

Master's Thesis

PIPING UNDER TRANSIENT CONDITIONS

Investigation of time-dependent
erosion under dikes

Renier Kramer

BSc, Civil Engineering (University of Twente, Enschede)

In partial fulfillment of the requirements
for the degree of

Master of Science in Civil Engineering and Management

University of Twente

October 9, 2014

Under supervision of the following committee:

Dr. ir. D.C.M. Augustijn

University of Twente, Department of Water Engineering and Management

Dr. J. J. Warmink

University of Twente, Department of Water Engineering and Management

J.P. Aguilar Lopez MSc.

University of Twente, Department of Water Engineering and Management

ir. J. Steenbergen-Kajabová

Grontmij Nederland B.V.

Abstract

Flood defenses have several failure mechanisms. One of those failure mechanisms is piping. Piping is the process of pipe formation in a sandy aquifer under river dikes. During high water periods, this process manifests itself by the formation of sand boils - formed by sand carried out of the aquifer by seepage – landwards of the dike. Piping will not lead to dike failure until the pipe length below the dike has reached the critical pipe length. From then, the piping process is irreversible and the dike will collapse.

The current piping safety assessment of Sellmeijer (1988) in the Netherlands assumes that dike failure will occur when the difference between the water levels on both sides of the dike, the hydraulic head difference, exceeds the critical hydraulic head difference. This is a constant value that can be calculated for each dike. The critical head difference is related to a critical pipe length approximately half the dike width. In reality, however, it takes time before the critical pipe length has been reached. It is likely that the critical pipe length will not be reached in case the hydraulic head difference equals or even exceeds the critical head difference for a brief moment and then quickly drops.

The influence of a variable head difference on piping has been investigated by, amongst others, Ozkan (2003) and Shamy et al. (2004). However, these studies do not involve the pipe length but focus on a process (exit gradient) that occurs before the start of piping, which is everywhere in the world, except for the Netherlands, used to indicate the chance of dike failure. Bonelli et al. (2007) researched the time-dependency of pipe widening (the last process of piping before dike failure) for a constant head difference. Recently, Van Esch et al. (2012) developed a piping model that is able to resolve the transient behavior of the groundwater pressure field of piping. Their model is meant to be part of the Dutch piping assessment and design from 2017. Until then, the model is not available and thus cannot be used for this study. Wang et al. (2014) derived formulae that can be used to determine the erosion velocity (pipe length increase per time step) under a constant head difference. It is, however, not clear what the effect of a variable head difference is on the erosion velocity.

This Master's thesis project investigates the effect of piping under transient conditions by taking into account the time dependency of the piping process. The objective of this study is to develop a piping model using existing theories of Sellmeijer (1988) and Wang et al. (2014) to investigate when progressive erosion occurs under realistic transient conditions. A transient piping model (TPM) has been developed in which the existing theory of Sellmeijer (1988) is extended with an erosion velocity formula of Wang et al. (2014) to account for time and to simulate piping under a variable head difference.

The most important limitation is that the TPM is only valid for piping under dikes and only for the idealized dike geometry of Sellmeijer. This dike consists of an impermeable clay dike is situated on top of a homogenous sandy aquifer with uniform thickness, the pipe entry and exit locations are predefined, and the slope of the pipe is zero. It is possible to simulate dikes that differ from the idealized Sellmeijer dike, but then this dike has to be simulated in the Sellmeijer model first and subsequently in the TPM.

The TPM has been validated on three IJkdijk full-scale piping experiments. The moment piping starts and the time to the critical situation were reasonably well predicted. The TPM (safely) underestimates the actual time to the critical situation. Also, the cumulative sand transport and sand transport rate predictions are satisfactory. Subsequently, the model has been used to determine the critical situation for constant and varying head differences for different dikes varying in seepage length, aquifer permeability, and aquifer thickness.

The results show that a dike declared as unsafe by Sellmeijer, does not have to be unsafe to piping, when taking into account the time dependent aspect. This is an important finding as it might save money because dike strengthening is not needed in that case. The more frequent a high water wave is expected to happen the more likely it is that the TPM predicts no dike failure whereas Sellmeijer predicts dike failure. The conclusion, however, only holds for high water waves with a return period of more than 10 years. The chance of a different prediction by Sellmeijer and the TPM is therefore the smallest for high waters waves with a return period of once in 1250 year.

Preface

This report represents my Master's thesis and it marks the end of my study in Civil Engineering and Management at the University of Twente. The objective of this research is gaining insight in the time dependency of piping under a variable river water level. Piping is the transport of sand below a dike (or structure) due to groundwater flow. Almost a year I had the pleasure to investigate the time-dependency of piping, which started with a two month literary study. The literary report is not included in the Master's thesis. During this research project I was supervised by Denie Augustijn, Jord Warmink, and Juan Pablo Aguilar Lopez from the University of Twente. I would like to thank them all for their useful feedback on my reports. I really appreciate the consistency of the feedback during the research project: for me it was always clear what was expected. The research has been carried out at Grontmij in the Bilt. I would like to thank Jana Steenbergen-Kajabová and Harm Rinkel for their guidance during the project.

By completing this Master Thesis, not only this research comes to an end, but also my time as a student here at the University of Twente in Enschede. I would like to thank my friends for the great time we had, already from the moment we met in the summer of 2007. Finally I would like to thank my family and especially my mom, who made it possible for me to achieve all this by their wholehearted support and encouragement.

Renier Kramer
Enschede, October 2014

Contents

Glossary	8
List of symbols.....	11
Chapter 1 – Introduction.....	12
1.1 Description of piping mechanism	12
1.2 State of the art.....	13
1.3 Problem definition	14
1.4 Research objective and questions	16
1.5 Research approach	17
1.6 Thesis outline.....	18
Chapter 2 - Development of the transient piping model.....	19
2.1 Piping models.....	19
2.1.1 Bligh	19
2.1.2 Lane.....	20
2.1.3 Sellmeijer	21
2.1.4 Wang et al.....	25
2.2 Transient piping model.....	28
2.2.1 Transient piping model setup	29
2.2.2 Neural network to simulate the Sellmeijer model	31
2.2.3 Hydraulic head in the pipe.....	33
Chapter 3 – Validation transient piping model.....	39
3.1 IJkdijk full-scale experiments.....	39
3.2 Transient piping model validation	42
3.2.1 Validation method	42
3.2.2 Validation results	43
3.2.3 Validation conclusion.....	50
Chapter 4 – Time dependent piping results.....	51
4.1 Time dependent piping with a constant head difference	51
4.1.1 Effect of seepage length with a constant head difference.....	51
4.1.2 Effect of aquifer permeability with a constant head difference	53
4.1.3 Effect of aquifer thickness with a constant head difference.....	55

4.1.4 Conclusion time dependent piping with constant head difference	57
4.2 Time dependent piping with a variable head difference	57
4.2.1 Effect of seepage length with a variable head difference	60
4.2.2 Effect of aquifer permeability with a variable head difference.....	62
4.2.3 Effect of aquifer thickness with a variable head difference	63
4.2.4 Effect of wave steepness under same wave period	64
4.2.5 Conclusion time dependent piping with variable head difference	65
Chapter 5 - Discussion.....	67
5.1 Model assumptions	67
5.2 Model limitations.....	68
5.3 Model uncertainties.....	69
5.4 Unaccounted physical processes.....	70
5.5 Comparison to literature	72
5.6 Added value of the transient piping model.....	73
Chapter 6 - Conclusions and recommendations	74
6.1 Conclusions	74
6.2 Recommendations.....	76
6.2.1 Academic recommendations.....	76
6.2.2 Practical recommendations.....	77
References	78
Appendix A - Historical research on piping	82
Appendix B - Sellmeijer.....	85
Appendix C - Sellmeijer (1988) versus Wang et al. (2014)	91
Appendix D - IJkdijk full-scale piping experiments.....	94
Appendix E - Transient piping model neural networks	95
Appendix F - Transient piping model dike parameters	98

Glossary

Aquifer - Sand layer under the dike with high permeability that allows for groundwater flow (water bearing layer)

Blanket - Covering or top layer in the dike that covers the aquifer. In many schematizations it is the first layer beneath a dike and consists of the same soil (mostly semi-pervious material)

Consolidation - In case soil gets unsaturated under the action of continuous (dike) material load above it. As a result, the material compresses due to expulsion of water or air from void spaces. Compression coincides with a volume decrease

Cutoff wall - A watertight screen constructed vertically in the ground, extending the line of seepage

Cracking - An open channel from aquifer to blanket. It is formed due to hydrostatic uplift pressure forces in the aquifer that exceed the downward ground pressure force at the underside blanket

Critical hydraulic head difference (ΔH_{CRIT}) - Head difference at which the dike will fail due to piping

Critical situation - when progressive erosion starts (see progressive erosion)

Effective stresses - Average stress in the matrix of a porous medium. It is the total soil stress minus pore water pressure at a certain point. Total stress at a certain depth in the aquifer remains constant as the river water level changes

Entry point - (Theoretical) point where the outside water enters the water-bearing sand layer, as a consequence of the hydraulic head over the flood defense

Erosion velocity - Pipe length increase per time step

Exit gradient - Exit gradient theory assumes a critical situation when the water level difference, between both sides of the dike, exceeds half the covering layer thickness next to the exit point of the pipe

Exit point - Location where seepage water first surfaces

Foreland - Area outside the dike, between dike and river; specifically in relation to piping

Heave - Vertical effective stresses in a sand layer fall away under the influence of a vertical groundwater flow, also called fluidization or the forming of quicksand

Hydraulic conductivity - Specific discharge per unit potential head gradient It describes the ease with which a fluid (usually water) can move through pore spaces or fractures. It depends on the intrinsic permeability of the material, on the degree of saturation, and on the density and viscosity of the fluid

Hydraulic head - Height of a column of fluid and thus expressed in units of length. In a well, the water will naturally rise to this height due to water pressure

Hydraulic head difference (ΔH) - Difference in head between two points, for example the two sides of a flood defense. The head difference is the driving force to groundwater flow

Hydraulic gradient - Gradient of the difference in head between the two points and the distance between those points. Hydraulic exit gradient is the quotient at the location of the exit point of the pipe

Inside toe - Most landward part of the dike (at the bottom). Inland of this point is hinterland area

Intrinsic permeability - Permeability of a material that is measured with a single fluid

Outside toe - Most riverside part of the dike (at the bottom). Any further towards the river, where foreland may exist, the river bedding is located

Phreatic surface line - Spatial surface in groundwater where pressure is equal to atmospheric pressure

Pipe formation - The onset of sand transport under dike as eventually consequence of uplift. Pipe formation is potentially followed by progressive erosion

Piping (forward & backward) - Forming of an open pipe from entry point to exit point: creation of hollow spaces under a dike or hydraulic structure, as a consequence of a concentrated seepage flow carrying ground particles. Backward erosion is piping from land- to riverside due to increasing ΔH . Forward erosion is the opposite process due to decreasing ΔH

Pipe length - Distance of the pipe from exit point (landward) to apparent tip of the pipe (not necessarily finished at riverside)

Polder level (or ground level) - Surface level of inland area (in Dutch referred to as 'maaiveld')

Polder water level - In this report the free water level landwards of the dike (in Dutch referred to as 'grondwaterpeil')

Pore water pressure - Pressure exerted by fluids within the pore space of a material. In and under the dike, this pressure is generated by the weight of the material (soil and water) above the pore's zone

Potential (hydraulic head) - Maximum hydraulic head in the aquifer determined by the weight of the blanket and pore water pressure in the aquifer. The potential is in relation to a reference level

Progressive erosion - When the pipe length equals the critical pipe length it starts to progressively erode towards the riverside of the dike: progressive erosion is irreversible and will result in dike failure

Relief well - An artificially crack in the top layer that needs to sufficiently relief the water pressure in the aquifer

Sand boil - Concentrated outflow of seepage water which carries sand out of the aquifer, for example through a crack channel or a hole in the covering

Seepage (horizontal, vertical) - Water flow through soil through and under dike. In this report ground water flow under the dike is considered when seepage is mentioned

Seepage length - Ground water flow distance from entry to exit point

Seepage line - Path of seepage from entry to exit point. It is assumed that during piping sand particles are transported along this line

Sellmeijer model - Three differential equations that describe physical equilibrium of the sand grains, groundwater flow and Poiseuille flow in the pipe

Sellmeijer rule (or formula) - Analytical formula developed by Sellmeijer that is used in practice as design and assessment rule

Tip of the pipe - Front side of the pipe that erodes towards the riverside of the dike

Transient - A transient event is a short-lived burst of energy in a system caused by a sudden change of state. In general "transient" and "unsteady" are considered to be equivalent.

Both indicate that the problem depends on time. However, transient is usually employed to indicate the evolution over time of the solution from an initial state until a steady state is reached (the solution does not change anymore). On the other hand, the term "unsteady" indicates that the solution does not reach such steady-state solution, it varies over time always. Such situation may arise, for example, when you have a source term within the solid, or boundary conditions that vary over time.

Transient Piping Model (TPM) - the model developed in this study to the time-dependency of piping

Uplift - Form of hydraulic soil failure by which a cohesive covering layer is lifted up as a consequence of water overpressure in the underlying aquifer. The uplift assessment questions whether uplift and possible rupture of the blanket in the form of a crack channel is expected.

List of symbols

Symbol	Unit	Description
ΔH	[m]	Hydraulic head difference over the dike
ΔH_{CRIT}	[m]	Critical hydraulic head difference over the dike (maximum permitted)
L	[m]	Seepage length (sum of horizontal and vertical seepage)
L_H	[m]	Total minimum horizontal seepage length
L_V	[m]	Total minimum vertical seepage length
C_{CREEP}	[-]	Creepfactor that depends on the median grain diameter
C_{W_CREEP}	[-]	Weighted creepfactor that depends on the median grain diameter
D_{blanket}	[m]	Thickness of the blanket
D	[m]	Thickness of the aquifer
K	[m/s]	Permeability of the aquifer
κ	[m ²]	Intrinsic permeability of the aquifer
h	[m]	Height of the pipe
$\partial\phi/\partial y$	[-]	Hydraulic head gradient normal to the pipe
$\partial\phi/\partial x$	[-]	Hydraulic head gradient along the pipe
$\partial\phi/\partial x_{\text{tip}}$	[-]	Hydraulic head gradient at the tip of the pipe
ϕ_{tip}	[m]	Hydraulic head at the tip of the pipe
F_R	[-]	Resistance term, being the strength of the sand
F_G	[-]	Geometry term (ratio of sand layer thickness and seepage length)
F_S	[-]	Scale term, relating particle size and seepage length
ν	[m ² /s]	Kinematic viscosity (1.33 10 ⁻⁶ m ² /s for groundwater at 10°C).
g	[m/s ²]	Acceleration of gravity (9.81 m/s ²)
d_{10}	[m]	10 percentile of the grain diameter of particles in the aquifer
d_{70}	[m]	70 percentile of the grain diameter of particles in the aquifer
d_{70m}	[m]	Mean value for the 70 percent grain diameter in small experiments (2.08 10 ⁻⁴ m)
γ^P	[kN/m ³]	Submerged unit weight of the particles in the aquifer (16.5 kN/m ³)
γ^W	[kN/m ³]	Unit weight of water (10 kN/m ³)
η	[-]	White's drag force factor (0.25)
ϑ	[deg.]	Rolling resistance angle of the sand in the aquifer (37 degree)
α	[m]	Slope of the pipe
RD	[-]	Relative density of the aquifer
C_3	[-]	Erosion coefficient of piping according (0.3)
u	[m/s]	Seepage velocity in the aquifer near the tip of the pipe
u_{crit}	[m/s]	Critical seepage velocity in the aquifer near the tip of the pipe
P_f	[%]	Percentage of particle weight that has to erode away before piping can occur
n	[-]	The initial porosity of the aquifer
n_{crit}	[-]	Critical porosity of the aquifer at which piping is possible (0.45)
h_{max}	[m]	Maximum pipe height at exit point
l	[m]	Apparent pipe length
l_{crit}	[m]	Critical pipe length
x	[m]	Distance along the pipe from exit point to tip of the pipe

Chapter 1 – Introduction

This Chapter addresses the outline of the research. First, Section 1.1 describes the piping mechanism, followed by the state of art of piping in Section 1.2. The context of the research problem is discussed in Section 1.3. Section 1.4 presents the objective and the main research questions of this study, followed by a brief research approach in Section 1.5. The outline of this thesis is given in Section 1.5.

1.1 Description of piping mechanism

Flood defenses have several failure mechanisms. One of those failure mechanisms is piping. In the factual definition, piping is the forming of an open pipe under a dike from entry point to exit point (TAW, 1999). The entry point and exit point is at the dike's riverside and polder side, respectively. The piping process can be split up in several steps, as shown in figure 1-1. In this figure the dike made of clay (red colored) and the sandy aquifer (yellow) are presented. On the left side the river is situated (blue) and on the right side is the polder. The water level difference between both sides of the dike causes water to flow under the dike. This water level difference is called the ΔH .

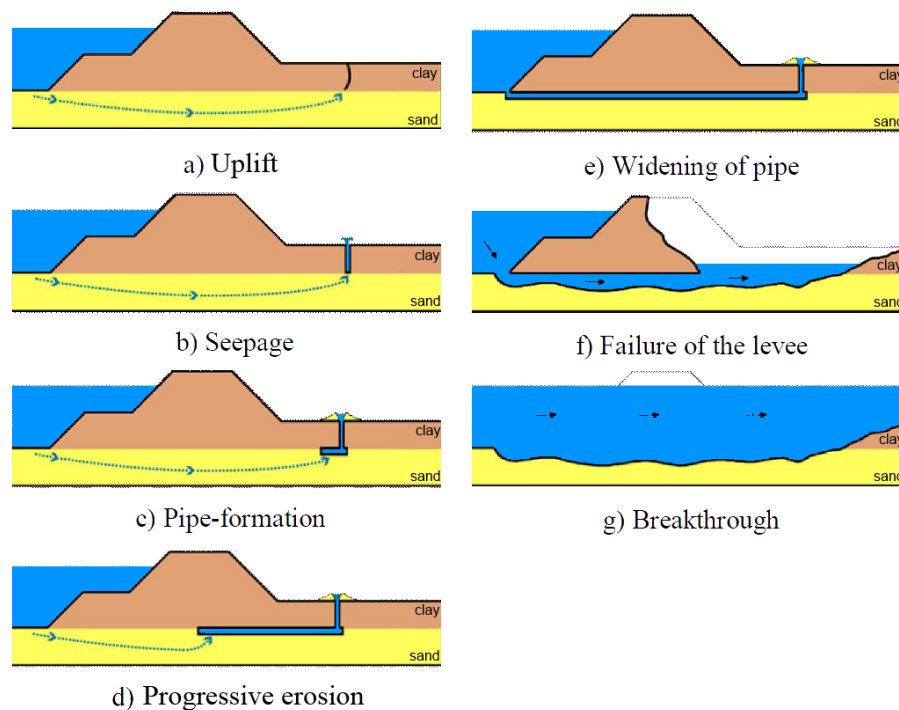


Figure 1-1 Steps in the process of piping (Van Beek et al., 2012a)

The process starts with uplift or heave at the polder side, depending on whether a cohesive top layer is situated on the polder side of the dike or not (figure 1-1 a). In case a cohesive top layer (clay) is present at the polder side piping can only occur if this top layer cracks (uplift). In case of no cohesive top layer (sand), the process starts with heave: vertical groundwater flow at the polder side causes fluidization of the sand (Van Beek et al., 2012).

Seepage water finds its way to the surface through the cracks (figure 1-1 b). This upward flow of groundwater erodes the cracks and creates a vertical channel. Since only water flows out and no sand is transported, this is not the pipe formation process yet (Van der Zee, 2011).

In case the velocity of groundwater flow (induced by ΔH) is large enough, sand grains may be transported along with the water flow (figure 1-1 c). This creates a pipe under the dike which erodes at the interface of the cohesive impermeable dike material and its granular permeable foundation. Due to higher permeability in the pipe, the pipe is able to discharge more water than the surrounding soil (Deltares, 2012). Note that the cohesive dike forms a “cover” over the pipe, allowing the pipe to exist. Without roofing the conceptual model has no potential. Since this erosion starts at the polder side and advances to the river side of the dike, in opposite direction of groundwater flow, it is also called backward erosion.

According to Sellmeijer (1988), the critical hydraulic head results in a critical pipe length which is about thirty to fifty percent of the flow path length (figure 1-1 d). Once the critical pipe length is reached the critical situation is reached and progressive erosion starts. Regardless of the ΔH the erosion velocity accelerates and the pipe erodes to the river side so that a direct connection between the river and protected landside is formed with dike failure as a result. For smaller ΔH s than the ΔH_{CRIT} , piping reaches a stable condition and the development of the pipe stops. As soon as the head increases, the erosion continues again.

Lengthening and widening of the pipe due to continued erosion finally results in significant dike deformation (figure 1-1 e). More than likely what will happen before the backward erosion reaches the river, as it somewhere under the dike, the dike sinks into the widened pipe (Van Beek et al., 2012).

Piping can lead to dike failure (figure 1-1 e). The river will start to flow through the damaged dike causing eventually a complete breach as indicated in figure 1-1 g (Van Beek et al., 2012).

1.2 State of the art

In the Netherlands, the empirical theories of Bligh (1910) and Lane (1935) and the mathematical model of Sellmeijer (1988) are used to calculate the critical situation of piping. In Section 2.1 these theories are elaborated in detail. According to these methods thirty-one percent of the primary water defenses is declared as unsafe due to piping (Vrijling et al., 2010). It is estimated that flood damage due to piping failure for a normative flood event is 2.2 million euros in the Netherlands. Water authorities need to improve their dikes but rather do not invest at the moment, knowing that new insights will become legally active around 2017. At the moment, it is unclear whether these new insights lead to less or more strict safety requirements.

A recently performed study by Vrijling et al. (2010) on the safety of Dutch dikes raised some doubts with respect to the validity of Bligh’s empirical rule (1910) which is applied as first piping safety check (Van Beek et al., 2012). Deltares (2012) concluded that this rule is not as conservative as one expected and therefore advises to disuse it.

The uncertainty in the current piping assessment of Sellmeijer is dominated by the aquifer permeability (Schweckendiek (2010)). The influence of heterogeneity at micro- and macro-scale has

not been investigated (van Beek et al., 2012a). Also, the behavior of piping in coarse sand is not yet well understood. Piping is mainly determined by the aquifer's soil composition. In the current assessment the aquifer is described by the aquifer permeability, the (seepage) length of aquifer and the thickness of the aquifer. The time dependent aspect of piping is not included in the current piping assessment, whereas this aspect certainly influences piping (Deltares, 2012).

Ozkan (2003) introduced a one-dimensional transient analytical flow model which was capable to determine the effect of variable ΔH s on the exit gradient. Everywhere in the world, except for the Netherlands, the exit gradient (see glossary) is used to indicate the dike failure chance. Ozkan (2003), however, did not include the erosion velocity.

Recently Van Esch et al. (2012) developed a new piping module in the Deltares groundwater flow simulator DgFlow that is able to resolve the transient behavior of the groundwater pressure field. Simulations demonstrate that the compressibility of the aquifer hampers the erosion velocity. Good quality laboratory experiments and field tests have to prove that the code simulates the concept of the piping mechanism well and supports Sellmeijer's rule (Van Esch et al., 2012). The research is carried out as part of the Wettelijk Toets Instrumentarium program (WTI2017). The model is meant to be part of the Dutch piping design and assessment rules from 2017. Until then, the model software is not available and cannot be used for this study.

Wang et al. (2014) investigated the erosion velocity for a constant ΔH . Their research resulted in formula that can be used to determine the erosion velocity for a constant ΔH . It is, however, not clear what the effect of a variable ΔH is on the erosion velocity.

1.3 Problem definition

Once piping has started it progresses in multiple small diverging “pipes” rather than a single “pipe” (figure 1-2). The natural heterogeneity in the aquifer causes the shallow pipes to be irregularly shaped which increases the complexity of the assessment. The trajectory of the pipe, and therefore also the time needed to eroded a certain distance, is difficult to predict since the pipe follows the path of least resistance. For computational reasons, the process of piping is modeled as one single straight pipe. The pipes are quite small with typical heights often less than two millimeter (Sellmeijer & Koenders, 1991).

As the aquifer is hidden, it is difficult to determine the piping phase. Yet, this time-dependency is important in interpreting historical failures, laboratory tests and to derive solutions to deal with piping. For instance if the pipe develops slowly; this might leave more room for emergency measures. The main difficulty is to determine whether the erosion process is in equilibrium (i.e. pipe length does not change) or that the pipe is still growing and just needs time to result in failure. Even when sand boils - formed by sand carried out of the aquifer by seepage - are suspected or detected, it is difficult to determine the piping phase (Bonelli et al., 2007). Also, for a high water situation that is below the ΔH_{CRIT} , where piping will lead to dike failure, the piping process may go slow. Hence, it is difficult to predict time to dike failure when sand boils are suspected or detected. History has shown that piping in the Netherlands occurs mainly along the upper reach of main rivers, most notably because the high water level is maintained for a

relatively long time (Deltares, 2012). This indicates that aquifer and/or time- dependency may play an important role.

After a flood wave, there are often sand boils observed while piping has not resulted in dike failure. This might be due to a reached equilibrium or due to limited time; failure might have occurred in the case the wave would have lasted longer. If the latter was the case, there is a high resilience in the mechanism for small gradients. However, what is often seen in real failures is that failure occurs fast. It might well be possible that no equilibrium is reached in these cases of high gradients. This implies that the resilience is a function of the gradient. Besides, there might be 'memory' in the mechanism, meaning that the formed pipe might remain open, after which the pipe might start growing again from its latest position during the next flood wave.

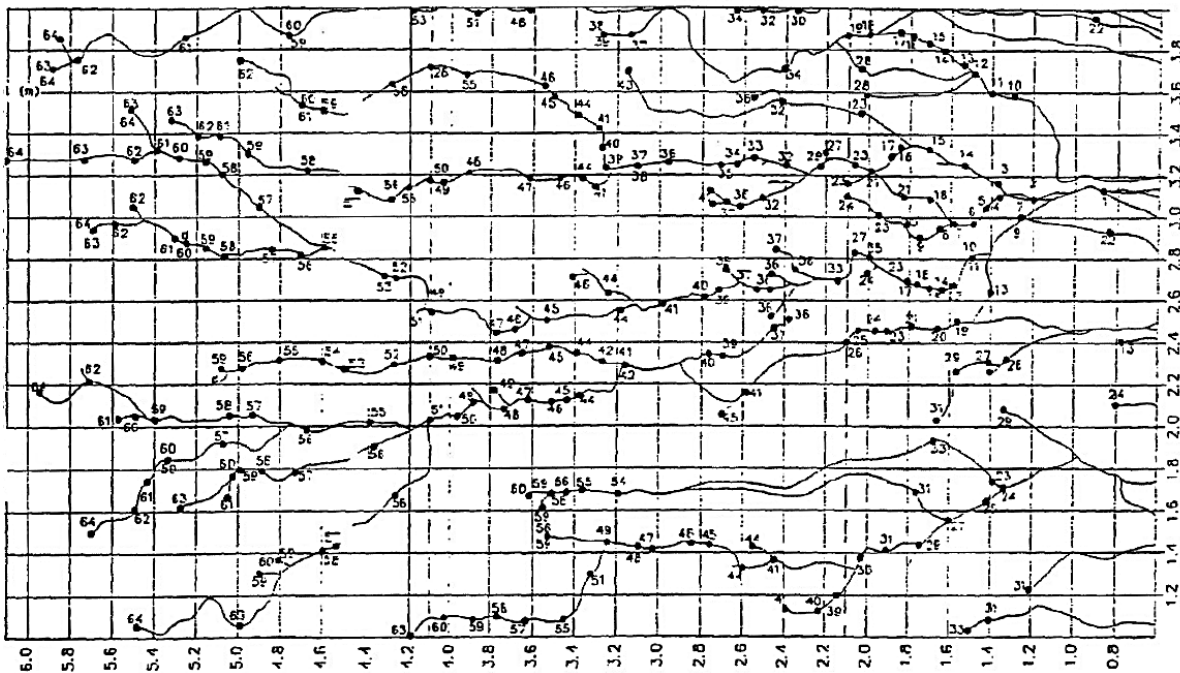


Figure 1-2 Top view of the aquifer for a full scale (length = 6m & width = 4m) piping experiment showing the arbitrary behavior of pipe growth. The pipes develop from the right side (downstream end) towards the left side (upstream side of dike). The numbers along the pipes indicate time of passing in minutes (Silvis, 1991)

As the pipe advances, the eroded soil is transported to the exit point of the pipe and appears as sand boils. By Dutch standards it is acceptable that sand boils form (TAW, 1999). However, when a sand boil is observed, it is unknown whether the erosion process is in equilibrium or that the pipe is still growing and just needs time to result in failure. A dangerous aspect of the time dependency is that for high water situations that are below the critical water level, the erosion may go slow. However, when the critical water level is reached, erosion may go fast.

The current piping safety assessment of Sellmeijer (1988) assumes that dike failure will occur when the ΔH equals or exceeds the ΔH_{CRIT} . In reality, however, it takes time before the critical situation has been reached. It is likely that the dike will not fail when the ΔH equals (or even exceeds) the ΔH_{CRIT} for a brief moment and then quickly drops. Assuming a constant ΔH in the current piping assessment may overestimate the design requirements for dikes.

The problem defined in the research is defined as:

“The current piping assessment in the Netherlands lacks a time dependent component”

1.4 Research objective and questions

This Master thesis project is intended to investigate the effect of piping under transient conditions by taking into account the time dependency of the piping process. The related objective of this study is:

“to develop a piping model using existing theories of Sellmeijer (1988) and Wang et al. (2014) to investigate when progressive erosion occurs under realistic transient conditions”

In the context of this objective we define progressive erosion as the critical situation of piping: the process is now irreversible and will result in dike failure. We define transient conditions as sudden or rapid changes in ΔH due to discharge waves in rivers. Based on the research objective, research questions are defined to further guide the research project. To achieve the objective, the following research questions were defined:

- 1. How can the effect of transient hydraulic head differences on piping be modeled?**
- 2. How does the modelled pipe length development compare to the IJkdijk measurements?**
- 3. When does piping result in progressive erosion considering dikes varying in aquifer permeability, aquifer thickness and seepage length?**
- 3. What is the added value of time-dependent piping analysis by the developed transient piping model compared to the Sellmeijer model?**

The outcomes of this study are expected to increase scientific understanding of the time dependency of piping. From a practical perspective, the outcomes can be used as scientific support for future research on piping under transient conditions which will lead to societal benefit: by knowing when progressive erosion cannot occur, due to for example a too short discharge wave period, further detailed (soil) investigation or advanced modeling is not needed. This research project will be one of the first projects to assess piping under transient conditions.

1.5 Research approach

This Section explains how the objective was to be reached and the research questions answered.

1. How can the effect of transient hydraulic head differences on piping be modeled?

For answering the first research question the theories of Wang et al. (2014) and Sellmeijer (1988) will be explored. A model needs to be developed that accounts for changing river water level. Possibilities to combine both theories of Wang et al. (2014) and Sellmeijer (1988) in a model to simulate piping under variable ΔH will be investigated. The model will be developed in MATLAB, which is a tool for numerical computation and visualization.

2. How does the modelled pipe length development compare to the IJkdijk measurements?

The full-scale piping experiments will be used to validate the TPM on four aspects. The start of piping is [h], the time required to reach the critical situation [h], the cumulative sand transport [kg], and the sand transport rate [kg/h]. All four aspects have been measured during the IJkdijk full-scale experiments. The IJkdijk tests will be simulated with Mseep. Mseep is a multipurpose program for numerical groundwater flow analyses that has an erosion module in which the Sellmeijer model is implemented. Sellmeijer used Mseep to conduct a great many numerical calculations of the ΔH_{CRIT} for various combinations of the parameters which play a role.

3. When does piping result in progressive erosion considering dikes varying in aquifer permeability, aquifer thickness and seepage length?

When progressive erosion occurs then piping will eventually lead to dike failure. Different dikes will be investigated differing in seepage length, aquifer permeability, and aquifer thickness. This research focusses on primary dikes as the time dependent effect of a variable ΔH plays a larger role compared to secondary dikes. A representative range of each of the three dike parameters for primary dikes in the Netherlands is defined by a Grontmij expert judgment call. The dikes are loaded with a constant and a variable ΔH and the critical time (pipe length is critical pipe length) is determined. Although the transient piping model (TPM) calculates the time to the critical situation, a 'critical time' comparison is not possible since the Sellmeijer model does not include time. However, both models predict whether a dike is going to fail due to piping and therefore a 'failure-no failure' comparison will be made. An existing dike (real case) is tested on piping with four different high water waves with a return period of 1250 years, 100 years, 10 years, and 1 year. The predictions by the TPM and the Sellmeijer model will be compared and discussed.

4. What is the added value of time-dependent piping analysis by the transient piping model compared to the Sellmeijer model?

To answer the fourth research question, the results obtained by the TPM will be discussed as well as the assumptions, limitations and uncertainties of the TPM. Also the processes that have not been modeled, but do have an impact on the results, are discussed. At the end of the true value of the TPM will be determined. The discussion is used to formulate the recommendations.

1.6 Thesis outline

The research is divided into four research questions each corresponding to one Chapter (figure 1-3). The first question focusses on the development of the TPM. This is elaborated in Chapter 2 which describes the underlying theory and setup of the TPM. The second research question, elaborated in Chapter 3, focusses on validation of the TPM on the IJkdijk full-scale piping experiments. The third research question is treated in Chapter 4. Performance of the TPM is investigated under constant and varying ΔH for dikes with varying seepage length, aquifer permeability, and aquifer thickness. The results are presented and compared with the Sellmeijer model. The fourth research question is elaborated in Chapter 5 in which the added value of the TPM (assumptions, limitations) is discussed. Finally, in Chapter 6 all the individual research questions are answered and conclusions and recommendations are given.

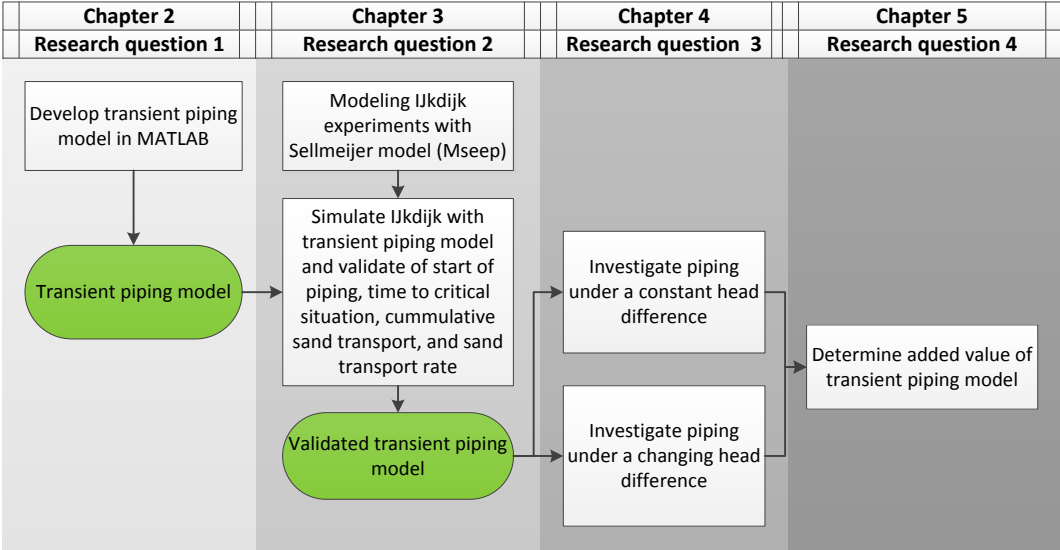


Figure 1-3 Research model flowchart

Chapter 2 - Development of the transient piping model

In this Chapter the first research question will be treated: How can the effect of transient hydraulic head differences on piping be modeled? Section 2.1 describes the existing piping theories on which the TPM is based. The similarities and differences between these theories are elaborated in Appendix C. Section 2.2 explains how the TPM is developed and elaborates the underlying assumptions. The limitations, assumptions of the TPM are discussed in Chapter 5 – Discussion.

2.1 Piping models

In the past a lot of research on piping has been done. In the Netherlands, the method of Bligh (1910), Lane (1935) and Sellmeijer (1988) are used to calculate piping. In this Section these methods are explained. In Appendix A, a chronological ordered overview of all research on piping is given.

2.1.1 Bligh

Bligh developed an empirical calculation rule in 1910, on the basis of a number of cases of collapse of steel-founded brick dams on diverse earth foundations in India. ‘The line of creep’ method developed by Bligh’s rule (1910) was applied in the Netherlands design practice till early nineties. The ‘line of creep’ represents a continuous line from entry- to exit point of the dike along which sand particles are transported. The critical line of creep, which is the total horizontal and vertical seepage line, is required to design a safe dike dimensions. Bligh (1910) analyzed several cases with dike failure due to piping and derived the following empirical rule of thumb:

$$\Delta H_{\text{CRIT}} = \frac{L}{C_{\text{CREEP}}} \quad (2.1)$$

In which is:

ΔH_{CRIT}	[m]	the critical head difference (maximum permitted)
L	[m]	the minimum seepage length (sum of horizontal and vertical seepage). The seepage length along a seepage screen is twice the screen length
C_{CREEP}	[-]	the creepfactor that depends on the median grain diameter (Bligh’s indications are listed in table 2-1).

Until recently, one considered no piping threat when Bligh’s safety assessment applies ($\Delta H < \Delta H_{\text{CRIT}}$). However, recent studies have shown that some exceptions exist in case the creep factor is not conservative enough. Bligh’s method then leads to an even more unsafe situation than results of Sellmeijer’s (1988) model (Vrijling et al., 2010). Ammerlaan (2007) also found that the maximum creep factor indicated safe situations for recorded failures in the USA. Hence, Deltares advises to disuse the method (Deltares, 2012).

2.1.2 Lane

Lane (1935) followed Bligh's empirical approach and extended his research for a few more soils, but argued that vertical seepage length weighs three times more than horizontal length and adjusted the empirical rule. Based on a total of 200 cases in the United States he developed an empirical formula called 'weighted line of creep'. When the pipe also follows a vertical path, for example in case of a vertical seepage screen, the formula of Lane can be used to assess the ΔH_{CRIT} . Lane's method is meant to include piping (horizontal erosion) and heave (vertical exit gradient). In case of uplift, the length of the crack channel is included in the vertical seepage length (Deltares, 2012). The aim of the simple test with Lane's rule is to assess if piping can occur along the shortest seepage length possible (Deltares, 2012). The empirical formula 'weighted line of creep' is based on a total of 200 cases in the United States:

$$\Delta H_{\text{CRIT}} = \frac{1}{3} \frac{L_H + L_V}{C_{W_CREEP}} \quad (2.2)$$

In which is:

ΔH_{CRIT}	[m]	the critical head difference
L_H	[m]	the total minimum horizontal seepage length
L_V	[m]	the total minimum vertical seepage length
C_{W_CREEP}	[-]	the weighted creep factor that depends on the median grain diameter (Lane's indications are listed in table 2-1).

The method mostly gives a conservative estimation. However, in case of aquifer with mainly coarse grains, or when no vertical seepage screen is installed, a dubious safety outcome is obtained (Deltares, 2012). A pipe with a higher slope than 1:2 is considered vertical and a pipe with a lower slope than 1:2 is considered horizontal.

Bligh vs Lane

If the vertical pipe length equals zero, results from Lane's and Bligh's method differ. One could argue that Bligh's creep factor should be three times Lane's creep factor, or Lane's creep factor one-third of Bligh's creep factor. Both rules are derived more or less the same. Many weirs and dams have been investigated of which was known a) the hydraulic head at which the water defense collapsed or b) the maximum ΔH ever occurred without collapsing of the water defense. The latter case might have caused discrepancy in the creep factors. From the method of Sellmeijer (1988), discussed in the next Section, it is known that the ΔH_{CRIT} is related to for example the grain size distribution and aquifer thickness. The difference between both creep factors might be caused by not taking this into account. For some soil materials the creep factor was not reported by Bligh or Lane (table 2-1).

Table 2-1 Creep factors of Bligh and Lane (TAW, 1999): a larger creep factor results in a lower piping resistance

Soil material	Median grain size	C_{CREEP} (Bligh, 1910) [-]	C_{W_CREEP} (Lane, 1935) [-]
Very fine sand	63 μm to 105 μm	-	8.5
Fine sand or silt	105 μm to 150 μm	18	-
Fine sand (micr.)	105 μm to 150 μm	18	7
Fine sand (quartz)	150 μm to 210 μm	15	7
Medium sand	210 μm to 300 μm	-	6
Coarse sand	300 μm to 2 mm	12	5
Fine gravel	2 mm to 5.6 mm	9	4
Medium gravel	5.6 mm to 10 mm	-	3.5
Coarse gravel	10 mm to 16 mm	-	3
Very coarse gravel	16 mm to 63 mm	4	3

2.1.3 Sellmeijer

Sellmeijer (1988) simulated the progression of a pipe with a mathematical model based on experiments. The initial movement of grains from the aquifer is based on the equilibrium forces on the grains in the pipe. Four distinct forces are considered in the particle force balance. The vertical forces are the weight of a particle and the vertical flow force. The horizontal ones are the drag force due to the channel flow and the horizontal flow force. Sellmeijer determined a relation between the ΔH and the pipe length at which the sand grains are in equilibrium and do not move out of position. The ΔH_{CRIT} is reached when the pipe reaches the critical pipe length. An equilibrium situation cannot occur anymore regardless of the ΔH and the pipe will progressively erode towards the river side of the dike.

His research resulted in three differential equations describing groundwater flow under the dike (Darcy and continuity), the water flow in the pipe (Poiseuille), and the physical equilibrium of the sand grains in the pipe (White). The equations cannot be solved analytically but need to be implemented in a numerical computation code (e.g. Mseep) (Van Esch & Sellmeijer, 2012). The last two processes together form the boundary condition for the first process. This implicates that the piping problem may be determined by ordinary groundwater flow computation with a special piping boundary condition. However, this is a cumbersome condition. It is highly nonlinear. It is not operative in a single point of the boundary, but affects the boundary on aggregate (van Zwieteren, 2013). By implication, only iteratively this condition may be applied. The three differential equations read:

1. A 2-D LaPlace equation (based on Darcy and continuity) to describe groundwater flow under a structure, with use of the following boundary conditions:
 - the riverside ΔH equals the river water level.
 - the landside ΔH equals the polder water level.
 - the hydraulic head around the pipe equals the hydraulic head in the pipe
 - the dike's blanket material is impervious

$$K_x \frac{\partial^2 \Delta H}{\partial x^2} + K_y \frac{\partial^2 \Delta H}{\partial y^2} = 0 \quad (2.3)$$

2. An equation (based on Poiseuille) to describe laminar flow in the pipe as a result of the increasing permeability:

$$h^3 \frac{\partial \varphi}{\partial x} = 12\kappa \int \frac{\delta \varphi}{\delta y} dx \quad (2.4)$$

3. An erosion formula (based on White) to describe equilibrium between forces on grains at the bottom of the pipe, assuming that rolling resistance is decisive for onset of grain's movement:

$$\frac{\partial \varphi}{\partial x} = \frac{d_{70} \pi \gamma^P}{h \cdot 3 \gamma^W \eta} \frac{\sin(\vartheta + \alpha)}{\cos(\vartheta)} \quad (2.5)$$

In which is:

K	[m/s]	the horizontal (K_x) en vertical (K_y) permeability of the sand layer which can be estimated using for example sieve analysis. The permeability in the Sellmeijer formula is the characteristic maximum value of the average permeability of the entire sand layer.
ΔH	[m]	the head difference over the dike
h	[m]	the height of the pipe
$\partial \varphi / \partial x$	[-]	the hydraulic head gradient along the pipe
$\partial \varphi / \partial y$	[-]	the hydraulic head gradient normal to the pipe
κ	[m ²]	the intrinsic permeability of the sand layer, which can be calculated by $\kappa = \nu / g * K$
ν	[m ² /s]	the kinematic viscosity ($1.33 \cdot 10^{-6}$ m ² /s for groundwater at 10°C).
g	[m/s ²]	the acceleration of gravity (9.81 m/s ²).
d_{70}	[m]	the 70 percentile of the grain diameter of particles in the aquifer
γ^P	[kN/m ³]	the submerged unit weight of the particles in the aquifer (16.5 kN/m ³). A volume weight of $\gamma^s = 26.5$ kN/m ³ can be assumed for Dutch sand that mainly consists of quarts. The submerged unit weight is then calculated as $\gamma^P = (\gamma^s - \gamma^W) / g$ (TAW, 1999)
γ^W	[kN/m ³]	the unit weight of water (10 kN/m ³)
η	[-]	White's constant (0.25 according to Sellmeijer (1988))
ϑ	[deg.]	the rolling resistance angle (37 degree according to Sellmeijer (1988))
α	[m]	the slope of the pipe. The factor $\sin(\vartheta + \alpha) / \cos(\vartheta)$ reduces to $\tan(\vartheta)$ if the slope of the pipe equals zero.

The mechanism of piping is conceptually modeled. The three differential equations cannot be solved analytically but need to be implemented in a numerical computation code (Van Esch &

Sellmeijer, 2012). It is implemented into the numerical groundwater flow program Mseep. Sellmeijer used Mseep to conduct a great many numerical calculations of the ΔH_{CRIT} for various combinations of the parameters which play a role. The piping rule is accommodated with the use of twenty-five thousand Mseep computations. Via accurate curve fitting to these calculation results an approximate analytical formula is derived. This formula was validated by a large-scale Delft Hydraulics model test in the Delta channel (Silvis, 1991). Sellmeijer proposed this formula as design and assessment rule for engineering practice. This rule can be used to design against piping in arbitrarily composed aquifer (TAW, 1999).

Sellmeijer (1988) used the so called idealized geometry in his research. This idealized dike geometry (figure 2-1) consists of a clay dike with a ditch on top of a homogeneous isotropic sand layer with constant and finite thickness: the permeability of the whole aquifer is represented by one value (that may change in time) and vertical permeability is equal to horizontal permeability (Deltares, 2012). A preassigned crack channel is assumed because of the convergence of streamlines at the exit point of the groundwater flow. The Sellmeijer model is a two dimensional model, and the pipe is assumed to be infinitely wide, and the outcome of the model is per running meter. Due to groundwater flow, the pipe length can increase in the direction of the river and sand boils occur at polder side of the dike. If the pipe reaches the river, a full passage under the dike is present (Van der Zee, 2011).

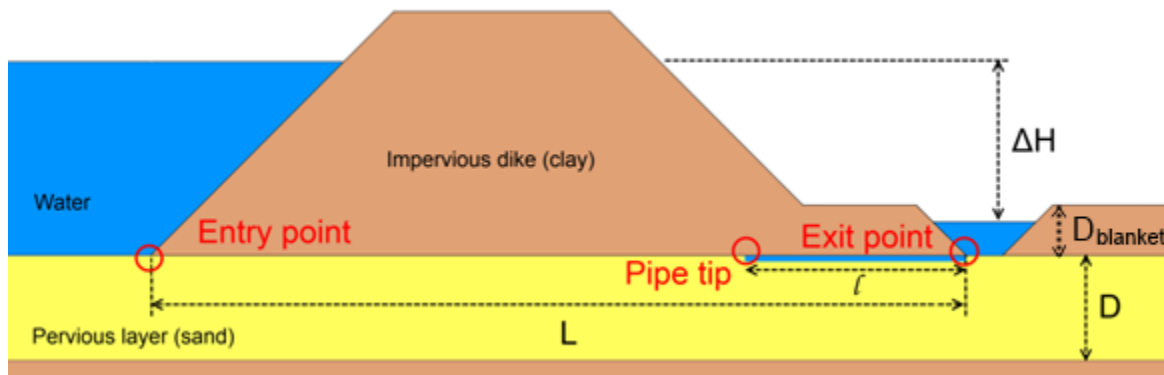


Figure 2-1 The idealized dike geometry for setup Sellmeijer's experiment (1988) with seepage length (L), ΔH (∂H), pipe length (l), and aquifer thickness (D)

The original version of the Sellmeijer rule (4-forces rule) that is used in Dutch practice dates back to 1994 (Deltares, 2012). The formula only applies when the seepage length is larger than ten times the ΔH over the dike (Ministerie van Verkeer en Waterstaat, 2007a). When this is not the case, more soil tests are needed. In 2006 the 4-forces rule has been altered in a 2-forces model (Sellmeijer, 2006). The role of the horizontal and vertical pressure gradient is questioned. It is put forward that in the pipe the particle at limit equilibrium sticks out, so that the pressure gradient does not affect it. Between the large grains substantial open space occurs. The forces due to the seepage gradients by no means can affect the grain at the top of the interface. Consequently, a 2-forces approach is selected where the drag force and weight of the particle are applied. The 2-forces model is implemented in the Mseep model that is used in this study.

Recently the 2-forces rule has been extended with a scaling factor and calibration ratio and validated in a full-scale experiment. The physics behind the revised rule have not changed; only the relation between the parameters and the ΔH_{CRIT} has been altered resulting in a more conservative piping rule so that a smaller ΔH_{CRIT} is obtained (ARCADIS, 2012). The latest version of the Sellmeijer rule that is used in Dutch practice dates back to 2009 (Deltares, 2012). The Sellmeijer 2-forces formula, which is currently used in Dutch practice and also implemented in Mseep, reads:

$$\Delta H - 0.3D_{\text{blanket}} \leq \frac{\Delta H_{\text{CRIT}}}{L} = F_R F_G F_S \quad (2.6)$$

with

$$F_R = \frac{\gamma^P}{\gamma^W} \eta \tan(\vartheta) \left(\frac{RD}{RD_m} \right)^{0.35} \quad (2.7)$$

$$F_S = \frac{d_{70}}{\sqrt[3]{\kappa L}} \left(\frac{d_{70}}{d_{70m}} \right)^{0.4} \quad (2.8)$$

$$F_G = 0.91 \left(\frac{D}{L} \right)^\alpha \quad \text{with } \alpha = \frac{0.28}{\left(\frac{D}{L} \right)^{2.8} - 1} + 0.04 \quad (2.9)$$

In which is:

F_R	[-]	the resistance term, being the strength of the sand
F_G	[-]	the geometry term, which depends on the ratio of the sand layer thickness and the seepage length
F_S	[-]	the scale term, relating the particle size and the seepage length
ΔH	[m]	the hydraulic head difference over the dike
D_{blanket}	[m]	the thickness of the blanket
ΔH_{CRIT}	[m]	the critical head difference over the dike
L	[m]	the horizontal seepage length
D	[m]	the thickness of the sand layer
γ^P	[kN/m ³]	the submerged unit weight of the particles in the aquifer (16.5 kN/m ³)
γ^W	[kN/m ³]	the unit weight of water (10 kN/m ³)
η	[-]	the drag force factor (coefficient of White with a value of 0,25)
ϑ	[deg.]	the rolling resistance angle of the sand in the aquifer (37 degree following Sellmeijer (1988))
RD	[-]	the relative density which defines how tight or loose soil is packed which influences the resistance of grains to move: the tighter, the more resistance. It is determined by the measured density of substance (kg/m ³) divided by density of the reference (kg/m ³) which is in most cases stated. $RD = (E_{\text{MAX}} - E)/(E_{\text{MAX}} - E_{\text{MIN}})$ in which E represent the dry density. RD_M

		represents the mean value for the relative density derived in small scale experiments (value set to 0,725)
d_{70}	[m]	the 70 percentile of the grain diameter of the sand in the aquifer
d_{70m}	[m]	the mean value for the 70 percent grain diameter derived in small scale experiments (value set to $2.08 \cdot 10^{-4}$ m)
κ	[m ²]	the intrinsic permeability of the sand layer which can be calculated as: $\kappa = \nu/g \cdot K$
ν	[m ² /s]	the kinematic viscosity ($1.33 \cdot 10^{-6}$ m ² /s for groundwater at 10°C)
g	[m/s ²]	the acceleration of gravity (9,81 m/s ²)
K	[m/s]	the initial isotropic hydraulic conductivity of the aquifer

The Sellmeijer model (implemented in Mseep) is used in this study to determine the relationship between the ΔH and the equilibrium pipe length. An example of the equilibrium curve is presented in figure 2-2. When the ΔH increases the pipe length increases until a new equilibrium is reached. This continues until the pipe length is approximately thirty to fifty percent of the seepage length (Sellmeijer, 1988). The curve maximum indicates the ΔH_{CRIT} and critical pipe length. Once the critical pipe length is reached progressive erosion occurs regardless of the ΔH : Piping accelerates with dike failure as a result: no equilibrium exists anymore, and the pipe grows fast until the entry point of the flow is reached and a full pipe has developed under the dike (TAW, 1999). The exact critical pipe length is calculated with the Sellmeijer model. In figure 2-2 this critical pipe length is about 70 percent of the seepage length.



Figure 2-2 Example of the Sellmeijer model (Mseep) output: the equilibrium curve with ΔH_{CRIT} (2.53 m) and critical pipe length (28 m). The total seepage length is 40 meters

2.1.4 Wang et al.

Recently Wang et al. (2014) developed a numerical quasi-steady state model to simulate the erosion velocity of piping. The transient process is divided into a number of successive steady phases which enables the application of a steady model. This approximation facilitates the

simplification of computation and holds for cases where the flow does not change quickly. Wang et al. (2014) proposed a mechanism of the soil particle inception in porous medium. Numerical analysis was carried out to investigate the effect of the upstream constant water head on piping below structures. The results coincide with physical model tests. Additionally, the numerical model gave an appropriate prediction of breaking through time for real situations.

The time it takes for the pipe to erode a certain distance depends on several aspects. If the local hydraulic gradient, which causes seepage flow, at the pipe tip is sufficient to take away the soil particles, fine particles are detached and transported through the pipe. This leads to an increase of soil porosity which increases hydraulic conductivity which influences groundwater flow around the pipe which will lead to more and more soil particles eroding. The natural soil has its maximum porosity ratio for a loosest condition. Piping occurs whenever the porosity exceeds this value. First the smallest grains erode. When the critical percentage is eroded, it is thought that the soil structure in the pipe tip has already broken, which means the pipe tip has changed from seepage domain to pipe flow domain (Wang et al., 2014). Smaller particles are quickly eroded away while the larger particles have larger resistance to the flow forces. The eroded particles are transported in the pipe flow, from tip to exit point of the pipe, which affects the rate of pipe progression. The pipe length increase, ∂L [m], within a time step, ∂t [s], can be calculated by:

$$\Delta L = \frac{C_3(u - u_{crit})}{P_f(1 - n)} \Delta t \quad (2.10)$$

In which is:

C_3	[-]	the erosion coefficient of the aquifer ($C_3=0.3$)
u	[m/s]	the seepage velocity in the aquifer near the tip of the pipe before piping occurs (equation 2.11). The direction of the seepage velocity is in opposite direction in which the pipe erodes
u_{crit}	[m/s]	the critical seepage velocity in the aquifer near the tip of the pipe (equation 2.11). Piping starts when the seepage velocity equals the critical seepage velocity
P_f	[%]	the percentage of particle weight that has to erode away from the soil composition before piping can occur. According to the model of Sellmeijer (1988), pipe flow occurs when the normative grain size d_{70} erodes (Van der Zee, 2011). Therefore P_f is taken as a constant value of 70%
n	[-]	the initial porosity of the aquifer

The (critical) seepage velocity is expressed by Darcy's law:

$$\text{with } u = \frac{K \frac{\partial \phi}{\partial x}}{n}; u_{crit} = \frac{K_{crit} \frac{\partial \phi}{\partial x}}{n_{crit}} \quad (2.11)$$

In which is:

- K_{crit} [m/s] the hydraulic conductivity
- $\partial \phi / \partial x$ [-] the local hydraulic gradient at the tip of the pipe. This is calculated by (seepage length – apparent pipe length) / (ΔH over dike – pressure at tip of pipe). The hydraulic gradient is updated each time step
- n [-] the initial porosity of the aquifer
- n_{crit} [-] the critical porosity of the aquifer. The natural soil has its maximum porosity value for a loosest condition and a structure beyond this maximum porosity value cannot exist. Wang et al. (2014) adopted a critical porosity n_{crit} of 0.45.

Chapuis (2004) has studied the saturated hydraulic conductivity of sand using effective diameter and void ratio, and proposed a relationship in which the hydraulic conductivity depends on the tenth percentile of the particle size distribution, d_{10} [m], and the initial (or critical in case of critical hydraulic conductivity) porosity. Wang et al. (2014) recommends this relation as the outcome is quite similar to the hydraulic conductivity of their experiment. According to Chapuis (2004) the (critical) permeability can be calculated by:

$$K = 1219.9 d_{10}^{1.565} \frac{n^{2.3475}}{(1-n)^{1.565}}; K_{crit} = 1219.9 d_{10}^{1.565} \frac{n_{crit}^{2.3475}}{(1-n_{crit})^{1.565}} \quad (2.12)$$

In which is:

- d_{10} [m] the 10 percentile of the grain diameter of the sand in the aquifer
- n [-] the initial porosity of the aquifer
- n_{crit} [-] the critical porosity of the aquifer (0.45 following Wang et al. (2014))

In table 2-2 an overview of the Wang et al. (2014) variables and parameters is given. For each of the variables and parameters is indicated whether they change or remain constant during piping.

Table 2-2 Wang et al. (2014) variables during piping

Constant (per dike case constant)			Same value for all dikes
Symbol	Unit	Description	
Δt	[s]	Time step (1 second)	Yes
P_f	[%]	Percentage of particle weight that has to erode for piping to occur (70%)	Yes
d_{10}	[m]	10 percentile of the grain diameter of the aquifer's sand	No
C_3	[-]	Erosion coefficient (0.3)	Yes
n	[-]	Initial aquifer porosity	No
n_{crit}	[-]	Critical porosity of the aquifer at which piping occurs (0.45)	Yes
K	[m/s]	Initial hydraulic conductivity of the aquifer depends on initial porosity and d_{10}	No
K_{crit}	[m/s]	Critical hydraulic conductivity of the aquifer depends on critical porosity and d_{10}	No
Variable (recalculated each time step)			In this study for all dikes the same
Symbol	Unit	Description	
ΔL	[m]	pipe length increase	No
$\partial\phi/\partial x$	[-]	horizontal hydraulic pressure gradient at the tip of the pipe	No
u	[m/s]	seepage velocity at the tip of the pipe depends on initial hydraulic conductivity, initial porosity (both constant) and hydraulic pressure gradient	No
u_{crit}	[m/s]	critical seepage velocity at the tip of the pipe depends on the critical hydraulic conductivity, critical porosity (both constant) and hydraulic pressure gradient	No

2.2 Transient piping model

In the TPM the existing theory of Sellmeijer (1988) is extended with an erosion velocity formula of Wang et al. (2014) to account for time and to simulate piping under a variable head difference. In Section 2.2.1 the setup of the TPM is described. Neural networks were developed in this study to emulate the Sellmeijer model so that the TPM alone could simulate piping. How these neural networks were developed is elaborated in Section 2.2.2. Section 2.2.3 holds the formulas of the TPM. In Section 2.2.4 the assumptions and limitations of the TPM are elaborated.

2.2.1 Transient piping model setup

The erosion velocity depends on the hydraulic gradient at the tip of the pipe (Wang et al., 2014). The erosion velocity changes when the ΔH over the dike changes. The TPM this study calculates the increase in pipe length based on the ΔH . In figure 2-3 the setup of the TPM is given.

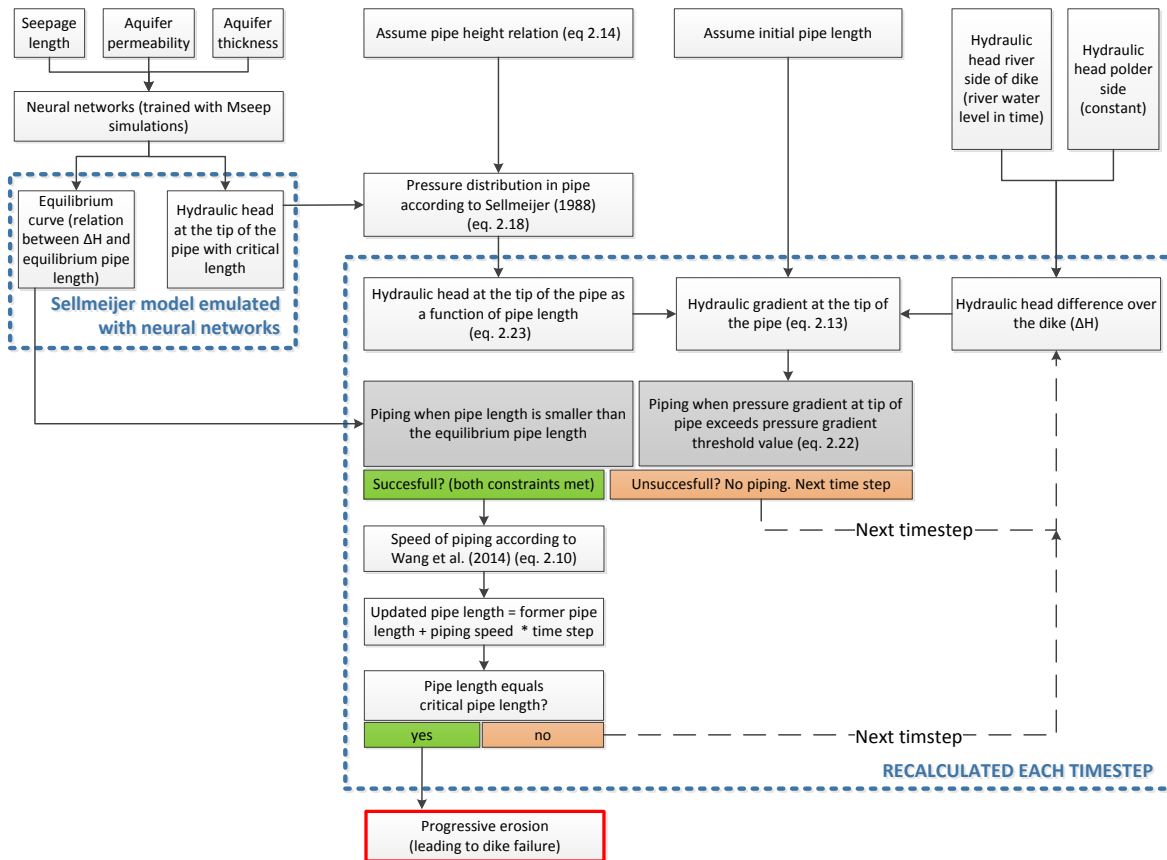


Figure 2-3 Model flow chart of the TPM

The erosion velocity depends on head gradient at the tip of the pipe. The gradient is calculated by difference between river head and the head at the tip of the pipe divided by seepage length where pipe did not occur.

To determine the hydraulic pressure distribution in the pipe, a relation for pipe height from entry to exit point (based on Sellmeijer) is assumed. As the pipe length increases, the exit hole height increases asymptotically from zero to a maximum value (h_{max}) at the time of critical pipe length. In Section 2.2.3 this is explained in more detail.

Neural networks have been used to emulate the Sellmeijer model and are included in the TPM. By doing so, piping can be simulated with only using the TPM. In Section 2.2.2 the neural networks are elaborated.

In figure 2-4, the idealized geometry of the Sellmeijer model (1988) is presented. This geometry represents also the TPM's dike geometry in which the seepage length is set: in case a clay blanket exists on the polder side of the dike, a preassigned pipe (crack channel) exists at the

inner toe of the dike (this is because of convergence of the streamlines). The slope of the pipe is zero.

It is assumed that the hydraulic pressure at the clay-sand interface increases linearly from inner toe to outer toe (figure 2-4). This assumption is discussed in Section 2.2.4. At the riverside, the head is equal to river water level and at the the polder side the head is zero, represented by the dark blue line. As the pipe erodes towards the river side of the levee, the pore water pressure around the pipe slightly decreases (Deltares, 2012), represented by the light blue line. When the river water level drops suddenly fast, in the TPM the pressure head in the soil around the pipe (the linear dark blue line) might become smaller than the pressure in the pipe. In practice this is not possible. The pressure in the pipe is always smaller than in its surrounding soil (Deltares, 2012). Therefore a first model constraint is defined: erosion velocity is set to zero when this is the case.

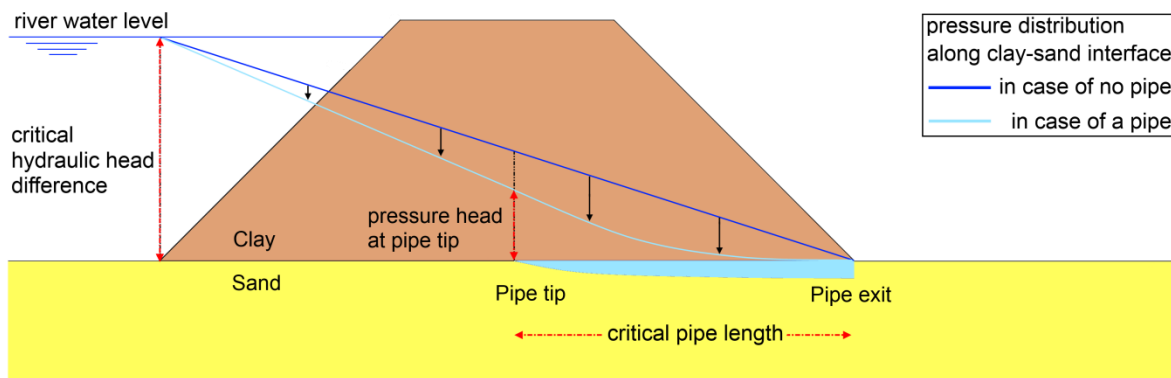


Figure 2-4 Schematic distribution of pore water pressure along clay and sand interface. The pipe erodes from right (polder side) to left (river side) of the clay dike

With the pressure at the tip of the pipe and the ΔH over the dike the hydraulic gradient at the tip of the pipe is calculated:

$$\frac{\partial \phi}{\partial x_{tip}} = \frac{\Delta H - \phi_{tip}}{L - l} \quad (2.13)$$

In which is:

$\partial \phi / \partial x_{tip}$	[-]	the hydraulic head gradient at the tip of the pipe
ΔH	[m]	the hydraulic head difference
ϕ_{tip}	[m]	the hydraulic head at the tip of the pipe is calculated according equation 2.19
L	[m]	the seepage length
l	[m]	the pipe length

The TPM calculates the increase in pipe length. Increase in pipe length can only occur when the hydraulic gradient at the tip of the pipe exceeds a threshold hydraulic gradient value that is proportional to the inverse of the cube root of the local flow velocity (equation 2.21). For a given time step, the pipe length might advance a certain length. The updated pipe length is the former pipe length plus erosion velocity times time step. The updated pipe length cannot exceed the

equilibrium pipe length that is related to a certain ΔH according to Sellmeijer (equilibrium curve). This forms a second constraint in the model.

The equilibrium curve and the pressure head at the tip of the critical pipe length pipe represent only a specific case with a certain dike geometry, aquifer thickness and soil composition, and other characteristics. The left column in figure 2-5 shows the input of the TPM (middle column). The output of the TPM (right column) contains maximum pipe length which is less than or equal to critical pipe length, elapsed time to reach that maximum pipe length, and the pipe length as a function of time.

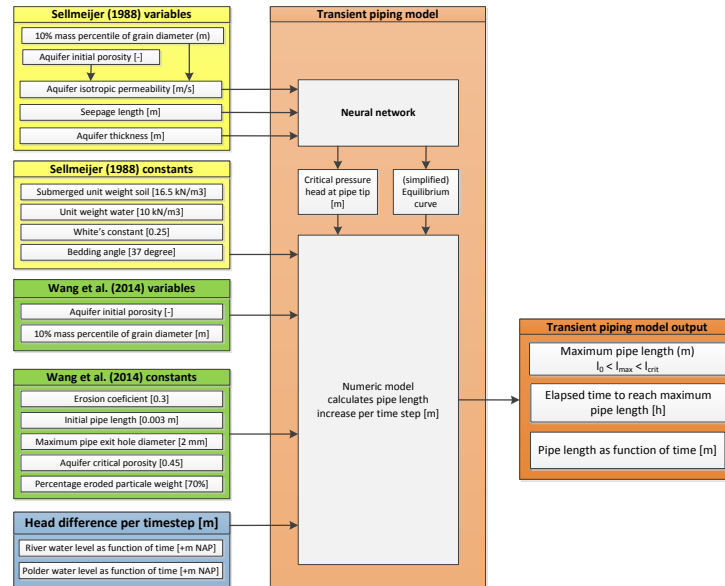


Figure 2-5 Model input and output of the TPM

2.2.2 Neural network to simulate the Sellmeijer model

To simulate piping with only using the TPM and not use the the Sellmeijer model for every simulation, the Sellmeijer model is emulated with neural networks. These neural networks are included in the TPM. The needed output from the Sellmeijer model consists of the equilibrium curve and the pressure head at pipe tip of the critical pipe.

Five parameters are simulated with five neural networks. Four of these parameters determine the simplified equilibrium curve, and one parameter determines the pressure head at pipe tip of the critical pipe. The five neural networks have been trained to predict these five parameters based on seepage length, aquifer thickness and aquifer permeability. As the relations are highly non-linear the Sellmeijer model cannot be fully applied (multiple regression is not possible). The neural networks are only valid within the lower and upper boundaries presented in table 2-3.

Table 2-3 Valid range of the five neural networks

	Parameter	Lower limit	Upper limit	Unit
Neural network input	Seepage length	20	70	m
	Aquifer thickness	5	50	m
	Aquifer permeability	10	100	m/day
Neural network output	ΔH first point equilibrium curve	1	7.8	m
	ΔH_{CRIT}	1	7.8	m
	Pipe length first point eq. curve	9.7	11.2	m
	Critical pipe length	10	34	m
	Pressure head at the tip of pipe with critical length	0.31	1.1	m

Neural networks training procedure

A script was developed to generate 312 Sellmeijer model input files (representing a dike) that were simulated with the Sellmeijer model (using a batch file). These 312 dikes vary in seepage length, aquifer permeability, and aquifer thickness. The seepage length range is 20 to 70 meters with a 10 meter interval (6 dikes). The aquifer permeability range is 10 to 100 meters per day with a 7.5 meter per day interval (13 dikes). The aquifer thickness range is 5 to 50 meters with a 15 meter interval (4 dikes). The intervals have been chosen with respect to the dominance of the dike parameter in the Sellmeijer model. The reliability of Sellmeijer’s rule is especially dominated by the uncertainty in permeability of the aquifer (Schweckendiek, 2010). The seepage length is split up into more samples than the aquifer thickness as the seepage length has a larger impact on piping (Sellmeijer, 1988).

Subsequently a script was developed to automatically collect the necessary information from the (6x13x4=) 312 Sellmeijer model output files: the ΔH related to the first point, the ΔH_{CRIT} , the pipe length related to the first point, the critical pipe length (all four related to equilibrium curve), and the pressure at the tip of the critical pipe length.

The neural networks have been developed with the fitting tool of the MATLAB neural network toolbox. The 312 training samples have been split up according to the default toolbox settings into training data (70%; 218 samples) to adjust the weights on the neural network, validating data (15%; 47 samples) to minimize overfitting, and testing data (15%; 47 samples) for testing the final solution in order to confirm the actual predictive power of the network. The testing results of the five networks are presented in table 2-4. To avoid ending up with an overtrained neural network the default settings of the network architecture panel (number of hidden neurons and number of layers) have been varied many times and each time the mean and normalize has been determined. The lowest normalized absolute error (NAE) between the predicted data and test data (47 samples) has been determined by trial and error. The NAE of all five networks is 0.012 at most (1.2% difference on average between predicted data and test data). Therefore it is assumed that all networks sufficiently emulate the Sellmeijer model. For all five

networks only one layer is used. This is kept as low as possible. More detailed information about the neural networks can be found in Appendix E.

Table 2-4 Specifications of the five neural networks

Neural network output	Number of hidden neurons	Number of layers	Normalized abs. error (NAE) [-]	Mean absolute error (MAE) [m]
ΔH first point	6	1	0.0022	0.004
ΔH_{CRIT}	4	1	0.0059	0.019
Pipe length first point	9	1	0.0052	0.056
Critical pipe length	10	1	0.0083	0.061
Critical pressure at pipe tip	14	1	0.0118	0.0079

Equilibrium curve

The equilibrium curve of the Sellmeijer model consists of a hyperbolic part and a linear part. The TPM simplifies this to two linear lines using the first and critical point predicted by the neural network. In figure 2-6 two examples of equilibrium curves are presented. It is possible that first point coincides with the critical point. The ΔH and pipe length of both points are predicted with the neural networks. Subsequently both coordinates are used to simplify the equilibrium curve as two linear parts. In between the first and critical point this results in a seemingly dangerous situation: according to the TPM equilibrium curve the pipe length is longer than the Sellmeijer model equilibrium curve for the same ΔH . However, the critical situations of both models share the same ΔH_{CRIT} implying that the TPM can only simulate dike failure when the Sellmeijer model simulates dike failure.

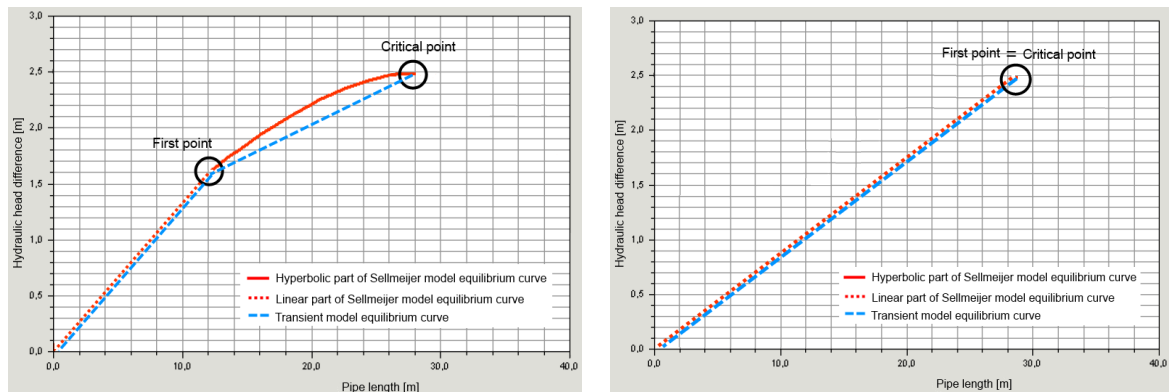


Figure 2-6 Sellmeijer model equilibrium curve (red) and the simplified equilibrium curve in the TPM (blue)

2.2.3 Hydraulic head in the pipe

To determine the hydraulic head distribution in the pipe, a relation for pipe height from entry to exit point is assumed. According to Van Esch & Sellmeijer (2012) the pipe height, h [m], is zero at the tip of the pipe and first steeply increases and then remains rather constant towards the exit point. An asymptotical relation for pipe height was adopted by Van Esch & Sellmeijer (2012):

$$h(x) = h_{max} \frac{\sqrt{l-x}}{\sqrt{l_{crit}}} \quad (2.14)$$

In which is:

- h_{max} [m] maximum pipe height at exit point (constant parameter for each dike case). When the critical pipe length is reached, the exit hole height equals this maximum value
- x [m] the distance along the pipe from exit point to tip of the pipe ($0 < x < l$)
- l [m] the apparent pipe length ($0 < l < l_{crit}$). Over time, as the pipe length increases towards the river side of the dike, the exit hole pipe height increases as well
- l_{crit} [m] critical pipe length predicted by the neural network (constant parameter for each dike case). When this length is reached progressive erosion occurs resulting in dike failure.

Figure 2-7 shows the pipe height development. Here the critical length (l_{crit}) of the pipe was set to 30 meters and h_{max} to a realistic exit pipe height in the critical situation of two millimeters (Van Esch & Sellmeijer, 2012). Water flows from the tip of the pipe $x = l$ (right) to the exit point $x = 0$ (left). From equation 2.14 it seems that the ΔH does not affect the pipe height. However, the equilibrium curve relates the ΔH and the pipe length (e.g. the critical pipe length can only be reached in case of a ΔH_{CRIT}). Therefore the ΔH influences the pipe height. In figure 2-7 no ΔH is defined, only a maximum pipe height and critical pipe length.

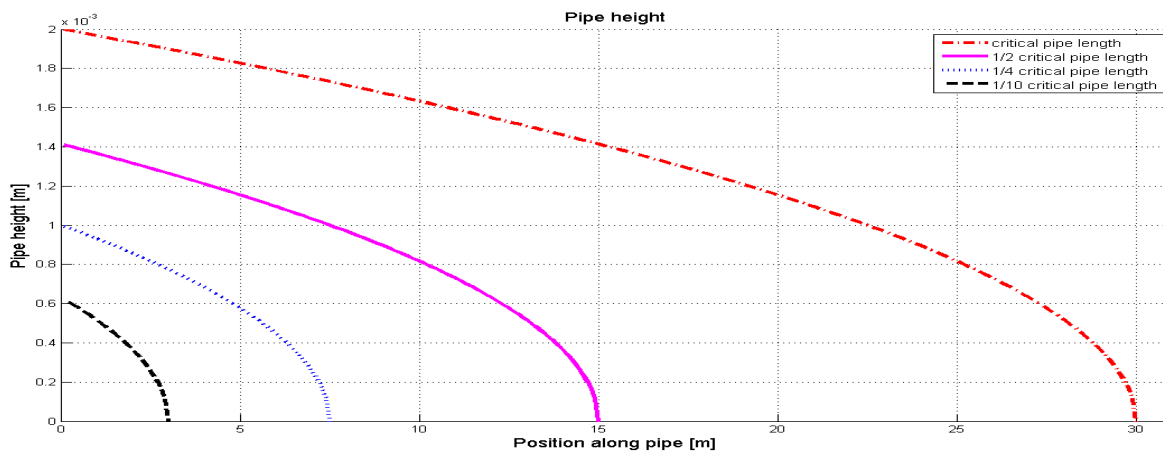


Figure 2-7 Pipe height at four different moments during increasing pipe length until the critical pipe length. The maximum pipe height at exit point is set to a realistic two millimeters (Van Esch & Sellmeijer, 2012)

In the pipe, soil particles are assumed to be in an equilibrium condition. This means that given a certain head gradient at a point particles do not move out of position (Sellmeijer, 1988). When pipe height decreases, a larger pressure gradient is needed to transport particles as the transport resistance increases (Sellmeijer, 1988). Sellmeijer assumes that the bottom and top of the pipe equally contribute to the shear stress. Sellmeijer's (1988) equilibrium condition reads:

$$\frac{\partial \varphi}{\partial x} = \frac{d_{70}}{h(x)} \frac{\pi \gamma^P}{3 \gamma^W} \eta \frac{\sin(\vartheta + \alpha)}{\cos(\vartheta)} \quad (2.15)$$

In which is:

$\partial \varphi / \partial x$	[-]	the hydraulic head gradient along the pipe
h	[m]	the height of the pipe
d_{70}	[m]	the 70 percentile of the grain diameter of particles in the aquifer
γ^P	[kN/m ³]	the submerged unit weight of the particles in the aquifer (16.5 kN/m ³)
γ^W	[kN/m ³]	the unit weight of water (10 kN/m ³)
η	[-]	White's constant (0.25 according to Sellmeijer (1988))
ϑ	[deg.]	the rolling resistance angle (37 according to Sellmeijer (1988))
α	[m]	the slope of the pipe. The factor $\sin(\vartheta + \alpha) / \cos(\vartheta)$ reduces to $\tan(\vartheta)$ if the slope of the pipe equals zero.

The only variable parameters in this equation are pipe height, which increases from tip to exit point of the pipe, and head gradient. All parameters in the right hand term are constant along the pipe, except pipe height, h (m). Substituting equation 2.14 into equation 2.15 assuming a pipe with flat slope gives the pressure gradient distribution in the pipe:

$$\frac{\partial \varphi}{\partial x} = \frac{\beta}{\sqrt{l-x}} \quad (2.16)$$

with pressure parameter β [m] representing constant parameters:

$$\beta = \frac{d_{70}}{h_{max}} \frac{2\pi \gamma^P}{3 \gamma^W} \eta \tan(\vartheta) \sqrt{l_{crit}} \quad (2.17)$$

Figure 2-8 shows the gradient of the hydraulic head over the pipe. This gradient is infinitely large at the tip of the pipe, which implies infinitely large erosion. This is because the pipe height is zero at the tip of the pipe. However, this hydraulic gradient according to Sellmeijer (1988) will not be used to calculate erosion velocity. Instead, the difference between the hydraulic head at the riverside of the dike and the tip of the pipe determines the hydraulic gradient (Wang et al. 2014).

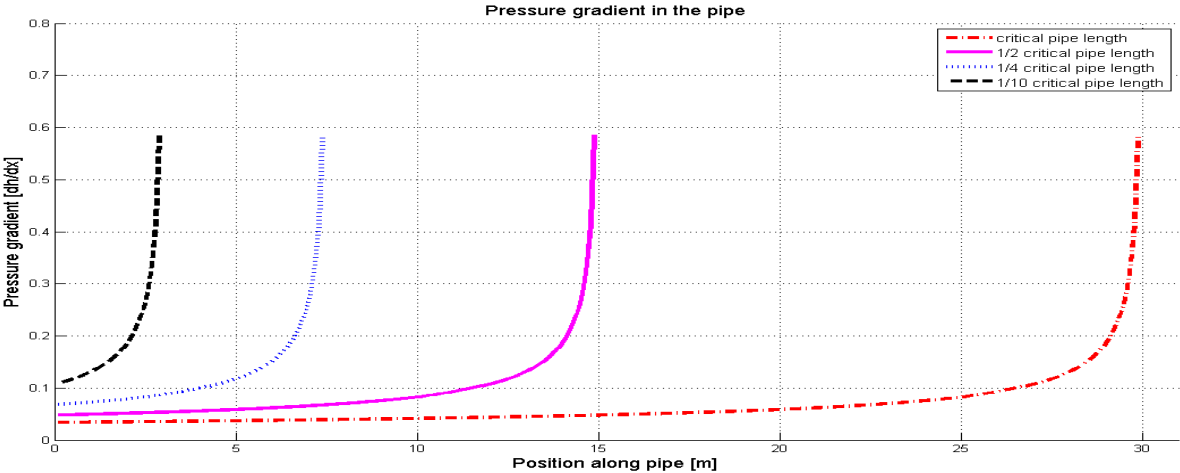


Figure 2-8 Pressure gradient along the pipe for four different pipe lengths

The head as a function of distance follows from head gradient integration. Setting the head at the exit point equal to zero gives the head distribution in the pipe depicted in figure 2-9.

$$\varphi(x) = \beta \int_0^x (l - x)^{-\frac{1}{2}} + C = -2\beta \sqrt{l - x} + 2\beta \sqrt{l} \tag{2.18}$$

The pressure in the pipe increases exponentially from the exit point to the tip of the pipe (figure 2-9). In equation 2.18 no ΔH is taken into account. The pressure in the pipe is related to the ΔH since the pipe length is related to the ΔH by the equilibrium curve of Sellmeijer.

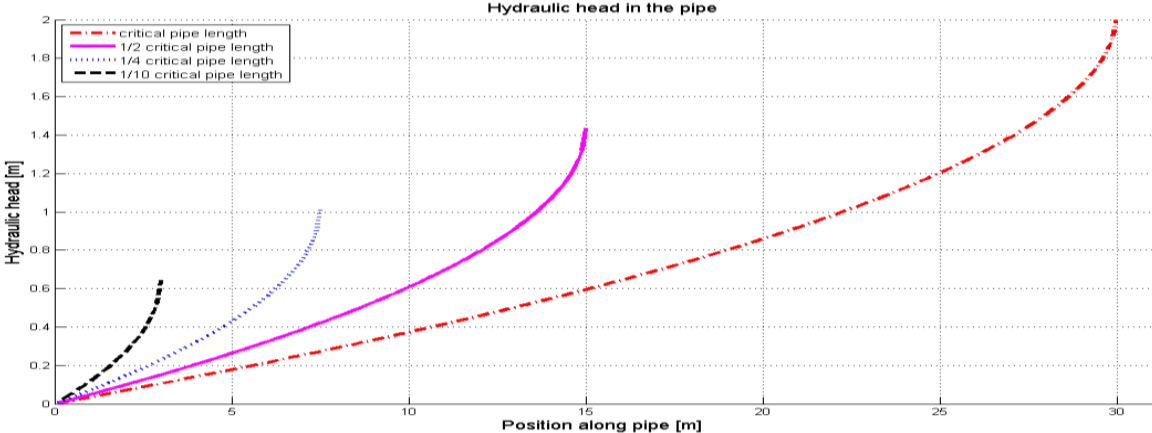


Figure 2-9 Hydraulic head distribution in the pipe for four different pipe lengths

The erosion velocity only accounts for the pressure head at the tip of the pipe. The hydraulic head at the tip of the pipe with length (l) reads:

$$\varphi_{tip}(l) = 2\beta\sqrt{l} \quad (2.19)$$

Only the pressure head at the tip of the pipe with the critical length is calculated by the Sellmeijer model. In case the $\varphi_{tip}(l_{crit})$ calculated by the TPM differs from the $\varphi_{tip}(l_{crit})$ calculated by the Sellmeijer model, equation 2.19 needs to be adjusted. The easiest way would be to adjust the pressure coefficient β . However, then all the variables within this parameter (equation 2.17) would be adjusted as well. Instead of changing the pressure coefficient β in equation 2.19, that represents the curviness of the relation, the curve is vertically shifted with γ_1 and horizontally shifted with γ_2 . Therefore equation 2.19 is rewritten so that the pressure head at the tip of the pipe with length (l) reads:

$$\varphi_{tip}(l) = -\gamma_1 + 2\beta\sqrt{l + \gamma_2} \quad (2.20)$$

with:

$$\gamma_1 = 2\beta\sqrt{\gamma_2 - l_{crit}} \quad (2.21)$$

$$\gamma_2 = \left[\frac{\beta}{\varphi_{crit}} \left(l_{crit} + \frac{\varphi_{crit}^2}{2\beta^2} \right) \right]^2 \quad (2.22)$$

Erosion threshold

The limit equilibrium condition of Sellmeijer (equation 2.15) determines whether particles in the pipe do move out of position given a certain head gradient. In this study this formula is used to estimate the pressure along the pipe. According to Van Esch & Sellmeijer (2012) the pipe height is zero at the tip of the pipe, hence, the onset of piping requires an infinitely large pressure gradient. To define the start-stop condition, a different threshold value related to flow velocity defined by Sellmeijer (1988) is introduced. Kanning (2012) states that the critical shear stress is proportional to the inverse of the cube root of the permeability (K), and hence proportional to the inverse of the cube root of the local flow velocity. For piping to occur the hydraulic gradient at the tip of the pipe needs to exceed the threshold value:

$$\frac{\partial \phi}{\partial x_{tip}} > \frac{\partial \phi}{\partial x_{threshold}} = \eta \frac{d_{70}}{\left(\frac{v}{g} K L\right)^{1/3}} \quad (2.24)$$

In which is:

η	[-]	White's constant (0.25)
ν	[m ² /s]	the kinematic viscosity (1.33 10 ⁻⁶ m ² /s for groundwater at 10°C)
g	[m/s ²]	the acceleration of gravity (9.81 m/s ²)
K	[m/s]	the permeability of the sand layer which can be estimated using Chapuis' formula (2004) displayed in equation 2.11.

As the permeability of the sand layer changes during piping, the minimum required head gradient for the onset of piping also changes. The threshold value decreases when the permeability increases due to an increasing porosity during piping. When the porosity decreases to a critical value, piping occurs. The iterative process of recalculating porosity and hydraulic conductivity is not included in the TPM. Instead, the critical porosity determined by Wang et al. (2014) is used to calculate the minimum required hydraulic gradient.

Chapter 3 – Validation transient piping model

In this Chapter the second research question will be treated: how does the modelled pipe length development compare to the IJkdijk measurements? A series of full-scale piping experiments are elaborated in Section 3.1. Section 3.2 explains the validation method and holds the validation results of the TPM.

3.1 IJkdijk full-scale experiments

It is rather difficult to predict the erosion velocity of piping. A case study is needed to validate the TPM predictions. Such a case will only be useful when the dike is actually threatened by piping, and information is available on for example dike configuration, soil compositions, sand boil observations, and hydraulic head measurements during the piping process.

In 2005 a large research program started to validate and possibly improve the Sellmeijer model. This program is part of a larger research program called Strength and Loading of Flood Defence Structures (SBW). Small-, medium- and full-scale experiments have been performed to study the process of piping in more detail. The Sellmeijer rule has been adapted based on several small and medium-scale tests and subsequently validated by the large-scale experiments. Four tests have been carried out in which is varied with fine or coarse aquifer sand and innovative monitoring techniques. These were carried out late 2009 at the location of the IJkdijk in the Northeast of the Netherlands (nearby Bad Nieuweschans). Here, the IJkdijk results will be used for calibration and validation of the TPM described in Chapter 2.

A schematic set-up of the IJkdijk test is presented in figure 3-1. First a 3 meter deep pit was excavated over a length of 33 meters and width of 15 meters. The bottom of the pit was covered with a watertight membrane. Subsequently the pit was filled with sand of homogeneous composition. A clay dike of 3.5 meters height and 15 meters width was built on top of the sand.

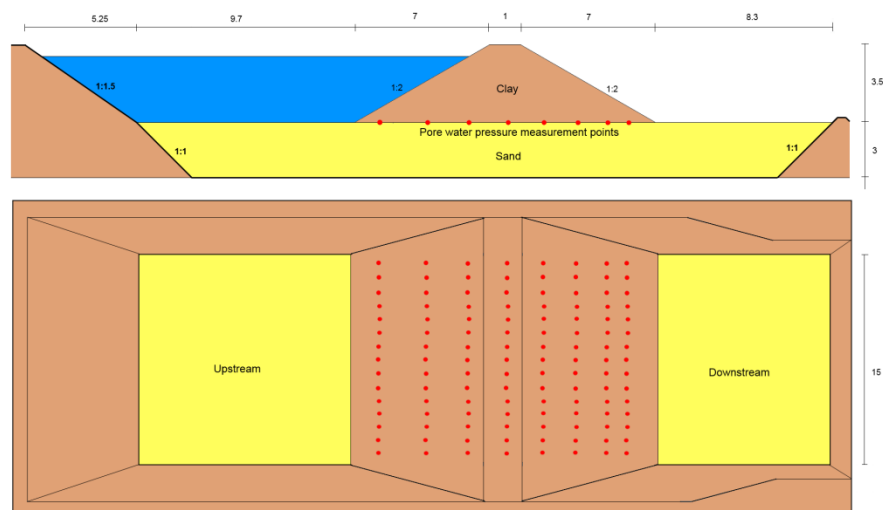


Figure 3-1 Cross section and top view of IJkdijk test site with a 15x8 matrix of water pressure gauges at the clay-sand interface (Van Beek et al., 2012)

At the upstream side of the dike, the water could be increased to 3 meters. At the downstream side the water level was kept constant by a small overflow approximately 0.1 meters above the sand. During the tests, the ΔH was increased 0.1 meter every hour. The first 15 minutes to raise the water and after that 45 minutes of observing if sand transport occurred. If this occurred, the ΔH was kept constant until the sand transport stopped. However, due to time constraints, in some cases the ΔH was increased despite of ongoing sand transport. Sand boils were removed to keep a constant hydraulic head gradient through the dike (Van Beek et al., 2012).

The erosion pattern is not observed directly, since the dike material is not transparent. Pore water pressure measurements, with a four second interval, have been used to assess pipe length. As the pore pressure in the pipe is somewhat smaller than its surrounding, a local pore water pressure decrease may indicate pipe formation (Sellmeijer et al, 2011). A matrix of gauges (eight by fifteen; see figure 3-1) was placed at the interface of sand and clay to be able to monitor the pipe formation. The upstream head was monitored with wells.

As the trajectory of piping is random, Sellmeijer et al. (2011) estimated pipe length by only using measurements of the eight rows at the location where the dike collapsed. This analysis was done with MATLAB scripts provided by Sellmeijer. An example of a situation during the second test is shown in figure 3-2 where the pipe length is 4.5 meters. The turquoise dots represent measured heads. The green regression line describes a fit of the likely behavior of the head, based on the measured heads. The red line represents the tangent line to the regression line at downstream (0 meters) and upstream side (15 meters) of the dike. The vertical part of the red line indicates the pipe length: 4.5 meter in test 2 at 70 hours. The blue line is the linear path between upstream and downstream head (Sellmeijer et al, 2011).

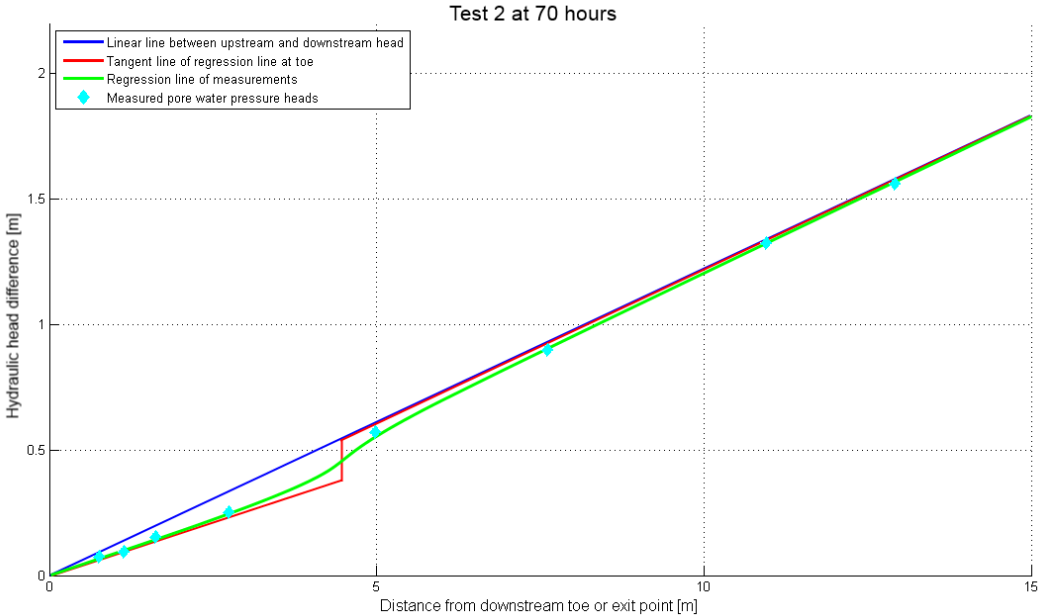


Figure 3-2 Water head below dike during test 2 after 70 hours (dike cross section where failure took place)

According to Sellmeijer et al. (2011) of the three full-scale tests the ΔH_{CRIT} of the tests with fine sand (first and third experiment) were well predicted by Sellmeijer's rule (table 3-1). In Appendix D a more detailed overview of the tests is given.

Table 3-1 IJkdijk full-scale experiment results

	Test 1	Test 2	Test 3	Unit
Dike height	3.5	3.5	3.5	m
Dike toe to toe width	15	15	15	m
Dike crest width	1	1	1	m
Dike length (parallel to seepage) / Seepage length	15	15	15	m
Dike width (normal to seepage)	16.9	19	16.9	m
Aquifer thickness	3	2.85	3	m
Aquifer length (parallel to seepage)	33	33	33	m
Aquifer width (normal to seepage)	9	11	9	m
Aquifer (initial) permeability	6.7	11.7	6.9	m/day
Aquifer initial porosity	0.4	0.3	0.3	-
Aquifer sand material	125-200	250-350	150-250	μm
Particle diameter d_{70}	180	260	180	μm
ΔH (first sand boil)	2.00	1.60	2.10	m
Predicted ΔH_{CRIT} (predicted to be critical)	2.15	2.25	2.10	m
Actual ΔH_{CRIT} (at moment of dike failure)	2.60	2.10	2.30	m
(1) Time to sand traces	5.3-20.0	2-26.3	24.6-42.5	hour
(2) Time to sand boils (piping)	20.0-95	26.3-94.5	42.5-79.2	hour
(3) Time to widening pipes	95-100	94.5-143	79.2-112	hour
(4) Time to dike failure	100	143	112	hour

In all tests four different phases were identified: sand traces, sand boils, pipe widening, and dike failure. Sand traces are spots of sand that suddenly appear without visual movement of sand. This occurred in an early stage of the experiment. When the ΔH was increased, sometimes sand boils appeared at the downstream side of the dike. The decreasing water pressure measurements from nearby pore water gauges indicated pipes. In the fine sand tests several sand boils occurred, while in the coarse sand experiment only one sand boil appeared. The sand transport continued at a stable pace of about 0.5 kg per hour.

Widening of the pipes started as soon as they reached the upstream side of the dike. This process moves from upstream to downstream side of the dike. The eroded sand is pushed through the pipe towards the downstream side and causes the pipes to clog. Therefore the sand boils stop to grow for some time. When the widening process reaches the downstream side of the dike two things may happen: the sand transport continues to increase until the dike collapses (tests 1 and 3) or the dike deforms (test 2) and causes the sand transport to decrease as the pipes will partially be closed. The IJkdijk experiments showed that the time necessary for the widening process can take up to a few days, which is longer than expected by Van Beek et al. (2011).

In all three tests the dike failed, which started with a large increase of turbulent flow and sand transport (mud flow). Before the toe of the dike eroded, cracks appeared in the downstream slope of dike. It is remarkable though that in the tests with fine sand a larger ΔH than the predicted ΔH_{CRIT} was needed for dike failure, while in the tests with coarse sand the dike failed before the predicted ΔH_{CRIT} was reached. According to Sellmeijer et al. (2011), the behavior of coarse sand is not yet well understood. A reason of less good prediction for coarse sand could be that fine sands develop as a front, while coarse sands tend to erode in smaller strips.

3.2 Transient piping model validation

3.2.1 Validation method

Here the three IJkdijk full-scale tests are used for validation. The TPM is validated on four aspects. The start time of piping [h], the time required to reach the critical situation [h], the sand transport rate [kg/h], and the cumulative sand transport [kg]. All four aspects have been measured during the IJkdijk full-scale experiments. The sand transport data is only available for the third test. In Section 3.2.2 the simulated results are compared with the IJkdijk measurements.

As mentioned before (Section 2.2.2), the neural networks, part of the TPM, are only valid for dikes that have a seepage length between 20 and 70 meters, an aquifer thickness in between 5 and 50 meters and aquifer permeability between 10 and 100 meters per day. The IJkdijk falls outside the valid range of the five networks. Hence, the three IJkdijk tests have been simulated in the Sellmeijer model to obtain five necessary parameters. The neural networks already have proven to emulate the Sellmeijer model (Section 2.2.2). Now the TPM itself will be validated.

Validation aspect 1: Start of piping

According to the TPM piping starts when the threshold pressure gradient at the tip of the pipe is exceeded (Section 2.2.3; equation 2.22). This simulated moment is compared with two measured moments. The start of piping is determined by Van Beek et al. (2012) by observing when sand boiling started. Moreover, the start of piping can also be estimated from pipe length records (thirty minutes interval).

Validation aspect 2: Time to reach critical situation

The model is also validated on when the critical situation has been reached. The TPM predicts the critical pipe length. The measured critical situation is, however, indicated as the moment pipe widening starts. The start of pipe widening is determined by Van Beek et al. (2012) based on the pore water pressure measurements. In between these two critical moments the pipe length has to develop the remaining seepage length (progressive erosion). The start of progressive erosion is not measured, so it unknown how long progressive erosion takes. Therefore in the validation analysis the start of progressive erosion (simulated) and pipe widening (measured) is considered as the critical situation.

The validation results of the first two aspects are presented in figures 3-3, 3-5, and 3-7. On the horizontal axis the time during the experiment is indicated. Four measured piping phases are indicated by vertical black lines in the figure: 1) sand traces, 2) sand boiling, 3) pipe widening and 4) dike failure. The first two phases are determined by observing sand boils. The third phase is determined by analyzing the pore water pressure measurements (pipe length measurements). Dike failure is visual observed and started.

The right axis represents the ΔH . The ΔH , represented by the blue solid line, is increased once in a while. The predicted ΔH_{CRIT} is depicted with a horizontal dashed blue line. The actual ΔH_{CRIT} at which the dike collapsed does not have to be the same as the predicted ΔH_{CRIT} .

On the left axis the pipe length is given up to 15 meters which equals the dike width (seepage length). The measured pipe length development is depicted by the fluctuating red line with black dots. The development of pipe length is predicted with the Sellmeijer model (green line) and the TPM (red line). The critical pipe length according to both models is presented with the horizontal green dashed line. The simulated pipe length is only plotted until the critical pipe length as beyond the predicted ΔH_{CRIT} the pipe length is not defined by Sellmeijer. The simulated erosion velocity by the TPM is presented in a separate figure.

Validation aspect 3 and 4: Cumulative sand transport [kg] and sand transport rate [kg/h]

During all experiments sand transport rate has been monitored by measuring the amount of sand that boiled out (in the sand boil) at the downstream end of the dike. Unfortunately only measurements of the third experiment are available. The validation results of the last two aspects are presented in figure 3-9. The amount of sand was measured and removed by hand to keep a constant hydraulic head gradient through the dike (Van Beek et al., 2012). The simulated (cumulative) sand transport rate is based on the pipe length and pipe height calculated by the TPM and the pipe length–volume relation determined by Sellmeijer et al. (2011) (Appendix B; equation B.14). With this information not only the sand transport can be estimated but also the width of the rectangular pipe in the two dimensional TPM. When the TPM predicts (cumulative) sand transport (rate) well it can be a useful tool to indicate piping in the field in an early stage.

3.2.2 Validation results

Test 1 with fine sand ($d_{70}=180 \mu\text{m}$)

In figure 3-4 and 3-5 the results of first IJkdijk test are presented. The measured pipe length shows more variation than the simulated pipe lengths. It seems that the measured pipe collapse and then grow again. This is not reflected by the TPM's pipe length as its pipe length can only increase.

The predicted ΔH_{CRIT} is smaller than actual ΔH_{CRIT} . This is a conservative (safe) prediction as the dike fails a larger ΔH . The predicted ΔH_{CRIT} coincides however with the observed start of piping as the measured pipe length does not increase and stabilize until the predicted ΔH_{CRIT} is loaded on the dike. Then the observed pipe length stabilizes at about 3.5 meters, which is half the pipe length by Sellmeijer. Once the predicted ΔH_{CRIT} is loaded on the dike it is remarkable that the pipe length stabilizes with some delay and then decreases. According to Sellmeijer the pipe should

progressively erode the remaining seepage length. Even when the ΔH is 2.5m, which is just above the predicted ΔH_{CRIT} but still below the actual ΔH_{CRIT} of 2.6m at which the dike failed, the pipe length retreats.

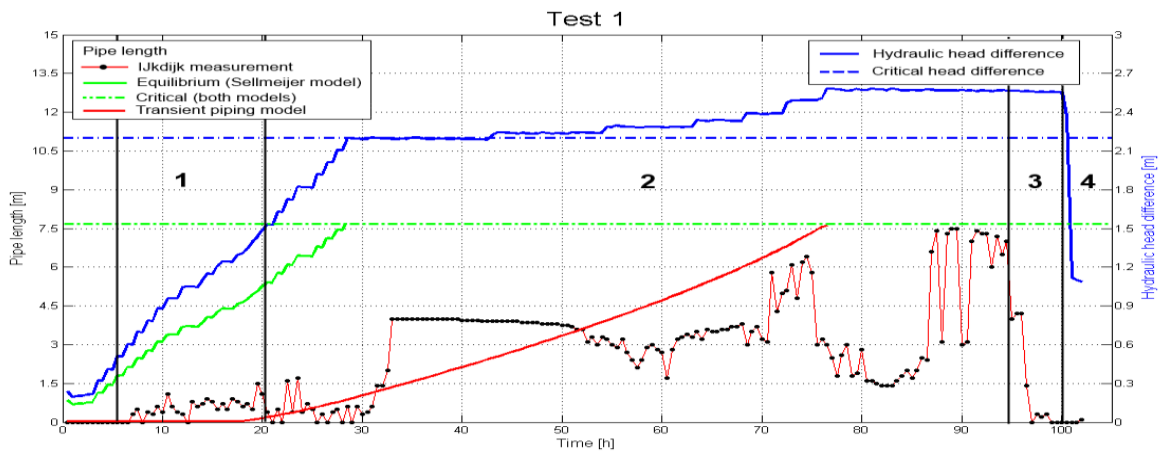


Figure 3-3 Pipe length development results of IJkdijk test 1 with four observed phases: 1) sand traces, 2) sand boiling, 3) pipe widening and 4) dike failure. The simulated pipe lengths stop when then reach the simulated critical pipe length indicating the critical situation

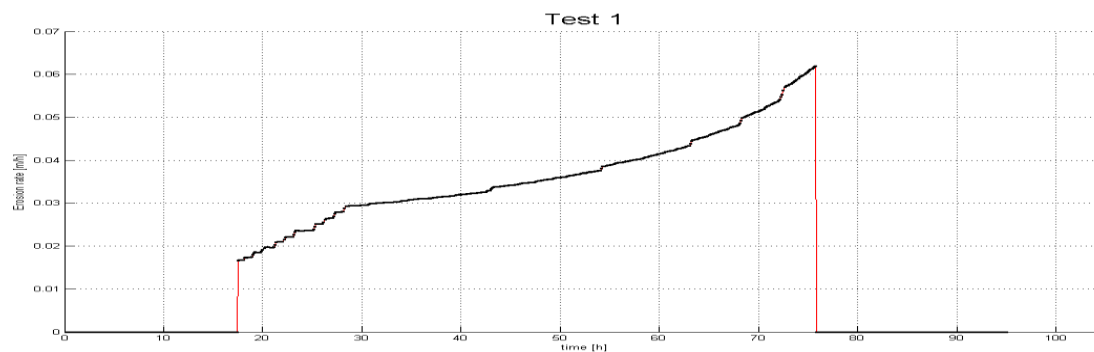


Figure 3-4 TPM simulated erosion velocity of IJkdijk test 1

Start of piping test 1

According to sand boil observations piping starts at 20 hours (phase two). When looking at the pattern of measured pipe length, one could indicate the start of piping at 30 hours (the last zero point). Therefore the actual start of piping is estimated to occur between 20 and 30 hours. The simulated start of piping by the TPM occurs at 18h (table 3-2) with a ΔH of 1.26 meters just before the observed start of piping (20 to 30h).

Time to critical situation test 1

The measured critical situation occurs at 95 hours since then pipe widening starts. The pipe widens when it reaches the upstream side of the dike. The measured pipe length drops because the pore water pressure measurements cannot be used anymore to determine the pipe length. Before pipe widening can occur the pipe has to develop all the way to the upstream side of the dike. Therefore it is remarkable that the measured pipe length never reaches 15 meters. The critical situation according to the TPM occurs at 75 hours. Then the critical pipe length of 7.5 meters has been

reached. This implies that progressive erosion of the remaining (15-7.5=) 7.5 meters of the seepage length required 20 hours.

Test 2 with coarse sand ($d_{70}=260 \mu\text{m}$)

In figure 3-5 and 3-6 the measured and simulated results of first IJkdijk are presented. The measured pipe length shows a dynamic trend likewise in the first test. The predicted ΔH_{CRIT} is too high (unsafe prediction) since the dike collapses before the predicted ΔH_{CRIT} is applied. The time to the critical situation cannot be compared since both models predict no dike failure and the critical pipe length has never been reached.

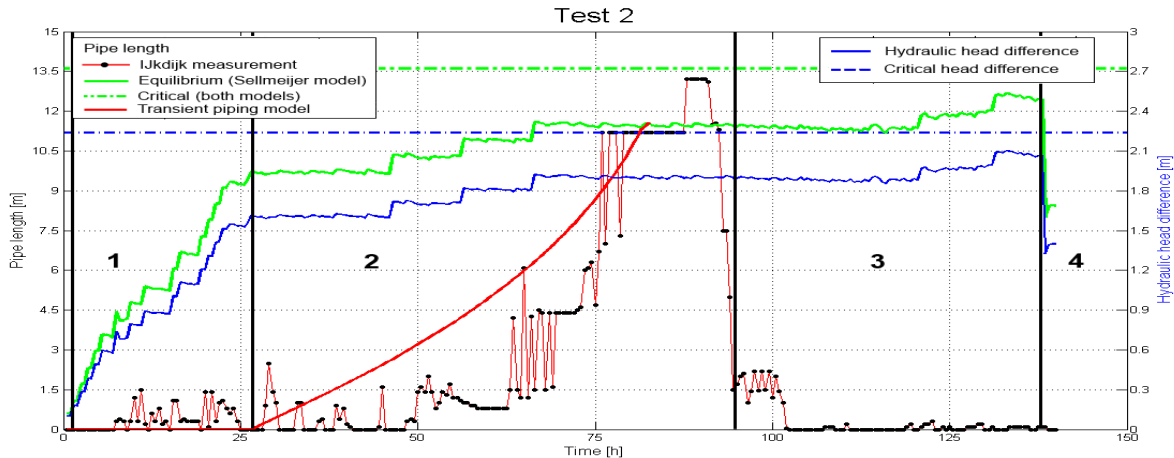


Figure 3-5 Pipe length development results of IJkdijk test 2 with four observed phases: 1) sand traces, 2) sand boiling, 3) pipe widening and 4) dike failure. The simulated pipe lengths do not reach the simulated critical pipe length (no critical situation) as the ΔH does not reach the predicted ΔH_{CRIT}

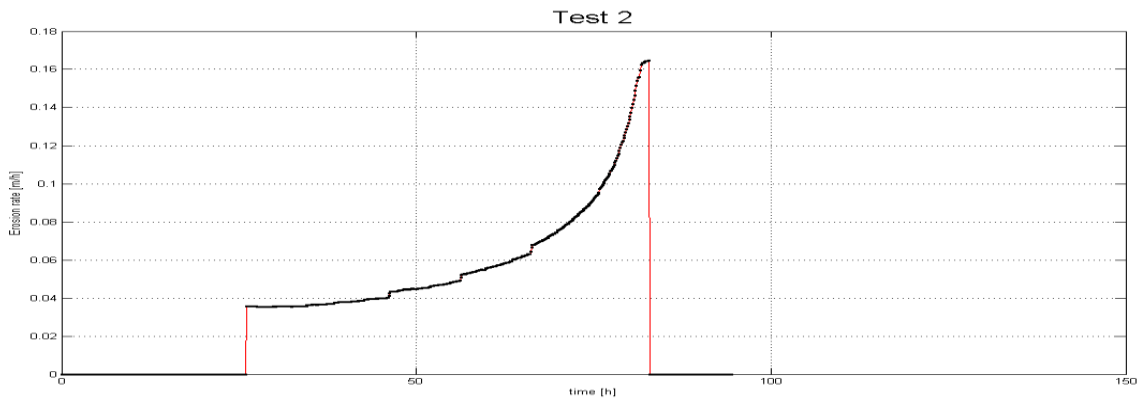


Figure 3-6 TPM simulated erosion velocity of IJkdijk test 2

Start of piping test 2

According to sand boil observations piping starts at 27 hours (phase two). According to the measured pipe length piping starts at approximately 50 hours. Therefore the actual start of piping is estimated to occur between 27 and 50 hours. The simulated start of piping by the TPM occurs (at 17h with a ΔH of 1.5 meters) at the start of sand boiling (27h).

Time to critical situation test 2

The measured critical situation occurs at 95 hours since then pipe widening starts. The predicted critical situation never occurs. Before pipe widening can occur the pipe has to develop all the way to the upstream side of the dike. It is remarkable that, just like in the first test, the measured pipe length never reaches the upstream side of the dike. Despite the dike failed, the TPM and the Sellmeijer model predicted that the dike would not fail. The predicted ΔH_{CRIT} is 10 centimeters above the actual ΔH_{CRIT} . Despite this dangerous prediction the Sellmeijer model predicts the critical pipe length of 13.5 meters well. The green and red solid lines do, however, not reach this length as the ΔH has not reached the predicted ΔH_{CRIT} .

Test 3 with fine sand ($d_{70}=180 \mu\text{m}$)

The third IJkdijk test is performed with the same aquifer sand as applied in the first test. In figure 3-7 and 3-8 the results of the third IJkdijk test are presented. The predicted ΔH_{CRIT} was 5 centimeters smaller than the predicted ΔH_{CRIT} in the first test, despite the same aquifer sand was applied. The different ΔH_{CRIT} prediction is because of different starting conditions (aquifer porosity and permeability). When the dike was loaded 60 hours with the predicted ΔH_{CRIT} , still no dike failure occurred. Due to time constraints during the experiment the ΔH was increased. In the IJkdijk reports it is stated that the dike would have failed in the end when the predicted ΔH_{CRIT} would have been applied (Sellmeijer et al. 2011). However, the pipe length measurements seem to indicate that the pipe length even retreats and stabilizes at a length of 1.5 meters.

Start of piping test 3

According to sand boil observations piping starts at 42 hours (phase two). When looking at the pattern of measured pipe length, one could indicate the start of piping at 38 hours (the last zero point). Therefore the actual start of piping is estimated to occur between 38 and 40 hours. When the predicted ΔH_{CRIT} is loaded on the dike for the first time then observed sand boiling starts. The measured pipe length increases and then remains constant for a while at one third of the Sellmeijer's predicted pipe length. It does, however, not develop till the critical pipe length.

The simulated start of piping by the TPM occurs at 23 hours with a ΔH of 1.23 meters: 2 centimeters smaller compared to the first test with the same sand but different starting conditions.

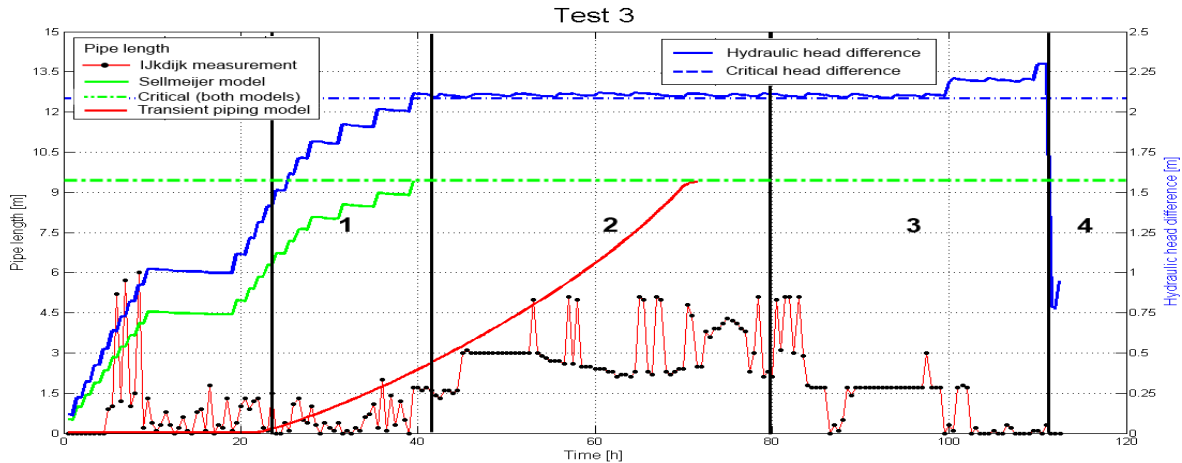


Figure 3-7 Pipe length development results of IJkdijk test 3 with four observed phases: 1) sand traces, 2) sand boiling, 3) pipe widening and 4) dike failure. The simulated pipe lengths stop when then reach the simulated critical pipe length indicating the critical situation

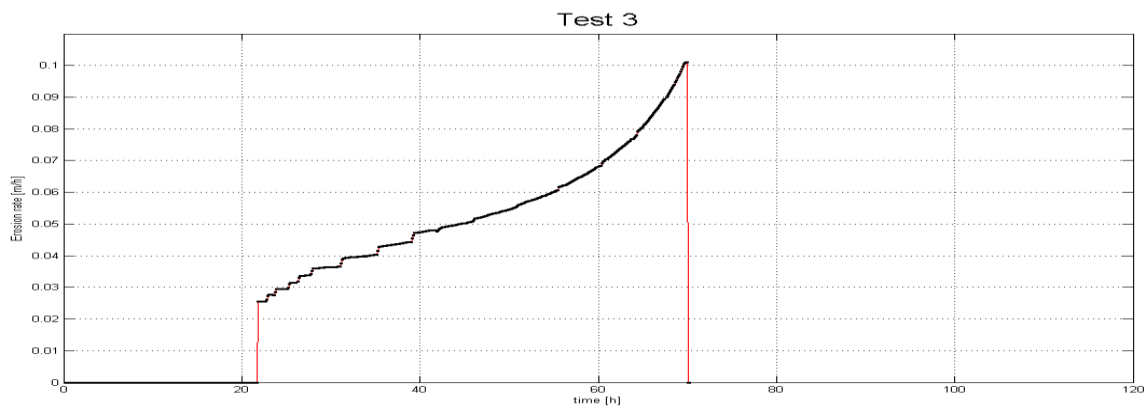


Figure 3-8 TPM simulated erosion velocity of IJkdijk test 3

Time to critical situation test 3

The measured critical situation occurs at 80 hours when pipe widening starts. Like in the first two tests the measured pipe length never reaches 15 meters but the dike fails anyway. This is likely due to that the pipe length cannot be estimated during progressive erosion. As the piping process is now speed up the pore water pressures perhaps fluctuate too much. This is also the case with pipe widening. The fluctuating pore water pressure measurements cannot be used to estimate the pipe length. Contrary to the first two tests, the observed pipe length does not reach the critical pipe length by far (4.5 meter difference). The critical situation according to the TPM occurs at 76 hours. Then the critical pipe length of 9.5 meters has been reached. This implies that progressive erosion of the remaining $(15-9.5=)$ 5.5 meters of the seepage length required 4 hours.

Cumulative sand transport [kg] test 3

Unfortunately only sand transport measurements of the third experiment are available. In figure 3-9 the sand transport of the third test is depicted. The red line with black dots represents the measured amount of sand downstream of the dike at the location where the dike failed. At 40 hours the predicted ΔH_{CRIT} is loaded on the dike. The pipe length measurements show that sand

transport starts almost as soon as the predicted ΔH_{CRIT} is applied (delay is approximately 2 hours). The start of sand transport coincides with the start of phase 2 in figure 3-9 which represents the observed start of sand boiling. The Sellmeijer model pipe length is the equilibrium pipe length, therefore the sand transport simulated by the Sellmeijer model can be seen as the amount of sand that is transported at most given a certain ΔH . Therefore the green line starts at the beginning of the experiment (without delay). The TPM predicts the start of sand transport 17 hours before the ΔH_{CRIT} is applied.

The cumulative amounts of transported sand at 80 hours predicted by both models are equal because their pipe lengths are then also equal. The measured cumulative amount of transported sand until pipe widening is 80 kg. The predicted cumulative amount of sand is 70 kg is (unsafely) underestimated by 13%.

Sand transport rate [kg/h] test 3

The slope of the lines indicate sand transport rate [kg/h]. The measured transport rate and the simulated rate by the TPM are similar (approximately 1 to 2 kg/h). However, at 60 hours the measurements show an intermezzo in the sand transport probably caused by pipe deformation or pipe clogging (Van Beek et al., 2012). When looking at the observed pipe length development in figure 3-7, one can see that the pipe length is decreasing at that moment. At 65 hours, the pipe length continues to increase and so does the measured sand transport in figure 3-9. It is remarkable that the observed pipe length already starts to retreat from 55 hours (figure 3-7) but this is not clearly indicated in the sand transport measurements (figure 3-9).

A reason why the simulated sand transport occurs too soon compared to the observed sand transport is due to the fact that the simulated line concerns sand transport at the tip of the pipe while the observed sand transport is at a set location at downstream side (pipe exit location). The sand that erodes at the tip of the pipe has to flow through the pipe towards the exit point where it is measured as actual sand transport. The distance between both points increases as the pipe length increases. When accounting for this the simulated line should have a less steep slope. In case it assumed that the sand particles travel through the pipe with the same velocity as the seepage velocity in the aquifer (critical velocity is 4,4 m/d at 70 hours), then the cumulative sand transport of 70 kg at 70 hours is delayed with 11 hours. This is closer to the observed cumulative sand transport. It should also be noted that the observed sand transport is the cumulative amount of sand that is eroded from from multiple pipes that merge into one pipe hole exit hole.

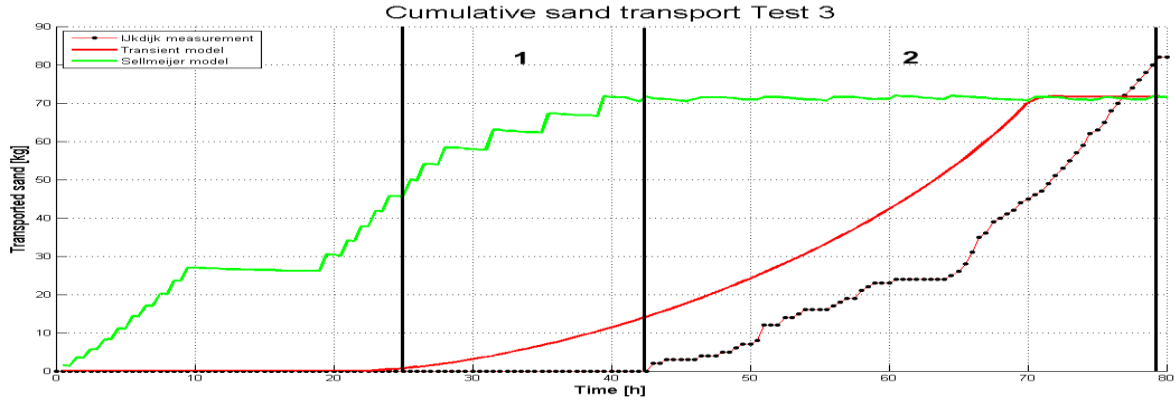


Figure 3-9 Cumulative sand transport at location of breakthrough in test 3 until pipe widening. Two observed phases are indicated 1) sand traces, 2) sand boiling

The sand transport of both models is calculated based on the pipe length-volume relation of Sellmeijer et al. (2011). This relation is determined by relating the observed sand transport to the measured pipe length in all three Ijkdijk tests. The pipe length-volume relation can also be used to determine the pipe width. In the Sellmeijer model and the TPM the pipe width is assumed to be infinitely wide (both 2D models). With use of the length-volume relation and the longitudinal pipe cross section, the uniform pipe width can be estimated and then compared to pipe width indications found in literature. In this way it is possible to check how realistic the assumed pipe height relation is. The uniform pipe width is calculated by dividing the pipe volume by the longitudinal cross section. The volume of the TPM's pipe at 80 hours is estimated to be (70 kg / 1650 kg/m³) = 0.042 cubic meters. The longitudinal cross section of the TPM pipe can be calculated by integrating the pipe height relation (equation 2.24):

$$\int_0^{l_{crit}} h_{max} \frac{\sqrt{l-x}}{\sqrt{l_{crit}}} dx = h_{max} \frac{2}{3} \frac{(l-x)^{\frac{3}{2}}}{\sqrt{l_{crit}}} = 0.0013 \text{ m}^2 \quad (3.1)$$

In which is:

- h_{max} [m] the maximum pipe height at exit point ($2 \cdot 10^{-4}$ meters)
- x [m] the distance along the pipe from exit point to tip of the pipe ($0 < x < l$)
- l [m] the pipe length at 80 hours (9.7 meters)
- l_{crit} [m] the critical pipe length in the third test (9.7 meters)

The uniform pipe width at 80 hours is calculated by dividing the pipe volume (0.042 m³) by the longitudinal cross section (0.0013 m²) and equals 32 centimeters which is wide compared to what was found in literature. Zhou et al. (2012) and Sellmeijer (1988) determined a pipe width of 3 to 5 centimeters and several centimeters respectively.

The pipe width overestimation is likely caused by underestimation of the longitudinal pipe cross section. The latter depends amongst others on the pipe height at the exit point when the critical situation is reached. A maximum pipe height at the exit point of 13 mm (instead of the used 2 mm) would result in a uniform pipe width of 5 cm at 80 hours. However, a 13 mm large

maximum exit hole pipe height results in a higher erosion velocity so that the predicted critical situation in the third test is reached 5 hours sooner compared to a pipe with a 2 mm maximum exit height. A maximum pipe height of 11 mm is large compared to what Van Esch & Sellmeijer (2012) assume to be a realistic value (2 mm). Since in all tests the pipe length prediction is reasonably well (Section 2.1.3) and a validated pipe volume-length relation (Sellmeijer et al. 2011) is used, it is assumed that sand transport is predicted reasonably well.

3.2.3 Validation conclusion

In this Section the validation results are summarized and a conclusion is drawn. Three full-scale tests were used to validate the TPM. Table 3-2 holds the validation results.

Table 3-2 Overview IJkdijk validation results

Test	Validation aspect	Measured based on		Simulated TPM
		Sand boils	Pipe length (pore water pressure measurement)	
1	Time to start of piping [h]	20.0	30.0	18
	Time to critical situation [h]	-	95.0	76
2	Time to start of piping [h]	26.3	50.0	26
	Time to critical situation [h]	-	94.5	Not reached
3	Time to start of piping [h]	42.5	38.0	22
	Time to critical situation [h]	-	79.2	71
	Sand transport rate [kg/h]	2.1	-	1.5
	Cumulative sand [kg]	80	-	70

The start of piping is well predicted by the TPM. Moreover, in all three tests a conservative (safe) prediction was obtained. In the third test the least good prediction was obtained: predicted start of piping occurs 15 hours before the actual start of piping (1 meter difference between ΔH), still the order of magnitude of the predicted start time is considered to be sufficient.

The time to the critical situation in the first and third test is well predicted by the TPM. The least satisfactory prediction differed 20 hours from the actual critical situation. Moreover, both predictions resulted in a conservative (safe) prediction. As for the second test the dike collapsed whereas it was predicted not to fail (also according to Sellmeijer). The actual ΔH_{CRIT} was (unsafely) overestimated by 15 centimeters. Overall, the critical time is predicted well for fine sands and for coarse sands a little unsafe outcome is obtained. In any case, the TPM will not predict dike failure when the Sellmeijer model predicts no dike failure.

The sand transport is only validated with the third test (only available validation data). The observed cumulative amount of transported sand (80 kg) at the moment the critical situation is reached is underestimated by 13%, which implies an unsafe prediction. The observed sand transport rate of 2.1 kg/h is (unsafely) underestimated by 25%. Overall, it can be concluded that the TPM is able to predict the start and the critical situation of piping, and the (cumulative) sand transport (rate) reasonably well. It will not predict dike failure when Sellmeijer declares the dike safe to piping.

Chapter 4 – Time dependent piping results

In this Chapter the third research question will be treated: When does piping result in progressive erosion considering dikes varying in aquifer permeability, aquifer thickness and seepage length? In Section 4.1 piping under a constant head difference is investigated. Section 4.2 involves piping under a changing head difference.

4.1 Time dependent piping with a constant head difference

For different dike configurations the possibility of dike failure by piping is investigated. For each dike one of the three dike parameters, seepage length (L), aquifer permeability (K), and aquifer thickness (D), was increased while the other two were kept at their low or high value to evaluate the effect. First the ΔH_{CRIT} is calculated and plotted for each combination of a specific parameter. Subsequently, the dike is loaded with its own constant ΔH_{CRIT} to investigate the critical time to progressive erosion. As a dike parameter (L, D, K) changes, the ΔH_{CRIT} also changes. One could argue that therefore the results of the four dikes are not comparable. Therefore the critical time is also indicated for dikes that are loaded with the highest ΔH_{CRIT} of all dikes configurations. By doing so, the direct relation between the seepage length and critical time becomes a bit clearer. The disadvantage of this approach is the difference between ΔH_{CRIT} of a dike and the larger applied ΔH (in the worst case $7.6 - 1.8 = 5.8$ meters. In that situation, the critical time is short. Combining the results of all three figures provides an overview of the dike parameter influence on the time dependency of piping.

4.1.1 Effect of seepage length with a constant head difference

Critical head difference

A larger seepage length requires the pipe to erode over a longer distance, therefore a larger seepage length results in a larger ΔH_{CRIT} (figure 4-1). According to the Sellmeijer model the relation is linear although not directly proportional. The slopes of the lines vary for the four different dikes. According to Sellmeijer, a dike with high permeability and large aquifer thickness is the most vulnerable to piping (the purple line has the lowest ΔH_{CRIT}).

Critical time under critical head difference

According to the TPM a dike with a low aquifer thickness and aquifer permeability is the most vulnerable to piping (the red line has the shortest critical time in figure 4-2). This dike is, however, loaded with a larger ΔH than the other three dikes. A larger ΔH implies a higher pressure gradient which increases the erosion velocity (Wang et al. 2014). The difference in critical time for dikes with large aquifer thickness is caused by a different ΔH_{CRIT} . The dike with low permeability (green line) has a larger ΔH_{CRIT} than the dike with high permeability (purple line) and therefore is simulated with a higher pressure gradient which increases the erosion velocity (Wang et al. 2014).

Figure 4-3 shows that the seepage length has almost no effect on the critical time in case of low aquifer thickness. According to the Sellmeijer model the critical pipe length is only

influenced by seepage length or aquifer thickness when one of these two has a high value. The critical pipe length remains half the seepage length in case of a large aquifer thickness (Appendix E). A longer critical pipe length requires the pipe to erode over a longer distance and therefore requires more time as figure 4-3 indicates.

Besides the critical pipe length the pressure gradient at the tip of the pipe affects the critical time. A longer seepage length decreases the pressure gradient at the tip of the pipe and therefore decreases the erosion velocity resulting in a higher critical time. This is shown by the dikes with low aquifer permeability (blue and red line figure 4-3). The critical time increases, while the critical pipe length remains the same (Appendix E). From figure 4-3 one can conclude that the critical pipe length influence is greater than pressure gradient influence on the critical time.

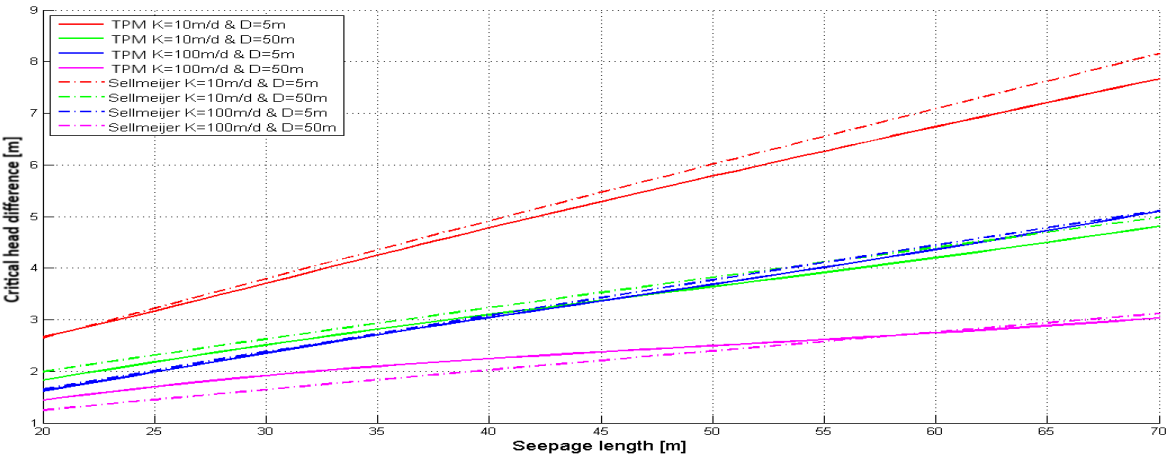


Figure 4-1 The ΔH_{CRIT} of four dikes with increasing seepage length

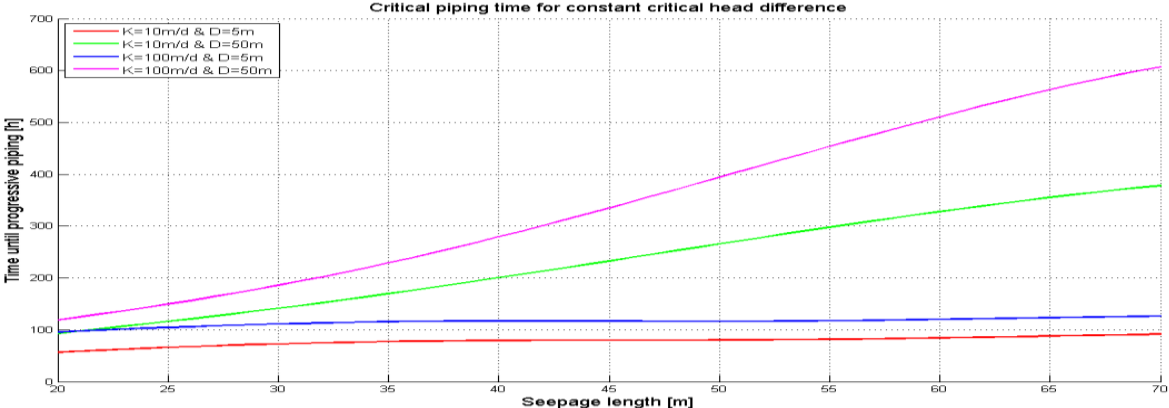


Figure 4-2 The critical time of four dikes (with increasing seepage length) loaded with their constant ΔH_{CRIT} which is different for each situation (see figure 4-1)

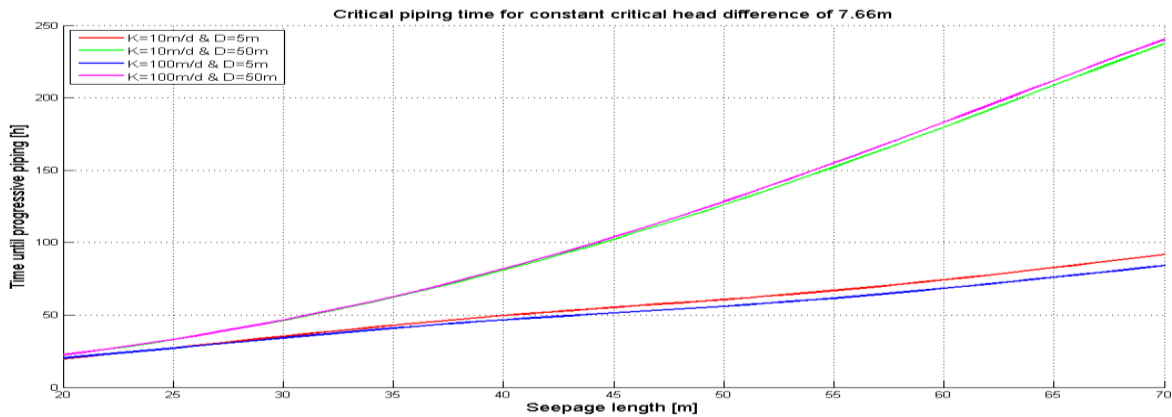


Figure 4-3 Critical time of four dikes (with increasing seepage length) loaded with a ΔH_{CRIT} of 7.66 meters

4.1.2 Effect of aquifer permeability with a constant head difference

Critical head difference

In figures 4-4 the ΔH_{CRIT} is given for four dikes scenarios with increasing aquifer permeability. The relation is almost linear and the ΔH_{CRIT} calculated by the TPM coincides well with the outcome of the current Sellmeijer rule. As the aquifer permeability increases, so do the aquifer grain sizes and aquifer porosity (Appendix F). As the lines decrease the ΔH_{CRIT} decreases as well indicating that the dike will become more vulnerable to piping. Permeability is mainly determined by the small grain size (d_{10}). This is generally accepted and confirmed by many researchers amongst others Terzaghi (1925), Hazen (1892), and Chapuis (2004). An increase of the smaller grain size (d_{10}), leads to a higher permeability, thus a higher erosion capacity, and therefore results in a smaller ΔH_{CRIT} (Sellmeijer, 1988). However, the neural networks in the TPM assume a uniformity coefficient of 1.7 (Section 2.2.4). So when the smaller grain size increases, also the larger grain size increases due to the uniformity coefficient. The resistance to piping is mainly determined by the larger grain size (Sellmeijer, 1988; Van der Zee, 2011). It turns out that the influence of the smaller grain size on the ΔH_{CRIT} is larger. Therefore the critical head drops for increasing aquifer permeability. The ΔH_{CRIT} is most sensitive (slope of lines) when the seepage length is large. Erosion has to take place over a longer distance, so the permeability has a larger distance to affect the pipe. The most vulnerable piping situation is for dikes with short seepage length and large aquifer thickness. How these two parameters influence piping is discussed in the next Sections.

Critical time under critical head difference

Figure 4-5 presents the time needed before the critical pipe length is reached (progressive erosion) for a constant ΔH_{CRIT} . For example, a dike with a seepage length of 20 meters, an aquifer thickness of 50 meters and aquifer permeability of 40 meters per day requires its ΔH_{CRIT} (4 meters) of 230 hours before the critical situation is reached. Below the curves, no progressive erosion will occur.

Figure 4-6 shows that aquifer permeability little affects the critical time in case of a small seepage length (green and red line). What is interesting is the hyperbolic shape of the critical time lines. At aquifer permeability of approximately 35 meter per day dike is the most vulnerable. It is

questioned why the critical time at a certain permeability increases. This is likely because of the how the porosity, particle sizes and permeability relate (Appendix F). The porosity is assumed to increase linear from 0.3 to 0.4 when the permeability increases from 10 to 100 m/d. Hence, the particle sizes increase asymptotic from low to high permeability according to Chapuis (2004). A higher porosity results in a longer critical time. As the particle sizes do not increase significantly, a longer critical time is the result when increasing the aquifer permeability. It would be interesting to see also how the critical time lines develop when the neural network in the TPM were trained with a constant porosity when the aquifer permeability increases. However, then new neural networks should be set up first. For a constant porosity the critical time likely decreases asymptotic when the permeability increases.

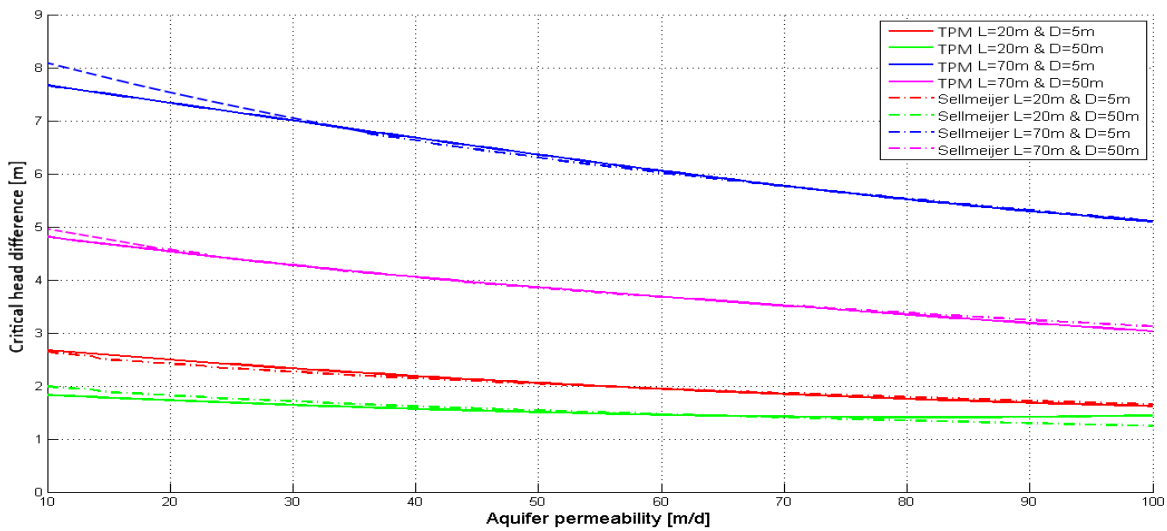


Figure 4-4 The ΔH_{CRIT} of four dikes with increasing aquifer permeability (d_{10} , d_{70} , n also change: Appendix F)

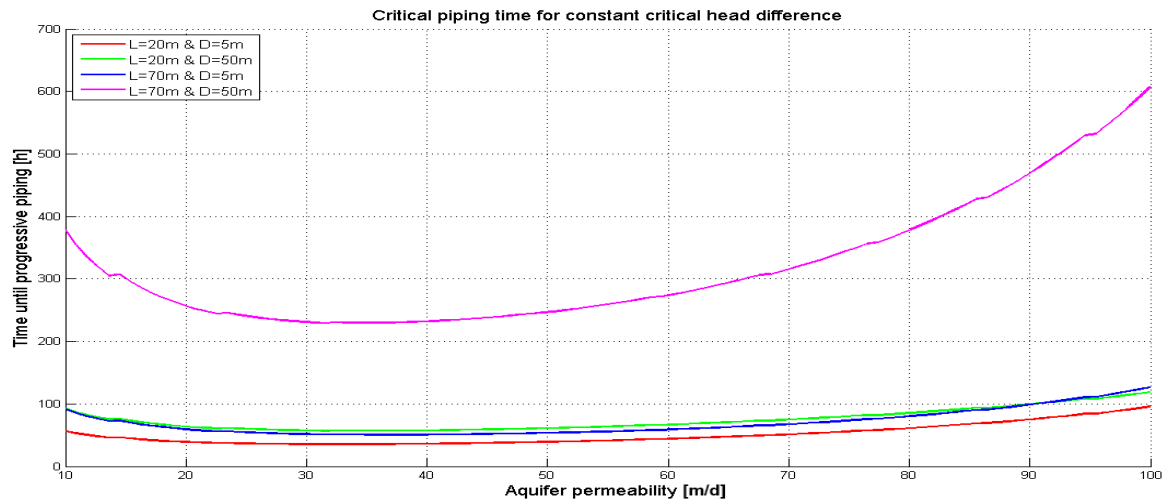


Figure 4-5 The critical time of four dikes, with increasing aquifer permeability (d_{10} , d_{70} , and n also change), loaded with their constant ΔH_{CRIT} which is different for each situation (see figure 4-4)

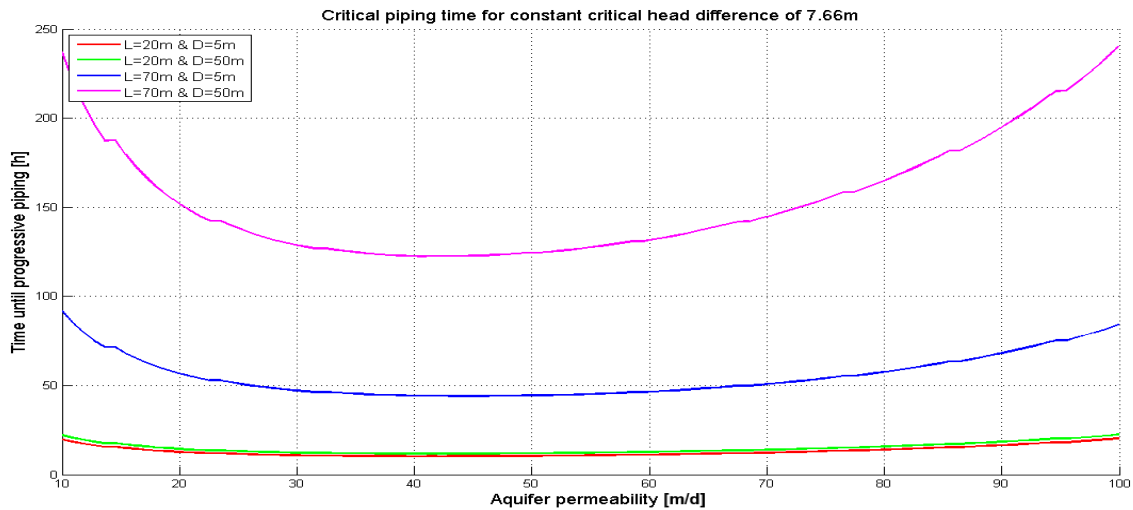


Figure 4-6 The critical time of four dikes, with increasing aquifer permeability (d_{10} , d_{70} , and n also change) loaded with a ΔH_{CRIT} of 7.66 meters

4.1.3 Effect of aquifer thickness with a constant head difference

Critical head difference

The aquifer thickness (and permeability) are decisive for the degree to which damping occurs of the outside water level (TAW, 1999). According to Darcy's law, the groundwater volume flux increases when the flow area (or aquifer thickness) increases with the same pressure gradient and aquifer permeability. A larger aquifer thickness allows the hydraulic pressure (of the river water level) in the aquifer to reach further landwards. The pressure head gradient at the exit point is therefore higher implying a higher driving force for piping to begin. So when the aquifer thickness increases, the ΔH_{CRIT} becomes smaller as indicated by the results figure 4-7. Contrary, a shallow aquifer has a high resistance to groundwater flow and leads to a larger ΔH_{CRIT} .

Critical time under critical head difference

The time dependent analysis shows again that the dike with a short seepage length and low permeability is the most vulnerable to piping (figure (4-8)). When all dikes are simulated with the same ΔH one can see that aquifer thickness does not influence the critical time in case the dike has a short seepage length. In Section 4.1.1 it was concluded that the seepage length had little influence on the critical time in case of a shallow aquifer. In figure 4-9 one can see that the aquifer thickness negligibly influences the critical time (with low seepage length). From this figure it appears that aquifer permeability does not affect the critical time. However, from the previous Section it is known that in between the low and high permeability the curve is hyperbolic and definitely influences the critical time line.

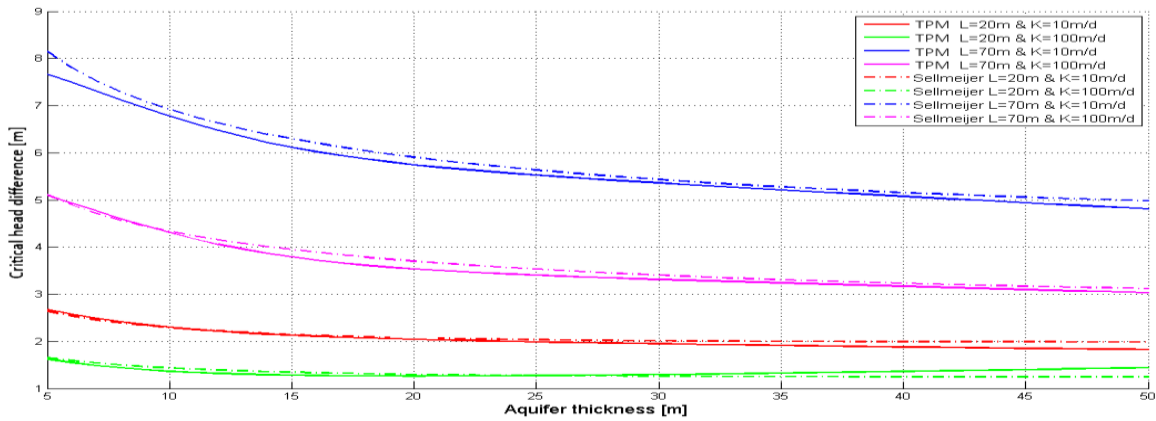


Figure 4-7 The ΔH_{CRIT} of four dikes with increasing aquifer thickness

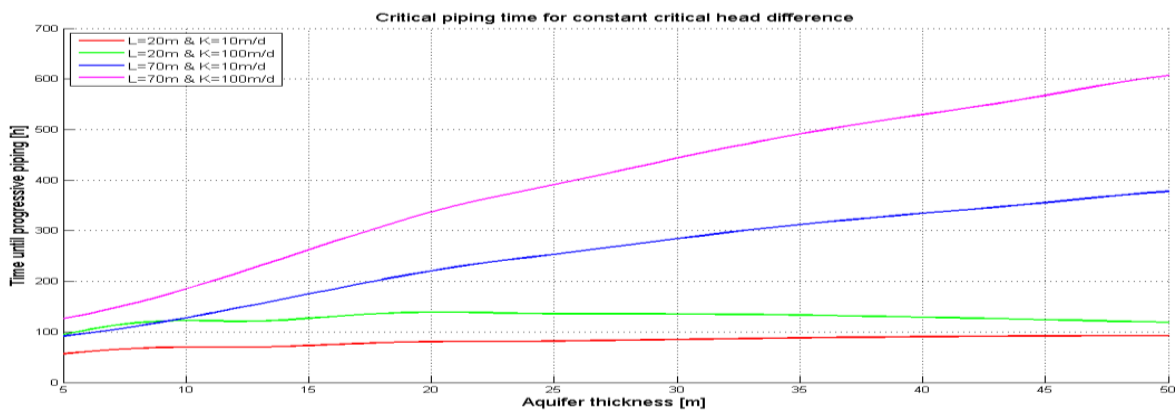


Figure 4-8 The critical time of four dikes (with increasing aquifer thickness) loaded with their constant ΔH_{CRIT} which is different for each situation (see figure 4-7)

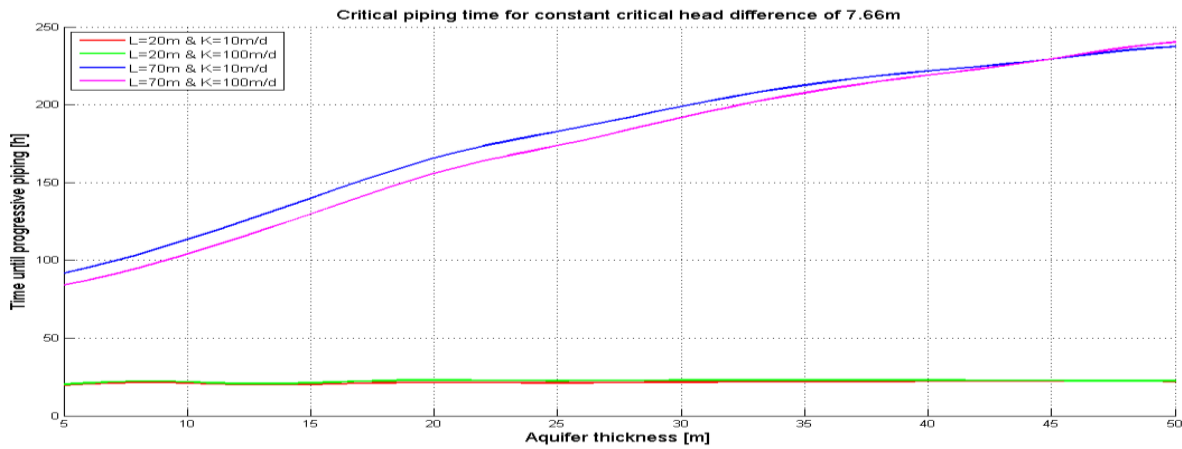


Figure 4-9 The critical time of four dikes (with increasing aquifer thickness) loaded with a ΔH_{CRIT} of 7.66 meters

4.1.4 Conclusion time dependent piping with constant head difference

When taking into account time-dependency, a different set of dike parameters makes the dike more vulnerable to piping (table 4-1). According to Sellmeijer (1988) the dikes with a high ΔH_{CRIT} have a low chance of dike failure. However, according to the TPM these are collapse sooner (when their loaded with their ΔH_{CRIT}) than dikes with a smaller (at first sight more vulnerable) ΔH_{CRIT} loaded with their ΔH_{CRIT} . The reason for this is that a larger ΔH increases the pressure gradient at the tip of the pipe and thus the erosion velocity (Wang et al. 2014).

Table 4-1 Dikes configurations with highest and lowest chance of dike failure based on ΔH_{CRIT} and time to progressive erosion

Piping analysis	Seepage length	Aquifer permeability	Aquifer thickness	Chance of dike failure
ΔH_{CRIT}	Short (20 m)	High (100 m/d)	Thick (50 m)	High (ΔH_c low)
ΔH_{CRIT}	Long (70 m)	Low (10 m/d)	Shallow (5 m)	Low (ΔH_c high)
Critical time	Short (20 m)	Low (10 m/d)	Shallow (5 m)	High (T_c short)
Critical time	Long (70 m)	High (100 m/d)	Thick (50 m)	Low (T_c long)

The TPM shows that the seepage length has almost no effect on the critical time in case of shallow aquifer thickness. The chance of dike failure does not change. This is remarkable since the seepage length significantly affects the ΔH_{CRIT} in case of a shallow aquifer: the chance of dike failure according to Sellmeijer decreases when the seepage length increases. The difference is caused by the critical pipe length (table 4-2): in case of a shallow aquifer the critical pipe length remains constant whereas in case of a thicker aquifer the critical pipe length increases (remains half the seepage length).

When not accounting for time-dependency, the ΔH_{CRIT} determines the chance of dike failure and the critical pipe length does not influence the chance of dike failure. In the time-dependent analysis a longer critical pipe length requires the pipe to erode over a longer distance and therefore requires more time.

Table 4-2 Chance of dike failure based on the ΔH_{CRIT} and the time to progressive erosion for an increasing seepage length

Piping analysis	Seepage length	Aquifer thickness	Critical pipe length	Chance of dike failure
ΔH_{CRIT}	Increasing	Shallow (5 m)	Constant	Decreasing
ΔH_{CRIT}	Increasing	Thick (50 m)	Increasing	Decreasing
Critical time	Increasing	Shallow (5 m)	Constant	Same chance
Critical time	Increasing	Thick (50 m)	Increasing	Decreasing

4.2 Time dependent piping with a variable head difference

In this Section the effect of a variable ΔH of one single wave on piping is investigated. A real dike is tested for piping with four different high water waves with a return period of 1250 years, 100 years, 10 years, and 1 year. The critical situation is indicated for each event with the same maximum ΔH and an increasing wave period.

The high waters have been schematized to triangular shaped hydrographs with a wave period and maximum ΔH . The river water level depends on the discharge-water level relation and is different for every location along the river. As the wave propagates downstream the wave is flattened out (diffusion process) and according to the Jones effect the front of the wave becomes a bit steeper due to flow resistance (Jones, 1916).

A primary dike nearby Tiel is chosen as a reference in this analysis: dike ring 43 km 917 along the Waal River, which branch of river Rhine. The dike protects its hinterland from floods with a return period of 1250 years. This dike reach has been chosen because of several reasons:

- The dike is located just upstream of the lower reach river area in the Netherlands: the wave is significantly flattened out but the tidal effect (from downstream) on the river water level is still negligible (Stijnen et al. 2006).
- The dike is located along a main river which was threatened by the high water waves in 1993 and 1995. The effect of high water waves will be investigated.
- The dike information required for the Sellmeijer model is available.

Two different wave shapes have been used: one with the maximum ΔH occurring at half the wave period and one with the maximum ΔH occurring at a third of the wave period (Jones effect). The most recent high water waves in the Netherlands show a more or less triangular shape (figure 4-10). The two high water waves can be characterized as events that have a return period in between once in 10 and once in 100 year (TAW, 1995). In 1993 and 1995 the main Dutch rivers dealt with extreme high water levels. Flood inundation almost occurred and a quarter million people and one million animals were evacuated (TAW, 1995). Figure 4-10 shows the water level at Tiel of both high water waves.

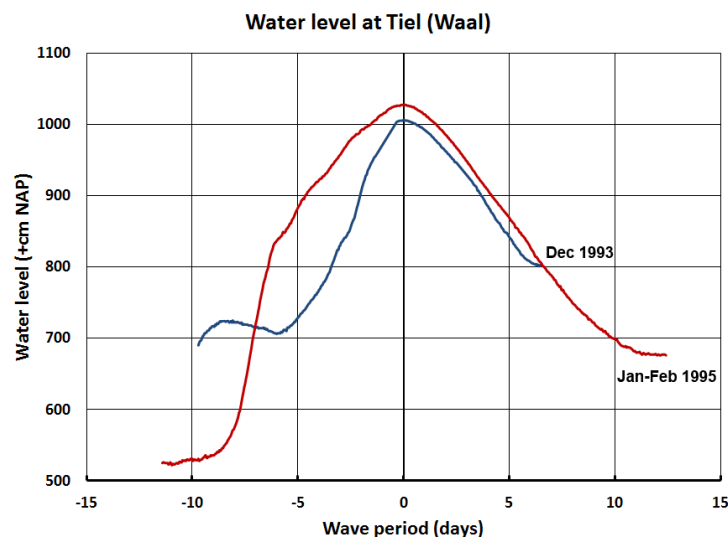


Figure 4-10 Observed flood events at Tiel (Waal) (Hydraulische randvoorwaarden primaire keringen, 2006; TAW, 1995)

In figure 4-11 a primary dike geometry near Tiel in 2006 is shown. According to the current Sellmeijer rule the dike is vulnerable to piping. The critical head difference is 4.7 m while the normative water level (MHW) results in a head difference of 7.1 m. One of the three dike parameters (aquifer thickness, seepage length, and aquifer permeability) is shifted likewise the piping analysis with a constant head difference in Section 4.1. The other two dike parameters are kept constant at the default value as indicated in figure 4-11. When these three parameters change, the ΔH_{CRIT} changes as well.

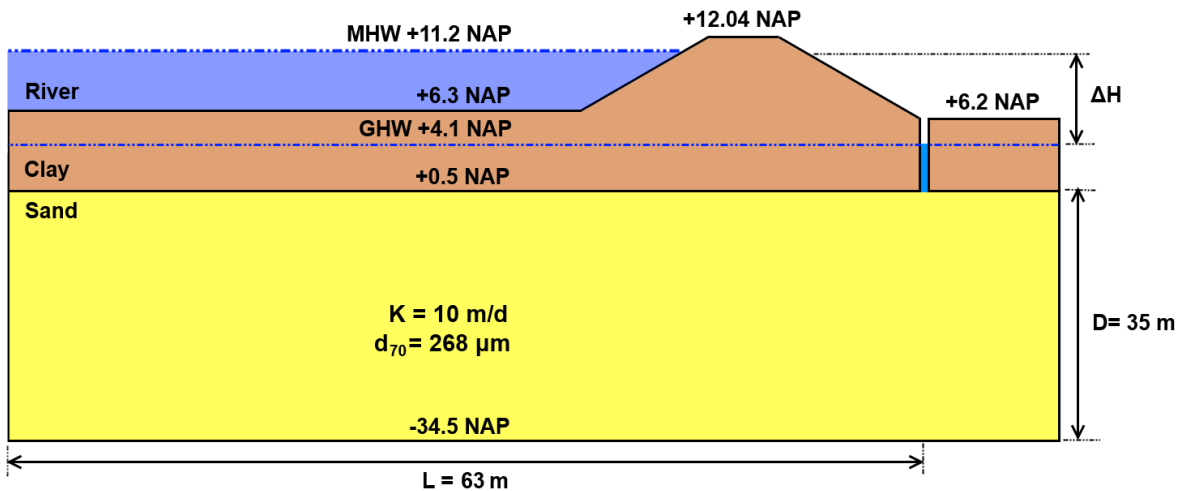


Figure 4-11 Primary dike cross-section dike ring 43 Tiel (Waal) km 917. Seepage enters the aquifer from the left, at the location where no clay blanket is situated, and flows until it reaches the crack channel at the inner toe of dike (polder side of the dike)

The average high water level (GHW = +4.1 NAP) is assumed to be the reference wave height (zero ΔH). A river water level above the normative high water level (MHW = +11.2 NAP) will lead to overtopping: water discharges over the top of the dike due to the wind. Therefore, the ΔH of the wave in the piping analysis ranges from 0 (GHW) to 7.1 meters (MHW). The four different high water waves are listed in table 4-3 and depicted in figure 4-12.

Table 4-3 Characteristics of the four tested hydrographs (Rijkswaterstaat, 2014; Stijnen et al. 2006)

High water wave [probability of occurrence per year]	Maximum river water level at Tiel [+m NAP]	Maximum ΔH [m]
1/1250	11.2 (= MHW)	7.10
1/100	10.45	6.35
1/10	9.55	5.45
1/1	8.00	3.90

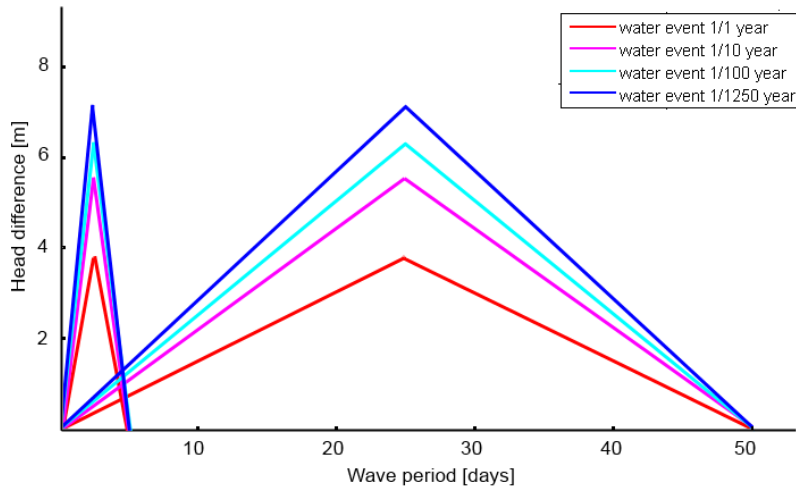


Figure 4-12 Four hydrographs nearby Tiel that will be investigated with a set maximum ΔH and variable wave period that will be increased from 0 days

4.2.1 Effect of seepage length with a variable head difference

In figure 4-13 the critical lines of the Tiel dike are presented considering four high water waves. The dike parameters as depicted in figure 4-11 are constant (aquifer thickness is 35 m and aquifer permeability is 10 m/d). The seepage length increases from 20 to 70 meters. Note that the y-axis represents the wave period and not the time to dike failure (which is sooner!). The critical wave period has been used so that different wave periods can be compared.

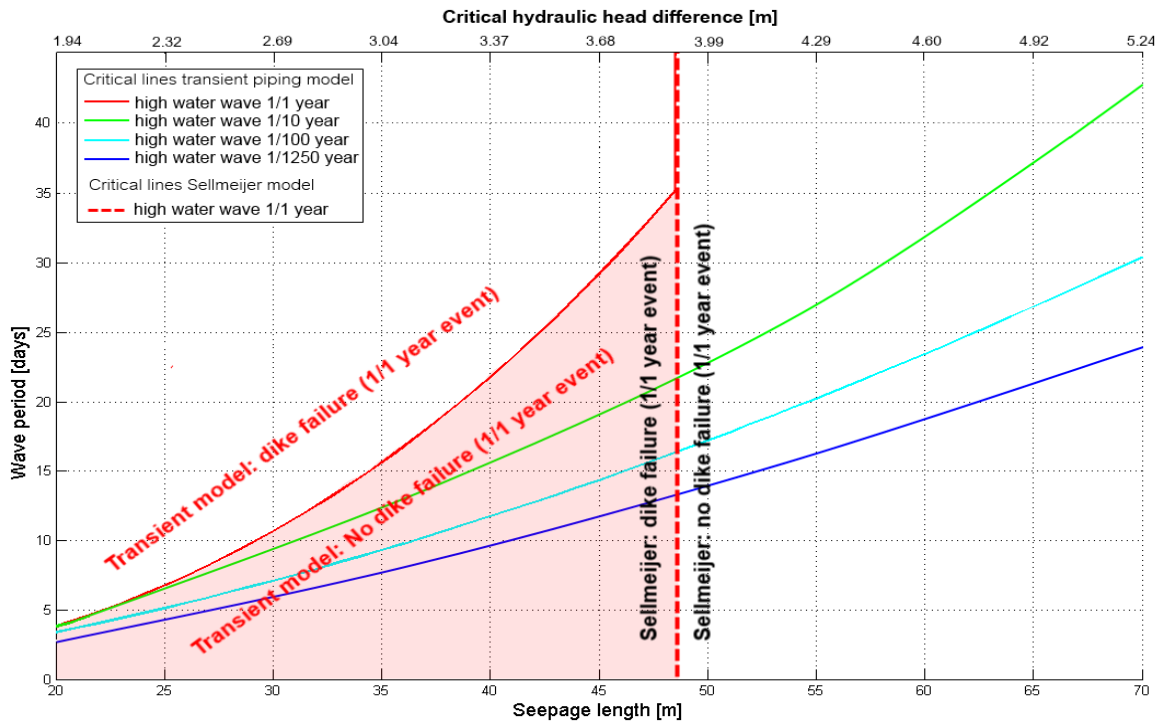


Figure 4-13 Critical lines of the Tiel dike (with aquifer thickness is 35 m and aquifer permeability is 10 m/d) for four high water waves

Sellmeijer

According to Sellmeijer the critical situation occurs when the ΔH_{CRIT} is reached. Therefore, the critical line according to Sellmeijer is vertical in this plot. The ΔH_{CRIT} increases when the seepage length increases (upper horizontal axis). The 1/1 year high water wave has a maximum ΔH of 3.9 m (related to a seepage length of 48.6 meters). Beyond this seepage length, the ΔH_{CRIT} is larger than the maximum ΔH of the 1/1 year event: dike failure cannot occur. For the 1/10, 1/100, and 1/1250 high water waves the critical seepage length is 72.8 m, 86.9 m, and 98.5 m respectively (outside the plotted seepage length range).

Transient piping model (TPM)

The TPM shows that it takes some time to reach the critical situation. The four curves are the critical lines according to the TPM. Below these lines no dike failure can occur. However, dike failure will occur when the dike is loaded with a longer wave period (represented by the area above the curve). Below the curves a discrepancy exists between Sellmeijer and the TPM. For the 1/1 year event this area is indicated by the red area: the dike fails when time dependency is not taken into account (Sellmeijer), whereas according to the TPM dike failure will not occur. The more frequent a high water wave is expected to happen the more likely it is that the TPM predicts no failure whereas Sellmeijer predicts dike failure. This only holds for high water waves with a return period of more than 10 years.

A high water wave that occurs once in 1250 years requires less time to reach the critical situation than the other high water waves. This is due to larger maximum ΔH (higher pressure gradient) and therefore higher erosion velocity. The time to the critical situation depends on the erosion velocity (with pressure gradient as the driving force) and the distance that has to be eroded (the critical pipe length). As the seepage length increases, the critical piping length also increases (Section 4.1.1). As more time is needed because of the longer distance that needs to be eroded, the critical wave period increases. This is the reason why the critical wave period lines increase when the seepage length increases. When the seepage length increases, the critical wave period lines of the four high water waves diverge. One can see that the critical wave period of the 1/1 high water wave increases faster than the critical wave period of the 1/1250 high water wave. This implies that the critical wave period with a low maximum ΔH is more sensitive to the critical pipe length and the steepness of the wave than the critical wave period with a high maximum ΔH .

When the Tiel dike has a minimum seepage length (20 m), none of the evaluated high water waves will lead to dike failure when the wave period is shorter than 2.5 days. When the Tiel dike has a maximum seepage length (70 m), no high water wave will lead to dike failure when the wave period is shorter than 24 days. The Tiel dike (in 2006) with a seepage length of 63 m would only fail due to piping when the normative wave period (1/1250 event) is longer than 20 days. A 1993 or 1995 high water wave (conservatively assumed to be comparable with a 1/100 high water wave) will lead to dike failure at Tiel when the wave period is longer than 25 days. From figure 4-10 it can be estimated that the wave period of the 1993 and 1995 high water was approximately 20 to 25 days (from reference water level of +4.1 NAP). Thus, according to the TPM both high water waves would not have resulted in dike failure, but a critical situation was almost reached. Likely the dike has been strengthened after the floods of 1993 and 1995. When accounting for

this, the critical situation might just have been reached during the high waters. It is unknown in literature whether at this location sand boils were observed.

4.2.2 Effect of aquifer permeability with a variable head difference

In figure 4-14 the critical lines of the Tiel dike are presented considering four high water waves. The aquifer thickness is 35 m and seepage length is 63 m (figure 4-11), while the aquifer permeability increases from 10 to 100 m/day.

Sellmeijer

The ΔH_{CRIT} decreases when the aquifer permeability increases. The 1/1 year high water wave has a maximum ΔH of 3.9 m (related to a permeability of 42.1 m/d). When the maximum ΔH is below the ΔH_{CRIT} no dike failure can occur. Hence, the 1/1 year event will not lead to dike failure for lower aquifer permeability than 42.1 m/d represented by the red vertical 1/1 year line). For the 1/10, 1/100, and 1/1250 waves the critical aquifer permeability is 7.1 m/d, 4.5 m/d, and 3.1 m/d respectively which are all outside the plotted permeability range.

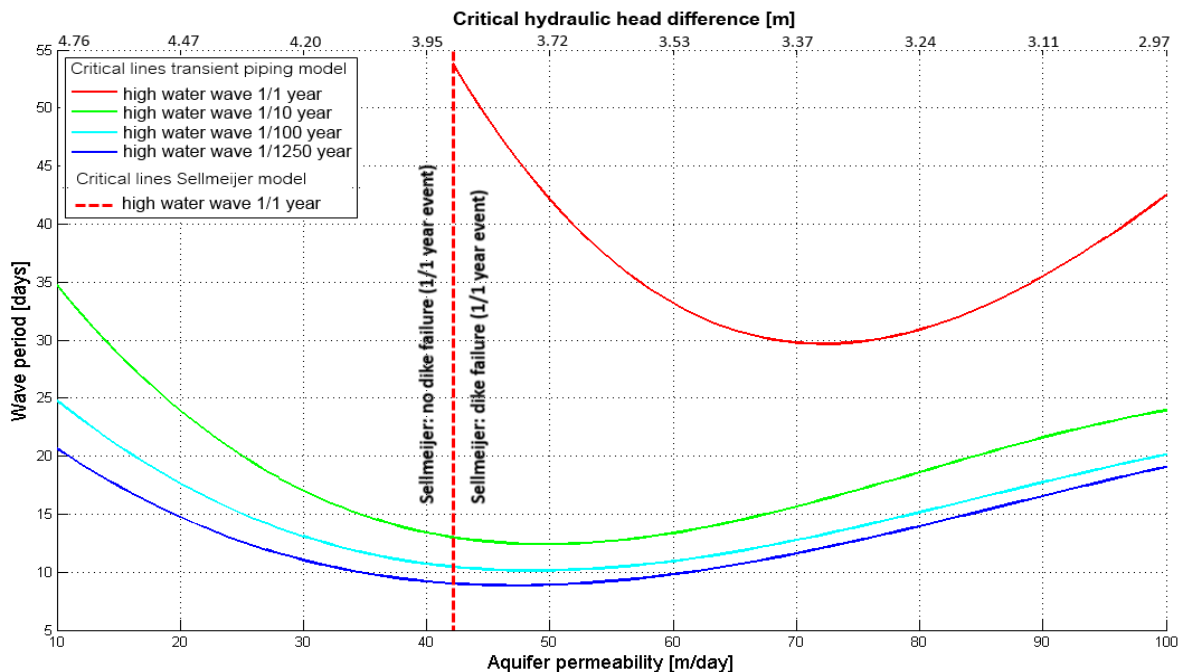


Figure 4-14 Critical lines of the Tiel dike (with seepage length is 63 m and aquifer thickness is 35 m) for four high water waves

Transient piping model (TPM)

The four curves are the critical lines according to the TPM. Below these lines no dike failure can occur. Likewise with the constant ΔH analysis, when the aquifer permeability increases, the required wave period for dike failure first decreases and then increases. When the aquifer permeability increases, the critical time line first decreases and then increases. This also occurred in the constant ΔH analysis (Section 4.1.2). However, for the 1/1 high water wave with the lowest maximum ΔH the minimum increases to higher aquifer permeability. This is because the TPM's

pipe length is stopped (slowed down) by the equilibrium curve before the peak of the wave occurred. Dike failure takes place after the peak of the wave. As for the other high water waves, the pipe length is not slowed down since a larger maximum ΔH and shorter wave period results in a “steeper” equilibrium curve.

The Tiel dike has an aquifer permeability of 10 m/d so no high water wave will result in dike failure when the wave period is shorter than 20 days. This is the same as in figure 4-12 with the actual seepage length of the Tiel dike of 63 m. The Tiel dike with a permeability of 50 m/d is the most vulnerable to piping. However, for the 1/1 year high water wave, the most vulnerable dike has an aquifer permeability of 70 m/d. No high water wave shorter than 5 days will lead to dike failure. The flood of 1995, comparable to approximately a 1/100 high water wave, would have led to dike failure when the wave period was longer than 25 days. This was also concluded in Section 4.2.1.

4.2.3 Effect of aquifer thickness with a variable head difference

In figure 4-15 the critical lines of the Tiel dike are presented considering four high water waves. The aquifer permeability is 10 m/d and the seepage length is 63 m while the aquifer thickness increases from 5 to 50 m.

Sellmeijer

When the aquifer thickness increases, the ΔH_{CRIT} decreases (Section 4.1.3) which can be seen on the upper horizontal axis of figure 4-10. The 1/10 year high water wave has a maximum ΔH of 5.45 m (related to an aquifer thickness of 16.5 m). When the maximum ΔH is below the ΔH_{CRIT} no dike failure can occur. Hence, the 1/10 wave will not lead to dike failure for a smaller aquifer thickness than 16.5 m). For the 1/1, 1/10, 1/100, and 1/1250 high water waves the critical aquifer thickness is 72 m, 16.5 m, 8.5 m, and 4.5 m respectively. The critical lines of the 1/1 and 1/1250 waves are not depicted as they are fall outside the plotted range.

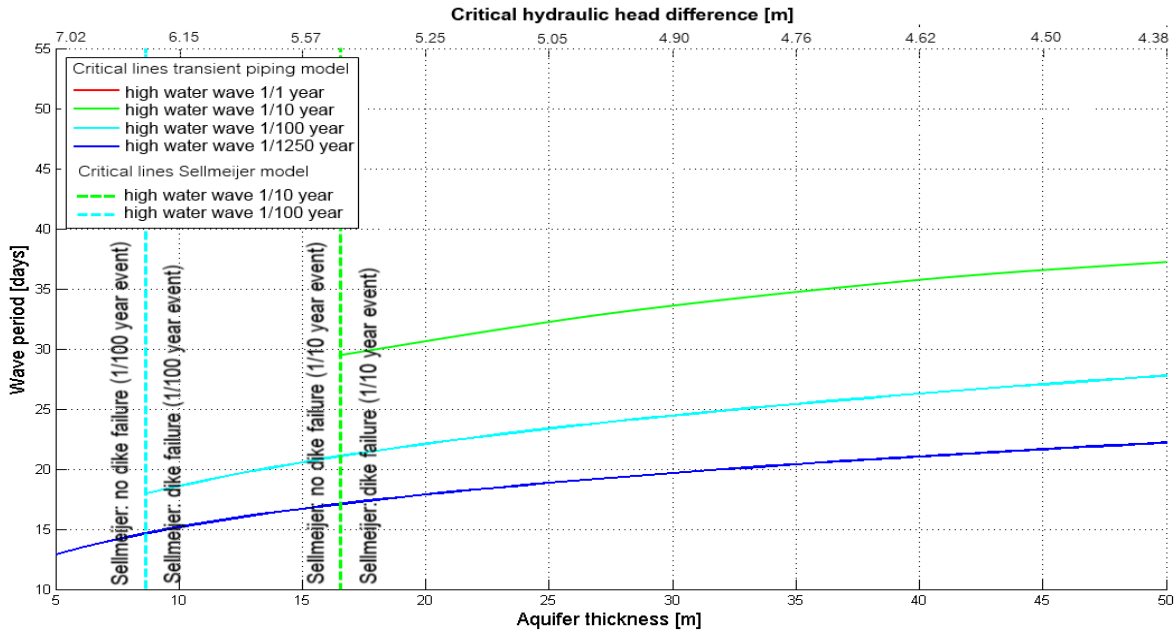


Figure 4-15 Critical lines of the Tiel dike (with seepage length is 35 m and aquifer permeability is 10 m/d) for four high water waves. The 1/1 high water wave is not indicated as it cannot lead to dike failure for an aquifer thickness smaller than 72 meters

Transient piping model (TPM)

According to the TPM dike failure cannot occur below the curve. According to the Sellmeijer model dike failure occurs on the right side of the vertical critical line, so below the curves a discrepancy exists between Sellmeijer and the TPM. The more frequent a high water wave is expected to happen the more likely it is that the TPM predicts no failure whereas Sellmeijer predicts dike failure. This only holds for high water waves with a return period of more than 10 years. Concerning high waters that occur 1/1250 year the possibility of a different prediction by Sellmeijer and the TPM is the smallest. This is a worrying conclusion at first. However, high water waves mainly occur along the main rivers where dikes are designed to protect against floods that occur 1/1250 year. A possible wrong prediction by Sellmeijer, dike failure while the dike would not fail when accounting for time dependency, is relatively small according to the TPM.

4.2.4 Effect of wave steepness under same wave period

Also waves with the maximum ΔH occurring at 1/3 and 2/3 of the wave period have been investigated. The maximum ΔH of the wave was kept constant (each high water waves has its own maximum ΔH), while the wave period was increased. The Tiel dike (figure 4-11) has been used in the analysis. In the upper graph of figure 4-16 the three wave types are presented for a 1/1250 high water wave. The ΔH_{CRIT} of the Tiel dike is 4.7 meters. The lower graph presents the equilibrium pipe length and the simulated pipe length for both high water waves.

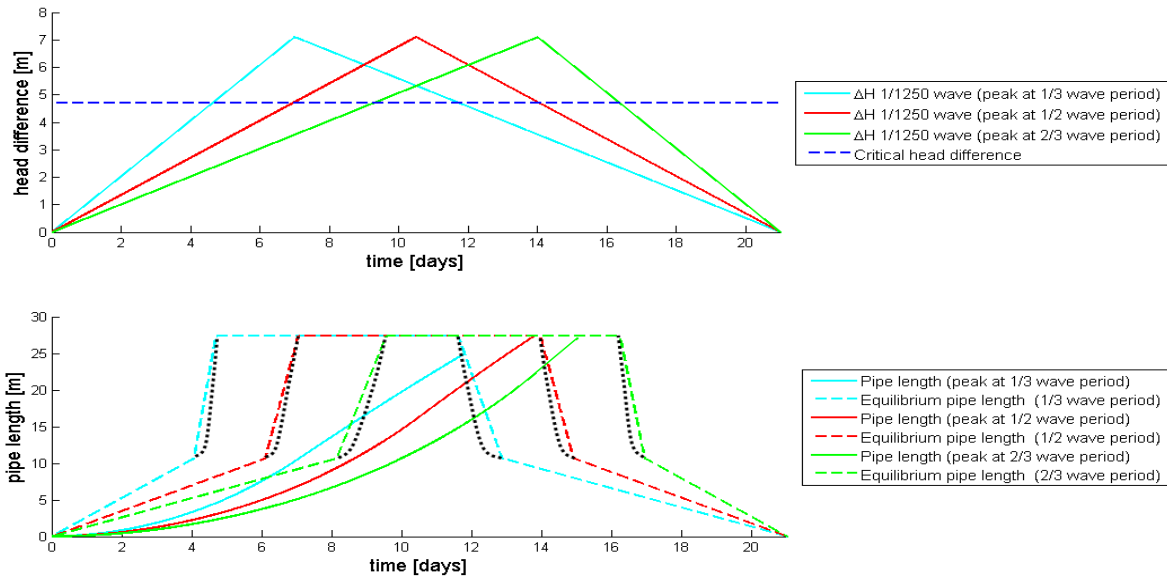


Figure 4-16 Wave steepness and its influence on erosion velocity. In the upper graph two waves with the same volume are plotted. In the lower graph the equilibrium pipe length (dashed line) and pipe length (solid line) is plotted. A part of the Sellmeijer model equilibrium curve (black dashed line) is simplified to a linear line in the TPM. The equilibrium pipe length reaches the critical pipe length (27 m) once the ΔH reaches the ΔH_{CRIT} (4.7 m)

Figure 4-16 shows that once the ΔH exceeds the ΔH_{CRIT} the equilibrium pipe length equals the critical pipe length (27 m) and stops increasing. The bump in the equilibrium pipe length is due to the simplification of the Sellmeijer model's equilibrium pipe length to two linear lines (Section 2.2.2). The part of the Sellmeijer model equilibrium pipe length that is simplified is depicted with the black dotted line.

It was expected that a faster increase of ΔH (the 1/3 wave) would result in a higher erosion velocity and therefore a smaller critical time. However, this turned out to be different according to the TPM. Given a maximum ΔH , the wave period of a 1/3 wave needs to be longer than the wave period of a 1/2 wave to result in dike failure. This applies for all high water waves even for short wave period with a high maximum ΔH . Despite the higher erosion velocity there is not sufficient time to reach the critical pipe length because the equilibrium pipe length of the 1/3 wave starts to decrease sooner than the 1/2 wave. The critical wave period of the 1/3 wave is longer than the critical wave period of the 1/2 wave. The high water wave with its wave peak at 2/3 of the wave period reaches the critical situation. When the wave period would be decreased with one day, the critical situation would still occur. The critical wave period of the 1/2 wave is longer than the critical wave period of the 2/3 wave.

It can be concluded that for a given wave period the later the wave peak, the more likely the critical situation will be reached.

4.2.5 Conclusion time dependent piping with variable head difference

Three main conclusions can be derived for piping with variable ΔH . The longer the wave period the smaller the maximum ΔH can be for progressive erosion to occur and to result in dike failure. Also a wave with a larger maximum ΔH required a shorter wave period to reach the critical situation. This is due to larger maximum ΔH (higher pressure gradient) and therefore higher erosion velocity.

The more frequent a high water wave is expected to happen the more likely it is that the TPM predicts no failure whereas Sellmeijer predicts dike failure. This only holds for high water waves with a return period of more than 10 years. Concerning high waters that occur 1/1250 year the possibility of a different prediction by Sellmeijer and the TPM is the smallest.

The critical wave period depends mainly on the critical pipe length and on the erosion velocity. The latter is dependent amongst others on the steepness of the wave. The steeper the front of the wave, the higher the erosion velocity the sooner the critical situation is reached. When the wave period increases and the maximum ΔH remains the same, the steepness of the wave decreases: the ΔH (and thus the pressure gradient) increases slower. Therefore the erosion velocity is lower and yet more time is needed to reach the critical situation.

When the peak of the wave is sooner, then the ΔH may drop too soon preventing the pipe length to reach the critical pipe length. It can be concluded that for a given wave period the later the wave peak, the more likely the critical situation will be reached.

Chapter 5 - Discussion

In this Chapter the fourth research question will be treated: What is the added value of time-dependent piping analysis by the transient piping model compared to the current piping assessment? The model assumptions, limitations and uncertainties are discussed in Section 5.1, 5.2 and 5.3 respectively. In Section 5.4, the processes that have not been modeled, but do have an impact on the results, are discussed. In Section 5.5, the results found in this study are compared to results found in literature. Finally in Section 5.6, the added value of the TPM is described. The discussion is used to formulate the recommendations.

5.1 Model assumptions

Linear pressure distribution in the aquifer

In the TPM the pressure head along the clay-sand interface is assumed to develop linearly, from the pressure head related to river water level at the outer dike toe to zero at the inner dike toe. The linear pressure assumption affects the pressure gradient at the tip of the pipe which determines the erosion velocity: for a certain ΔH it is irrelevant whether the river water level is increasing and decreasing at that moment. Due to the linear pressure assumption, there is no difference between increasing and decreasing river water level on the pressure distribution along the interface. In reality this is different: The hydraulic pressure distribution along the clay-sand interface is affected by the permeability: low permeability delays the hydraulic pressure propagation (TAW, 1994). An increasing river water level would result in a lower pressure gradient at the tip of the pipe than assumed. On one hand, the TPM (safely) overestimates the actual erosion velocity when the head difference increases. On the other hand, the TPM (unsafely) underestimates the actual erosion velocity when the head difference increases. For a constant ΔH the issue does not influence the simulated erosion velocity.

Equilibrium pipe length

The simulated pipe length cannot exceed the equilibrium pipe length determined by Sellmeijer who related all ΔH below the ΔH_{CRIT} to different equilibrium pipe lengths (the equilibrium curve). The simulated erosion velocity is set to zero in case the updated pipe length exceeds the equilibrium length. This implies that for a given ΔH the TPM never will predict a less conservative (more dangerous) pipe length than the Sellmeijer model does. The Sellmeijer model is a valid model, generally accepted and used in design practice. The equilibrium curve of the Sellmeijer model was simplified to two linear lines in the TPM. The critical pipe lengths of both models still share the same ΔH implying that the TPM can only simulate dike failure when the Sellmeijer model simulates dike failure.

Pipe height

The model is two dimensional and the cross-sectional shape of the pipe, and thus its volume is not included in the TPM. The pipe height is determined based on observations by Sellmeijer: “from the pipe tip the pipe height steeply increases and then remains rather constant towards the exit point.

A realistic exit point pipe height is two millimeters". An asymptotical pipe height relation was adopted based on Van Esch & Sellmeijer (2012). During the validation of the TPM on sand transport it was concluded that the actual longitudinal cross section of the simulated pipe probably is underestimated. A larger longitudinal pipe cross section leads to a higher erosion velocity. Hence, the actual erosion velocity is (unsafely) underestimated which implies an (unsafe) overestimation of the actual time to the critical situation. The TPM validation results show, however, that the time to the critical situation is (safely) underestimated.

The pipe height at the exit hole is assumed to increase when the pipe length increases, to a maximum when the critical pipe length is reached. The initial pipe length has a small pipe height at the exit point, so small that it is physically impossible for the coarse grains to pass through the pipe. These coarse grains are only able to erode when the pipe length increases. According to Sellmeijer the pipe length increases when the 70 percentile of the grain diameters (d_{70}) of aquifer particles is able to erode. This is a theoretical based assumption. In practice it is unknown if the pipe length can increase when only the small grains erode (Sellmeijer, 1988).

Wang et al. (2014) parameters

In this study all piping simulations have been carried out with one value for the critical aquifer porosity, at which piping occurs ($n = 0.45$). Wang et al. (2014) state that for most natural soils the maximum porosity is 0.41-0.44. They adopted a critical porosity of 0.45. Den Rooijen (1992) states that the packing is dependent on porosity and the uniformity coefficient. Rough indications are - for uniform sands ($U < 2$) and a pore content larger than 0.39 the packing is loose. For sand with a uniformity coefficient of about 10 the pore contents which indicate the transition between normal and loose packing is 0.33. For a still greater uniformity coefficient ($U = 40$), the pore content at which the packing becomes loose is 0.32. Overall, according to literature a critical porosity of 0.45 is a high value. Given a certain initial aquifer porosity, the higher the critical porosity the longer it takes before piping starts. Therefore the TPM might (unsafely) overestimate the time to the critical situation.

The TPM used the same erosion coefficient ($C_3 = 0.3$) that was adopted by Wang et al. (2014). Midgley et al. (2012) and Fox et al. (2007) reported a range of 0.027-0.65 m^3/m^3 for C_3 in their experiments. A higher erosion coefficient results in higher erosion velocity. Compared to the range defined by Midgley et al. (2012) and Fox et al. (2007), the used erosion coefficient is low. Therefore the TPM might (unsafely) underestimated the erosion velocity and thus (unsafely) overestimated the critical time.

5.2 Model limitations

Idealized dike geometry

The most important limitation is that the TPM is only valid for piping under dikes and only for the idealized dike geometry of Sellmeijer. This dike consists of an impermeable clay dike is situated on top of a homogenous sandy aquifer with uniform thickness, the pipe entry and exit locations are predefined, and the slope of the pipe is zero. In case a clay blanket exists on the polder side of the dike, a preassigned pipe (crack channel) exists in the clay layer so that the seepage length is

determined. In reality this idealized dike (e.g. IJkdijk) is very rare. The slope of the pipe is zero the model is not capable of calculating piping around for example seepage screens. The slope of the pipe may have a constant angle (this is possible in the Sellmeijer model), but then the neural networks within the TPM are not valid: the dike should be simulated first with the Sellmeijer model and subsequently with the TPM.

Valid range of the research results

Neural networks were used to emulate the Sellmeijer model, so that TPM alone could simulate piping. First the accuracy of the neural networks was investigated and declared as sufficient. The neural networks, however, are only valid for limited number of dikes with a seepage length between 20 and 70 m, an aquifer thickness between 5 and 50 m, and aquifer permeability between 10 and 100 m/d. These ranges are representative for primary dikes in the Netherlands according to a Grontmij expert judgment call. Moreover, the aquifer permeability depends on the aquifer porosity, and the 10 and 70 percentile of the grain diameter of particles in the aquifer. For the given permeability range of 10 to 100 m/d the relationship between the three parameters is predetermined. This implies that the research results are only valid for dikes with the same relationship. As mentioned earlier, the slope of the pipe in the TPM is assumed to be zero. It may, however, have a constant angle. It is possible to simulate dikes outside the neural networks range, but then the dike has to be simulated in the Sellmeijer model first.

5.3 Model uncertainties

IJkdijk measurements

The TPM is validated on three IJkdijk full-scale tests. The erosion pattern is not observed directly, since the dike material is not transparent. The pipe length was determined by analyzing the pore water pressure measurements below the dike. This analysis was carried out with MATLAB scripts provided by Sellmeijer (figure 3-1), in which the pipe length was estimated using a regression technique which introduces some statistical uncertainty. The analyzed measurements only include the measurements of the row from the location where the dike failed to the exit hole. This row of measurements is parallel to the groundwater flow in the aquifer. The rest of the pore water measurements (a matrix of eight by fifteen below the dike) were not included in the analysis. As piping is a three dimensional process and the trajectory of the pipes is random, it is likely that multiple pipes merged into the “measured pipe” increasing the erosion capacity of the pipe. The cumulative sand transport of the TPM is compared with the observed sand transport at the pipe exit point. The IJkdijk results show also that the measured pipe length fluctuates, probably caused by pipe deformation or pipe clogging (Van Beek et al., 2012). The TPM’s pipe length, that is not able to decrease, is validated on this fluctuating pipe length. According to Sellmeijer (1988) and Bonelli (2007) pipe widening starts when the pipe reaches the riverside of the dike. In all tests pipe widening occurred while the observed pipe length in all tests did not reach the river side of the dike. Overall it can be concluded that the observed pipe length involves some uncertainty. The TPM (safely) underestimates the observed pipe length as the TPM’s pipe length sooner starts to erode and sooner reaches the critical situation.

Cumulative flood effect on piping

The IJkdijk full-scale experiments showed that pipe lengths seemed to retreat and then suddenly grew again. According to Deltares (2012) until now it is not clearly understood when and how this happens. Hesami and Zwanenburg (2009) found that short pipes at the downstream side of the dike do not collapse. Long pipes, however, may collapse when they reach the upstream side of the dike. Glynn and Kuszmaul (2011) studied piping along the Mississippi and state that previous piping occurrence is the most influential factor in the prediction of future piping. This is confirmed by sand boil observation in the Netherlands. At many locations where sand boils were observed during the flood of 1993, sand boils appeared again with the flood of 1995. At a few locations this did not happen and at some new locations sand boils were also spotted (TAW, 1995). This means that those locations are sensitive to piping and/or there is 'memory' in the mechanism, meaning that the formed pipe might remain open, after which the pipe may start growing again from its latest position during the next flood wave. The initial pipe length of the TPM is almost zero and the simulated pipe length cannot decrease. The cumulative flood effect on piping is not taken into account in the TPM. Therefore it may (unsafely) overestimate the time to progressive erosion.

Aquifer permeability

The reliability of the Sellmeijer model, and therefore also the TPM, is especially dominated by the uncertainty in permeability of the aquifer (Schweckendiek, 2010). This is caused by a high spatial variability (heterogeneity) in the aquifer combined with the limited availability of direct measurements (Zwanenburg, 2011). The 10 and 70 percentile of the grain diameter of particles in the aquifer often varies greatly over a small distance (Van Swieteren, 2013; Deltares, 2012). It is rather difficult to determine the effective aquifer permeability. Despite the artificial (controlled) conditions even in the IJkdijk experiments this was a challenge. The largest difference (between the laboratory and field measurement) was about 10 meters per day according to Sellmeijer. The TPM predicts the shortest critical time for an aquifer permeability of 30 to 50 meters per day. The aquifer permeability is calculated in the TPM with Chapuis (2004) as recommend by Wang et al. (2014). A different result (7% higher) is obtained with Den Rooijen (1992) which is mainly used in design practice. The higher the aquifer permeability the higher the (Sellmeijer, 1988). Hence, the TPM predicts a higher (less conservative) ΔH_{CRIT} than Den Rooijen (1992),

Sellmeijer prediction

Since the TPM is dependent on the Sellmeijer model it is interesting to know how accurate it is. The Sellmeijer model is considered to be conservative. However, the IJkdijk tests showed that the dike with coarse sand failed at 15 centimeter smaller ΔH than the predicted ΔH_{CRIT} (2.25 m). This is a worrying conclusion as the dike can fail while no dike failure is predicted by Sellmeijer. The TPM is, however, not less safe than the Sellmeijer model. The TPM can only simulate dike failure when the Sellmeijer model simulates dike failure.

5.4 Unaccounted physical processes

Sand boil resistance to piping

The TPM is validated on three Ikdijk full-scale tests, all three identical to the idealize dike geometry of Sellmeijer. In these tests everything was controlled: for example the sand was sieved, the water was sieved (the smallest silt was removed), and sand boils were removed to keep a constant hydraulic head gradient through the dike (Van Beek et al., 2012). A sand boil increases the resistance to piping as the head difference becomes smaller when the polder water level increases inside the sand boil. In reality (without these interventions) the dike perhaps would have failed at a larger ΔH . The only piping emergency measure applied in practice also concerns reduction of the ΔH : sand bags are put around the sand boil (TAW, 1999). The resulting dike failure probability reduction is not included in the Dutch piping safety assessment. The TPM does also not account for sand boil resistance to piping and therefore (safely) overestimates the hydraulic head difference.

Vertical hydraulic pressure gradient in the aquifer

According to Sellmeijer the discharge in the pipe depends on the vertical pressure gradient development along the pipe. The pipe height is calculated based on the discharge in the pipe, the particle force balance, and the horizontal pressure gradient. In the Sellmeijer model the horizontal and vertical pressure gradient in the aquifer and the pressure in the pipe affect each other. The equilibrium situation is iteratively calculated for different constant ΔH s. The TPM does not include the vertical pressure gradient. One can argue this unrealistic, but according to Koning (2012) the influence of the vertical pressure gradient on piping is small. Instead a pipe height relation is assumed and based on the pipe height and the condition limit equilibrium (Sellmeijer, 1988) the pressure in the pipe is calculated. The pressure at the tip of the critical pipe length is compared with the Sellmeijer model and adjusted when needed. The simulated pressure in the pipe for shorter pipe lengths than the critical pipe length is considered to coincide with the Sellmeijer model.

Aquifer compressibility

According to Van Esch & Sellmeijer (2012) the compressibility of the aquifer delays the increase of water pressures in the aquifer in time. Compression is mainly due to clay inclusions in the sandy aquifer. The delay in water pressure generation hampers the growth of the piping channel in time and increases the ΔH_{CRIT} if rapid variations of river water level are considered relative to the system response in time. By accounting for aquifer compressibility the pipe length increases relatively slower. As the TPM does not do this, the erosion velocity is (safely) overestimated.

Foreland

In case the aquifer is not directly connected with the river water, but separated by a clay top layer (foreland) then the time dependency process of piping significantly changes. This clay layer damps and delays the fluctuating pressure head in the aquifer due to the fluctuating river water level significantly (TAW, 1999). The current piping assessment assumes a constant water level so in the calculation the delay of the fluctuating pressure head does not play a role (only damping and a longer seepage length due to foreland). In the TPM also not accounts for the delay of the

fluctuating pressure head. The erosion velocity therefore is higher than in reality. Hence, the TPM (safely) overestimates the erosion velocity.

Three dimensional piping

Piping is a three dimensional process. The TPM and current piping assessment are two dimensional. Recently a three dimensional piping approach is presented by Van den Boer et al. (2014). Large three dimensional volumes are drained by the pipe, resulting in a significantly larger pipe exit velocity and thus higher erosion velocity. Hence, the TPM (unsafely) underestimates the actual erosion velocity by not accounting for three dimensional piping.

5.5 Comparison to literature

Ozkan (2003) introduced a one-dimensional transient analytical flow model which was capable to determine the effect of variable ΔH s on the exit gradient. Everywhere in the world, except for the Netherlands, the exit gradient (see glossary for explanation) is used to indicate whether piping may occur. Ozkan (2003), however, did not include the erosion velocity. He found that multiple flood events increase probability that piping might start. The TPM is not able to simulate the effect of multiple flood events; therefore a comparison is not possible.

Expertise Network for Flood Protection (ENW), an independent advisory committee on water safety, indicates two aspects that may have significant impact on piping: time dependency and heterogeneity of the aquifer. Especially, the former is expected to lead to less conservative piping safety rules in the coastal zone due to dynamic and short high water levels (Expertise Network for Flood Protection, 2013). This can be confirmed by the TPM. The TPM leads also to less conservative piping safety rules compared to the current piping assessment.

Shamy et al. (2004) developed a model to study the flood-induced effect on deformation of the soil system below structures. Their results showed that failure of such structures may occur before the predicted critical situation has been reached due to combined action of weight of the structure and water flow. Likewise in the study of Ozkan (2003) the critical exit gradient is used. It is likely that the weight of the dike does influence the piping process. The more weight, the more tightly the soil is packed, the higher flow velocity is needed to move the particles, the more difficult for piping to occur. Moreover, a higher weight on top of the pipes, the more likely they will collapse. According to Sellmeijer and the TPM, the weight of the dike (as well as the dike height) does not influence the piping process. The compressibility of the dike is not taken into account. By accounting for aquifer compressibility the erosion velocity is lower.

Bonelli et al. (2007) investigated the characteristic time of pipe widening under a constant head difference: the process that starts when the critical pipe length has been reached and ends with dike failure. Based on a series of hole erosion tests in laboratory they deduced an estimation of the time for breaching in hydraulic works (dams and dikes) when pipe widening starts. The TPM estimates time until pipe widening and therefore the findings regarding the critical time cannot be compared. However, the observed time from pipe widening until dike failure in the IJkdijk tests is the same magnitude of order as the estimation by Bonelli et al. (2007). In this estimation the

maximum exit hole of 2 mm is used (likewise in the TPM). By combining both models - TPM and Bonelli et al. (2007) – the time from start of piping until dike failure can be estimated.

Wang et al. (2014) studied the time of piping below structures for a constant head. Numerical analysis was carried out to investigate the effect of the (constant) upstream water head on the channel development. The results indicate that the greater the water head, the faster the erodible pipe progressed, which is confirmed by the TPM.

5.6 Added value of the transient piping model

The added value of time-dependent piping analysis by the transient piping model compared to the current piping assessment is that a dike declared as unsafe by Sellmeijer does not have to be unsafe to piping when taking into account the time dependent aspect (scenario 2 in table 5-1). On one hand the TPM (safely) underestimates the actual time to progressive erosion as it does not account for aquifer compressibility and, when a foreland is situated, the delay of fluctuating pressure head. On the other hand the TPM (unsafely) overestimates the time to the critical situation as it does not account for three dimensional piping and the cumulative effect of floods. How much these processes affect the under or overestimation has not been investigated. The validation results showed that the time to the critical situation was (safely) underestimated.

Table 5-1 Scenarios of dike failure prediction by the Sellmeijer model and the TPM. The second scenario represents the added value of TPM

Scenario	Prediction by Sellmeijer	Prediction by TPM	Remark
1	Dike failure	Dike failure	The research results showed that high water waves with a long (enough) wave period with a maximum ΔH that equals or exceeds the ΔH_{CRIT} will lead to dike failure.
2	Dike failure	No dike failure	This scenario concerns the added value of the TPM. The research results show that a dike declared as unsafe by Sellmeijer does not have to be unsafe when taking into account the time dependent aspect (short wave period). The more frequent a high water wave is expected to happen the more likely the TPM predicts no failure whereas Sellmeijer predicts dike failure. The conclusion only holds for high water waves with a return period of more than 10 years
3	No dike failure	Dike failure	This scenario is not possible. The TPM cannot predict 'dike failure' when the Sellmeijer model predicts 'no dike failure'.
4	No dike failure	No dike failure	The TPM will always predict 'no dike failure' when the Sellmeijer model predicts 'no dike failure'

Chapter 6 - Conclusions and recommendations

The main objective of this research was: “to develop a piping model using existing theories of Sellmeijer (1988) and Wang et al. (2014) to investigate under which circumstances dike failure due to piping can occur under realistic transient conditions”. Four research questions were used as a guideline to reach the goal. This Chapter recaps the answers to these questions in the same order as they were answered throughout this thesis.

6.1 Conclusions

1. How can the effect of transient hydraulic head differences on piping be modeled?

For answering the first research question the theories of Wang et al. (2014) and Sellmeijer (1988) have been explored. Sellmeijer (1988) describes the equilibrium situation of piping (when piping stops) for a given head difference. In this study the Sellmeijer model is extended with a erosion velocity formula of Wang et al. (2014). Wang et al. (2014) developed a model to simulate piping with a variable angle (piping around structures) for a constant head difference. Moreover they determined the erosion velocity which depends on the hydraulic gradient at the tip (front side) of the pipe. The erosion velocity is higher when the constant head difference over the dike is larger. The TPM is an extension of the Sellmeijer model - that uses input from the Sellmeijer model and the erosion velocity formula of Wang et al. (2014) - to account for time and to simulate piping under a variable head difference. The effect of transient hydraulic head difference on piping can be modeled with the TPM.

2. How does the modelled pipe length development compare to the IJkdijk measurements?

The TPM was validated on three full-scale piping tests. The start of piping is well predicted by the TPM and in all three tests a conservative (safe) prediction was obtained. The time to the critical situation in the first and third test was well predicted by TPM. Both predictions resulted in a conservative (safe) prediction. However, for the second test the dike collapsed whereas it was predicted not to fail (also according to Sellmeijer): the predicted critical head difference (2.25 m) was 15 cm larger than the actual critical head difference at which the dike failed. The observed cumulative amount of transported sand of 80 kg is (unsafely) underestimated by 13%. The observed sand transport rate of 2.1 kg/h is underestimated by 25%. Overall, it can be concluded that the TPM can serve as a useful tool to estimate time until progressive erosion as an extension to the Sellmeijer model. The TPM will not predict dike failure when Sellmeijer declares the dike safe to piping.

3. *When does piping result in progressive erosion considering dikes varying in aquifer permeability, aquifer thickness and seepage length?*

When loading dikes with their own critical head difference, then progressive erosion occurs sooner for dikes with a high critical head difference. The reason for this is that a larger head difference increases the pressure gradient at the tip of the pipe and thus the erosion velocity (Wang et al. 2014). When accounting for time-dependent piping it turns out that the seepage length has almost no effect on the critical time in case of shallow aquifer thickness: in case of a shallow aquifer the critical pipe length remains constant whereas in case of a thick aquifer the critical pipe length increases (remains half the seepage length). A longer critical pipe length requires the pipe to erode over a longer distance and therefore results in a longer time to progressive erosion. The longer the wave period the smaller the maximum head difference has to be for progressive erosion to occur and to result in dike failure. Also a wave with a larger maximum head difference required a shorter wave period to reach the critical situation. This is due to larger maximum head difference (higher pressure gradient) and therefore higher erosion velocity. The critical wave period depends mainly on the critical pipe length and on the erosion velocity. The latter is dependent amongst others on the steepness of the wave. The steeper the front of the wave the higher the erosion velocity the sooner the critical situation is reached. However, in case of an early wave peak the head difference drops too soon which may prevent the pipe length to reach the critical pipe length. Hence, given a certain wave period the sooner the wave peak the lower the change the critical situation will be reached.

4. *What is the added value of time-dependent piping analysis by the transient piping model compared to the current piping assessment?*

The TPM might result in less conservative piping safety rules compared to the current piping assessment as the research results show that a dike declared as unsafe by Sellmeijer does not have to be unsafe to piping when taking into account the time dependent aspect. This is an important finding. The more frequent a high water wave is expected to happen the more likely it is that the TPM predicts no dike failure whereas Sellmeijer predicts dike failure. This discrepancy can be seen as the added value of the TPM. The conclusion, however, only holds for high water waves with a return period of more than 10 years. The chance of a different prediction by Sellmeijer and the TPM is therefore the smallest for high waters waves with a return period of once in 1250 year.

On one hand the TPM (safely) underestimates the actual time to progressive erosion as it does not account for aquifer compressibility and, when a foreland is situated, the delay of fluctuating pressure head. On the other hand the TPM (unsafely) overestimates the actual time to the critical situation as it does not account for three dimensional piping and the cumulative effect of floods. How much these processes affect the under or overestimation has not been investigated. The validation results showed that the time to the critical situation was (safely) underestimated.

6.2 Recommendations

The conclusions of this study primarily serve a scientific purpose, which is to increase the understanding of the time-dependency of piping. However, the findings are also of practical importance since they point out that current piping assessment can be improved by accounting for time-dependent piping. Even though the benefits of time-dependent piping are demonstrated by this study, additional studies are necessary to further improve the TPM.

6.2.1 Academic recommendations

From the academic point of view, further research needs to improve the understanding of the time-dependent aspect of piping. Firstly, the TPM should be validated on different cases than the IJkdijk tests, as the IJkdijk situation is rare in practice. Piping tests with a fluctuating head difference on a dike with a blanket (without a predefined crack channel) landwards of the dike, and a foreland on the riverside of the dike (damping of fluctuating pressure head) should be investigated. This would help to understand the time dependent behavior of piping for dikes that are more common in practice. During this test sand boils should not be removed as increase the resistance to piping and they are neither removed during piping in practice.

The pressure distribution along clay-sand interface should be investigated as, it is most likely not linear as in the TPM, and it affects the pressure gradient at the tip of the pipe and therefore erosion velocity.

Scientific research should focus on the effect of multiple floods on piping. This can be done by increasing the period in between the high water waves in the test. More insight is needed into how the erosion channel, which developed during a period of high river water levels, will be preserved until a next period of high water levels. A combination of further field, laboratory, and model studies are needed to document changes in pipe lengths during multiple high waters.

The effect of different pipe height relation in the TPM should be investigated. It seems that the TPM's pipe height is underestimated which results in a (unsafe) underestimation of the actual erosion velocity. Also different Wang et al. (2014) parameters should be explored: the erosion coefficient (0.3 used in this study) ranges from 0.0027 to 0.65, and the critical porosity (0.45 used in this study) ranges from 0.41 to 0.44 according to Wang et al. (2014).

Scientific research should also focus on the effect of three dimensional piping on the time-dependency. Different pore water measurements, than used in this study, can be used to do so.

By combining the TPM with insights from Bonelli (2007) the time from start of piping until dike failure can be estimated. As the TPM simulates until the critical pipe length has been reached and Bonelli (2007) simulation starts when pipe has already reached the river side of the dike, the process in between both models (progressive erosion) is not described. It is recommended to investigate the time-dependency of progressive erosion to get a better indication of the total time from start of piping to dike failure. Also the time of pipe widening for a variable head difference should be research as Bonelli (2007) is only valid for a constant head difference.

6.2.2 Practical recommendations

This research has shown that the time to progressive erosion can be modeled under a variable head difference. It is recommended to use the transient model in practice so that it can be estimated which high water waves will lead under which circumstances to dike failure. It is interesting to investigate dikes are loaded with a variable head difference and are declared as unsafe by the current piping assessment. The TPM might show that these dikes are safe when taking into account the time dependent aspect.

To be able to investigate dike configurations different from dike configurations within the neural networks, the dike should first be simulated in the Sellmeijer model and subsequently simulated with the TPM.

The time-dependency of piping is important in interpreting historical failures, laboratory tests and to derive solutions to deal with piping. To roughly estimate the time from start of piping until dike failure The TPM should be combined with the time-dependency insights of the widening process by Bonelli (2007). The time of progressive erosion is not included in both models (see academic recommendations).

References

- Ammerlaan, P.R.M., 2007. Levees and levee evaluation The Dutch and US practice compared, MSc thesis, Delft University of Technology, Delft.
- Bligh, W.G., 1910. Dams Barrages and Weirs on Porous Foundations, *Engineering news*, p. 708.
- Bonelli, S., Brivois, O. & Lachouette, D., 2007. The scaling law of piping erosion. In *Francais de Mécanique*. Grenoble, 2007. Cemagref, Hydraulics Engineering and Hydrology Research Unit.
- Chapuis, R. P., 2004. Predicting the saturated hydraulic conductivity of sand and gravel using effective diameter and void ratio, *Canadian Geotechnical Journal*, 41(5): 787-795.
- Deltares, 2012. Zandmeevoerende Wellen. Research report. Delft: Rijkswaterstaat Ministerie van Infrastructuur en Milieu.
- Den Rooijen, H., 1992. Literatuuronderzoek doorlatendheid- korrelkarakteristieken. Grondmechanica Delft Rapport CO-317710/7
- Expertise Network for Flood Protection, 2013. [Online] Available at: <http://www.enwinfo.nl/upload/ENW-13-01%20Advies%20concept-TR%20Zandmeevoerende%20Wellen%20en%20Bijlage%20Pipingvoorbeeld%20%20scan.pdf> [Accessed 12 October 2013].
- Fox, G. A., Wilson, G. V., Simon, A., Langendoen, E. J., Akay, O. and Fuchs, J. W., 2007. Measuring streambank erosion due to ground water seepage: correlation to bank pore water pressure, precipitation and stream stage, *Earth Surface Processes and Landforms*, 32(10), 1558-1573.
- Fujisawa, K., Murakami, A. and Nishimura, S., 2010. Numerical analysis of the erosion and the transport of fine particles within soils leading to the piping phenomenon, *Soils and foundations*, 50(4), 471-482.
- Hazen, A., 1892. Some physical properties of sand and gravel, with special reference to their use in filtration. Massachusetts State Board of Health, 24th Annual Report, Boston.
- Hegen, D., 1996. Element-free Galerkin methods in combination with finite element approaches, *Computer Methods in Applied Mechanics and Engineering*, 135, 143-166.
- Hesami, F., Zwanenburg, C. (2009): *SBW Piping HP3. Gedrag van klei*. Rapport 1200187-007-GEO-0001, Deltares
- Howard, A. D. and McLane, C. F., 1988. Erosion of cohesionless sediment by groundwater seepage, *Water Resources Research*, 24(10), 1659-1674.

- Janssen P.H.M., Slob, W., en Rotmans, J., 1990. Gevoeligheidsanalyse en Onzekerheidsanalyse: een inventarisatie van ideeën methoden en technieken. RIVM Rapport nr. 958805001 Ministerie van Verkeer en Waterstaat, 2007. *Hydraulische Randvoorwaarden primaire keringen*. Rijkswaterstaat.
- Jones, B. E., 1916. A method of correcting river discharge for a changing stage. US Geological Survey Water Supply Paper 375-E.
- Kanning, W., 2012. *The Weakest Link*, PhD Thesis. Delft: Delft University of Technology.
- Lambe, T.W. and Whitman, R.V., 1979. Soil Mechanics, SI version, John Wiley & Sons, 67
- Midgley, T., Fox, G., Wilson, G., Heeren, D., Langendoen, E. and Simon, A., 2012. Seepage-induced streambank erosion and instability: In-situ constant-head experiments, *Journal of Hydrologic Engineering*, 18(10), 1200-1210.
- Ministerie van Verkeer en Waterstaat, 2007. *Voorschrift Toetsen op Veiligheid Primaire Waterkeringen*. Rijkswaterstaat
- Lane, A.W., 1935. Security from Under-Seepage Masonry Dams on Earth Foundations, Transactions American Society of Civil Engineers, vol. 100 paper no. 1919.
- Ojha, C.S.P., 2011. Influence of porosity on piping models of levee failure, Journal of geotechnical and environmental engineering.
- Schweckendiek, T., 2010. Reliability benchmarking task group 3. Benchmark example number 9 (version 1). Delft: Deltares & Delft University of Technology.
- Sellmeijer, J.B., 1988. On the mechanism of piping under impervious structures, PhD Thesis. Delft University of Technology, Delft.
- Sellmeijer J.B., Koenders M.A., 1991. "A mathematical model for piping", *Applied Mathematical Modelling*, vol. 115, pp. 646–661.
- Sellmeijer, J.B. 2006., Numerical computation of seepage erosion below dams (piping), Proceedings of Third International Conference on Scour and Erosion, p. 596-601.
- Sellmeijer, J.B., López de la Cruz, J., Van Beek, V.M. & Knoeff, H., 2011. Fine-tuning of the backward erosion piping model through small-scale, medium-scale and IJkdijk experiments. *European Journal of Environmental and Civil*, 15(8), pp.1139 - 1154.
- El Shamy, U. & Aydin, F., 2008. Multiscale Modeling of Flood-Induced Piping in River Levees. *GEOTECHNICAL AND GEOENVIRONMENTAL ENGINEERING*, pp.1385 - 1398.
- Silvis, F., 1991. Verificatie Piping Model; Proeven in de Deltagoot. Evaluatierapport. Rapport Grondmechanica Delft CO317710/7

- Stijnen, J.W., Wouters, C.A.H., Calle, E.O.F., Knoeff, H., Vrouwenvelder, A.C.W.M., 2006. *Vergelijk Leidraad Waterkeringen*. Rijkswaterstaat DWW / RIZA
- TAW, 1999. *Technisch rapport Zandmeevoerende wellen*. Technical Report. Delft: Technical Advisory Committee on flood defence.
- TAW, 1995. *Druk op de dijken 1995*. Delft: Technical Advisory Committee on flood defence.
- Terzaghi, K., 1925. Principles of soil mechanics. *Engineering News-Record*. v. 95, p. 832
- Van Beek, V.M., Knoeff, J.G., de Bruijn, H.T.J., Bezuijnen, A., & Förster, U., 2012. Levee failure due to piping: A full-scale experiment. p.1-10.
- Van den Boer, K., Van Beek, V., Bezuijnen, A., 2014. *3D finite element method (FEM) simulation of groundwater flow during backward erosion piping*. Deltares, Delft. Department of Civil Engineering Ghent University, Ghent.
- Van der Zee, R.A., 2011. *Influence of sand characteristics on the piping process*. MSc Thesis. Delft: Delft University of Technology.
- Van Esch, J. M. & Sellmeijer, J. B., 2012. *Delft Modelling transient Groundwater Flow and Piping under Dikes and Dams*
- Van Swieteren, T. J. A., 2013. *Spatial variation in dike safety management for uplift*. MSc Thesis. Delft: Delft University of Technology.
- Vrijling, J.K., Kok, M., Calle, E.O.F., Epema, W.G., van der Meer, M.T. & van der Berg, P., 2010. *Piping - Realiteit of Rekenfout?* ENW.
- Wang, D., Fu, X., Jie, Y., Dong, W., Hu, D., 2014. Simulation of pipe progression in a levee foundation with coupled seepage and pipe flow domains. *Journal of soils and foundations*, pp. 100084, State Key Laboratory of Hydrosience and Engineering, Tsinghua University Beijing.
- Zhou, X. J., Jie, Y. X. and Li, G. X., 2012. Numerical simulation of the developing course of piping, *Computers and Geotechnics*, 44, 104-108.
- Zwanenburg, C., 2011. PIPING: OVER 100 YEARS OF EXPERIENCE. *A feeling for soil and water – A tribute to prof. Frans Barends*. Deltares Select Series . ISSN 1877-5608.

Appendices

Appendix A - Historical research on piping

Below a chronological ordered overview of all research on piping is given:

Clibborn & Beresford	1902	Found that the ratio between ΔH_{CRIT} and seepage length is a constant that depends on soil properties.
Bligh	1910	Empirical rule of creep theory ($L = C_{\text{CREEP}} * H$) in which percolation factors were established for different soil types, thereby determining a safe head to prevent piping.
Griffith	1913	Further development of Bligh's empirical creep theory.
Harza	1934	Proposes the electric analogy method, where groundwater flow is simulated with electric currents.
Lane	1935	Argued that vertical length contributes more to safety than horizontal length and adjusted the empirical rule, based on a total of 200 cases in the United States ($L_V + 1/3 * L_H = C_{W_CREEP} * \Delta H$).
Terzaghi	1948	Proposed a formula for heave near sheet piles, which takes into account the vertical gradient of the water flow.
Müller-Kirchenbauer	1978	Experiments with test facilities to research the multiple aquifer layers of sand on the influence of piping process. The grain size was not varied in these experiments.
De Wit & Sellmeijer	1984	Laboratory theory. Investigated influence of soil characteristics, such as grain size, porosity, dimensions of the sand bed and type of exit point, on the ΔH_{CRIT} .
Kohno	1987	Researched the influence of multiple sand layers on the ΔH_{CRIT} with a test facility.
Sellmeijer	1988	Simulated the progression of a pipe with a theoretical model, by using the equilibrium of grains in the bed of the pipe as a criterion for the initial movement of grains.
Calle et al.	1989	Probabilistic calculation for analyzing the likelihood of piping beneath sea dikes and river dikes considering the dynamic equilibrium necessary to accelerate or terminate erosion and material movement once piping has initiated.
Silvis	1991	Large-scale tests performed in the Delta flume allowed for validation of the model at different scales.
Calle & Weijers	1994	New guideline with updated Sellmeijer (1988) calculation rule.
Griffiths & Fenton	1998	Employed two- and three-dimensional finite-element models to study seepage in spatially random soil with statistically variable soil permeability and steady state flow.
Schmertmann	2000	Found that the results of the piping experiments were independent of the applied effective stresses.
Ojha	2001	Researched the influence of the porosity on piping, and found that the outcome of the study supports the formula of Bligh.

Zeping	2001	Investigated the difference between the Dutch and the Chinese method of calculating piping and concluded that in the Netherlands a critical gradient is determined, while in China a critical exit gradient is normative.
Schmertmann	2002	Provides, based on the failure (and damage) probability of dams due to piping, an excellent economical substantiated argument to invest heavily in piping experiments.
Lu & Zhang	2002	Developed an unsteady groundwater flow model using finite-element difference technique that accounts for heterogeneous soils.
Sellmeijer III	2003	Presents neural network including other geometries that the idealized geometry can be used, and a fast and accurate computation can be performed.
Ozkan	2003	Most of the analytical work found in the literature considers piping under steady state conditions (Sellmeijer 1988; Sellmeijer and Koenders 1991; Weijers and Sellmeijer 1993; Ojha et al. 2001). Ozkan (2003) introduced a one-dimensional transient analytical flow model with changing water level to study the effects of transient flow and repetitive flood events.
Fell et al.	2004	Estimated the probability of failure of embankment dams by internal erosion and piping by historic performance and event tree methods.
Shamy et al.	2004	Developed a model to study the flood-induced effect on deformation of the soil system below structures. Their results showed that failure of such structures may occur before the predicted critical situation has been reached due to combined action of weight of the structure and water flow.
VNK1 (Veiligheid Nederland in Kaart)	2005	Performed safety assessment of Dutch dikes using the model of Sellmeijer (1988). A discrepancy emerged between calculated probabilities of failure and the opinion of dike managers of the actual resistance to piping.
Ter Horst	2005	Investigated the conditional failure probability of several failure mechanisms of dikes in the Netherlands, and concluded that piping is the most dangerous failure mechanism in the Netherlands because of the high uncertainty in the resistance of a dike.
Achmus	2006	Defined a critical exit gradient for piping. The method of a critical exit gradient method is used in several countries.
Sellmeijer	2006	Sellmeijer's model has also been implemented in a numerical groundwater flow program (Mseep) for safety assessment for other configurations, such as multi-layer aquifers.
Ding et al.	2007	Performed experiments to investigate the piping process in multi-layer aquifers. However, this experimental work did not allow for validation of Sellmeijer's model for multi-layer aquifers, because for some experiments the necessary parameters were unavailable and the sand

types used in other experiments were out of the validity range of Sellmeijer's model.

Ammerlaan	2007	Compared safety standards from the Netherlands and the USA. He concluded that in the USA sand boils are not allowed by safety standards, in the Netherlands, the creation of sand boils is allowed, as long as the critical gradient is not exceeded. In the USA values of C_{Bligh} of 43 or 44 are used.
Bonelli et al.	2007	Investigated the characteristic time of pipe widening under a constant head difference: the process that starts when the critical pipe length has been reached and ends with dike failure. Based on a series of hole erosion tests in laboratory they deduced an estimation of the time for breaching in hydraulic works (dams and dikes) when pipe widening starts.
Hoffmans and Sellmeijer	2009	Suggests that piping can be described with the Shields equation that the solution gives a better fit with the experiments than the formula.
ENW	2010	'Expertise Netwerk Waterveiligheid' concluded that piping a more serious threat is than was assumed (Vrijling et al., 2010).
Sellmeijer et al	2011	Sellmeijer's model has been validated for different homogeneous sand types from which an adapted rule is derived. The new rule predicts well the outcome of the large-scale IJkdijk tests, when the aquifer is composed by fine sand. For coarse sands the original model appeared to overestimate the ΔH_{CRIT} . The behavior of coarse sand is not yet well understood. It is presumed that the width of the erosion channel is significant. In the theoretical piping rule, this width is supposed to be large (2D). A reason could be that fine sands develops as a front, while coarse sands tend to erode in smaller strips.
Van Beek	2012	A series of full-scale tests allowed for validation of Sellmeijers' adjusted rule as well as the observation of the piping process. It was concluded that failure of a dike due to piping is certainly possible and that the model of Sellmeijer is able to predict the ΔH_{CRIT} well. It is noticed that in all experiments sieved sands are used, where as in practice heterogeneity both at micro-scale and at macro-scale can influence the process. This has not yet been investigated.

Appendix B - Sellmeijer

Sellmeijer's (1988) research resulted in several equations, describing the relation between pipe length and ΔH at which the sand grains are in equilibrium piping process: the ΔH_{CRIT} is the point where the pipe under the dike starts to grow explosively. The equations cannot be solved analytically but need to be implemented in a numerical computation code (e.g. Mseep) (Van Esch & Sellmeijer, 2012). The mathematical model of Sellmeijer (1988) consists of three differential equations (van Zwieteren, 2013). The last two equations together form the boundary condition for the first equation. This implicates that the piping problem may be determined by ordinary groundwater flow computation with a special piping boundary condition. However, this is a cumbersome condition. It is highly nonlinear. It is not operative in a single point of the boundary, but affects the boundary on aggregate. By implication, only iteratively this condition may be applied:

1. A 2-D LaPlace equation (based on Darcy and continuity) to describe groundwater flow under a structure, with use of the following boundary conditions:
 - a. the riverside ΔH equals the river water level.
 - b. the landside ΔH equals the polder water level.
 - c. the hydraulic head around the pipe equals the hydraulic head in the pipe
 - d. the dike's blanket material is impervious

$$\nabla^2 \varphi = 0 \quad (\text{B.1})$$

2. An equation (based on Poiseuille law) to describe laminar flow in the pipe as a result of the increasing permeability:

$$h^3 \frac{\partial \varphi}{\partial x} = 12\kappa \int \frac{\partial \varphi}{\partial y} dx \quad (\text{B.2})$$

3. An erosion formula (based on White) to describe equilibrium between forces on grains at the bottom of the pipe, assuming that rolling resistance is decisive for onset of grain's movement:

$$\frac{h}{d} \frac{\partial \varphi}{\partial x} = \frac{\pi}{3} \eta \frac{\gamma^P}{\gamma^W} \frac{\sin(\theta + \beta)}{\cos \theta} \quad (\text{B.3})$$

$\partial \varphi / \partial x$	the hydraulic head gradient along the pipe
h	the height of the pipe
x	the horizontal coordinate
y	the vertical coordinates
κ	the intrinsic permeability
η	the drag force factor (coefficient of White)
γ^P	the volumetric weight of submerged sand grains
γ^W	the volumetric weight of water
θ	the rolling friction angle of sand grains
β	the slope of the pipe. In case of idealized geometry, the pipe slope equals zero, then the last part of the last term of equation B-3 becomes $\tan(\theta)$.

The mechanism of piping is conceptually modeled. It is implemented into the numerical groundwater flow program Mseep. A single piping computation requires preparation skills and takes time in the order of dozens of minutes. In order to minimize this effort, an advanced piping rule for a schematized geometry has been worked out. This is accomplished by applying the technique of artificial neural networks. The piping rule is accommodated with the use of 25000 Mseep computations. Fitting of results of the numerical outcome, results in simplified formula that are used as design and assessment rule in engineering practice to design against piping in arbitrarily composed aquifer (TAW, 1999).

Original Sellmeijer rule (4-forces):

$$\Delta H - 0.3D_{blanket} \leq \frac{\Delta H_{CRIT}}{L} = \left(\frac{D}{L}\right)^\alpha \frac{\gamma^P}{\gamma^W} \eta \tan(\theta) \eta \frac{d_{60}}{\sqrt[3]{\kappa L}} \left\{0.685 - 0.094 \ln\left(\frac{d_{60}}{\sqrt[3]{\kappa L}}\right)\right\} \quad (B.4)$$

$$with \alpha = \frac{0.28}{\left(\frac{D}{L}\right)^{2.8} - 1} \quad (B.5)$$

ΔH_{CRIT}	[m]	the critical head difference over the flood defense.
D	[m]	the thickness of the sand layer
L	[m]	the horizontal seepage length.
γ^P	[kN/m ³]	the volumetric weight of submerged sand grains (16.5 kN/m ³)
γ^W	[kN/m ³]	the volumetric weight of water (10 kN/m ³)
η	[-]	the drag force factor (coefficient of White with a value of 0,25)
θ	[deg.]	the angle of friction of sand (41 degree suggested by TAW (1994))
d_{60}	[m]	the 60 percentile of the grain diameter of the sand.
κ	[m ²]	the intrinsic permeability of the sand layer
g	[m/s ²]	the acceleration of gravity (9,81 m/s ²).

Current Sellmeijer rule (2-forces) used in Dutch practice

In 2006 the 4-forces rule has been altered in a 2-forces model (Sellmeijer, 2006). The role of the horizontal and vertical pressure gradient is questioned. It is put forward that in the pipe the particle at limit equilibrium sticks out, so that the pressure gradient does not affect it. Between the large grains substantial open space occurs. The forces due to the seepage gradients by no means can affect the grain at the top of the interface. Consequently, a 2-forces approach is selected where the drag force and weight of the particle are applied. The 2-forces model is implemented in the Mseep model that is used in this study. The latest version of the Sellmeijer rule that is used in Dutch practice is displayed in equation B-6 through B-9 with an added scaling factor d_{70m} and a calibration ratio defined by relative densities RD and RD_m (Sellmeijer et al. 2011):

$$\Delta H - 0.3D_{blanket} \leq \frac{\Delta H_{CRIT}}{L} = F_{Resistance} F_{Geometry} F_{Scale} \quad (B.6)$$

$$F_{Resistance} = \frac{\gamma^P}{\gamma^W} \eta \tan(\theta) \left(\frac{RD}{RD_m} \right)^{0.35} \quad (B.7)$$

$$F_{Scale} = \frac{d_{70}}{\sqrt[3]{\kappa L}} \left(\frac{d_{70}}{d_{70m}} \right)^{0.4} \quad (B.8)$$

$$F_{Geometry} = 0.91 \left(\frac{D}{L} \right)^\alpha \text{ with } \alpha = \frac{0.28}{\left(\frac{D}{L} \right)^{2.8} - 1} + 0.04 \quad (B.9)$$

ΔH_{CRIT}	[m]	the critical head difference over the flood defense
D	[m]	the thickness of the sand layer
L	[m]	the horizontal seepage length
γ^P	[kN/m ³]	the volumetric weight of submerged sand grains (16.5 kN/m ³)
γ^W	[kN/m ³]	the volumetric weight of water (10 kN/m ³)
η	[-]	the drag force factor (coefficient of White with a value of 0,25)
θ	[°]	the angle of friction of sand (37° suggested by Sellmeijer)
d_{70}	[m]	the 70 percentile of the grain diameter of the sand.
g	[m/s ²]	the acceleration of gravity (9,81 m/s ²)
κ	[m ²]	the intrinsic permeability of the sand layer, which can be calculated as : $\kappa = v/g \cdot K$
K	[m/s]	the initial isotropic hydraulic conductivity of the aquifer
ν	[m ² /s]	the kinematic viscosity (1.33 10 ⁻⁶ m ² /s for groundwater at 10°C.)
RD	[-]	the relative density which defines how tight or loose soil is packed which influences the resistance of grains to move: the tighter, the more resistance. It is determined by the measured density of substance (kg/m ³) divided by density of the reference (kg/m ³)

which is in most cases stated. $RD = (E_{MAX} - E)/(E_{MAX} - E_{MIN})$ in which E represent the dry density. RD_M represents the mean value for the relative density derived in small scale experiments (value set to 0,725).

Sellmeijer multi-layer formula (2012)

The latest version of the Sellmeijer rule is not (yet) in used in Dutch practice. In the past, the resistance factor has been extended by adding the influence of relative density, uniformity and particle roundness. This has been validated for one uniform sand layer. In reality aquifers often consist of multiple sand layers: a fine sand top layer overlying a more permeable layer consisting of coarse grains is often encountered in the Netherlands. Therefore, the model has been extended with a multi-layer function, so that more complex layer configurations can be predicted. Recently, this new rule has been successfully validated on small-scale experiments (Van Beek et al., 2012b). The physics behind the new rule have not changed; only the relation between the parameters and the ΔH_{CRIT} has been altered resulting in a more conservative piping rule (ARCADIS, 2012). The Sellmeijer rule below is not in use in Dutch practice and is therefore not called latest version but Sellmeijer multi-layer rule this thesis. The Sellmeijer multi-layer rule reads:

$$\Delta H - 0.3D_{blanket} \leq \frac{\Delta H_{CRIT}}{L} = F_r F_s F_g \quad (B.10)$$

$$F_r = \frac{\gamma^P}{\gamma^W} \eta \tan \theta \left(\frac{RD}{RD_m} \right)^{0.35} \left(\frac{U}{U_m} \right)^{0.13} \left(\frac{KAS}{KAS_m} \right)^{-0.02} \quad (B.11)$$

$$F_s = \left(\frac{d_{70}}{\kappa_{h,avg} L} \right)^{1/3} \left(\frac{d_{70}}{d_{70m}} \right)^{0.4} \text{ with } \kappa_{h,avg} = \sum_{m=1}^n \frac{\kappa_{h,m} D_m}{D_{tot}} \quad (B.12)$$

$$F_g = 0.91 \left(\frac{D}{L} \right)^\alpha \text{ with } \alpha = \frac{0.28}{\left(\frac{D}{L} \right)^{2.8} - 1} + 0.04 \quad (B.13)$$

D_M	[m]	the thickness of the water bearing aquifer number m (figure B-1)
D_{TOT}	[m]	the total thickness of all water bearing aquifers added. The model assumes no in between impervious layers.
θ	[°]	the rolling friction angle of sand grains (37 suggested by Sellmeijer (2012)).
d_{70}	[m]	the 70 percentile of the grain diameter (d_{70M}), which represents the mean value for the 70 percent grain diameter derived in small scale experiments (value set to $2.08 \cdot 10^{-4}$).
U	[-]	Uniformity coefficient calculated by grain size d_{60} divided by d_{10} . Estimation of these sizes requires a grain size curve. U_M represents the mean value of uniformity derived in small scale experiments (value set to 1.81)

- KAS [-] the grain angularity (roundness of particles) which can be visually obtained using microscopes. KAS_M represents the mean value of roundness of particles derived in small scale experiments (value set to 49.8).
- $K_{H,AVG}$ [m^2] the averaged horizontal intrinsic permeability of all sand layers
- $K_{H,M}$ [m^2] the horizontal intrinsic permeability of the sand layer m , which can be calculated as: $k_{h,m} = v/g \cdot K$. Note that this is calculated the same as for the 'normal' intrinsic permeability, but now per layer.

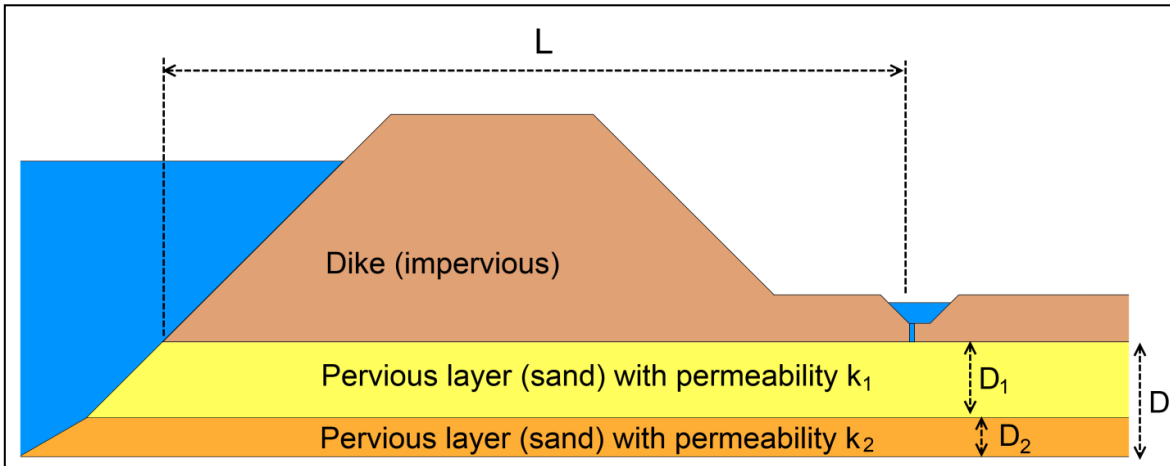


Figure B-1 Idealized geometry for Sellmeijer's multiple sand layer model

Discussion Sellmeijer's method

The method is developed in the Netherlands and was, and nowadays still is, only used in the Netherlands (Ammerlaan, 2007). Sellmeijer's method is more complex than the methods of Bligh (1910) and Lane (1935) and mostly provides a more precise assessment. However, much more input information is needed like thickness of layers, grain distribution and permeability of pervious layers (TAW, 1999). In case the necessary input information can be obtained and when the seepage length exceeds the total thickness of the sand layers, use of Sellmeijer's method is suggested (TAW, 1999). However, it should be mentioned that the method (all versions) is only valid in case seepage length is larger than ΔH over the dike multiplied by ten (Ministerie van Verkeer en Waterstaat, 2007). Although a safety assessment with Sellmeijer avoids pipe formation until riverside, it allows sand boil formation. These boils can be seen as indication of piping threat. The model does not serve a heave or uplift assessment, since a pipe is already present in the blanket. The latest version of Sellmeijer's rule (multiple sand layers) is only validated in small scale test, containing 0,15 to 0,43 mm grain sizes, but appears to predict large-scale experiment results well in case of aquifers also composed by fine sand (Sellmeijer et al., 2011). The method (all versions) does not account for in between impervious layers. Also, the geometrical shape term is valid only for a sand layer of constant thickness. More complex geometries can be dealt with by a numerical approach (Sellmeijer et al., 2011).

Sellmeijer pipe volume estimation

For the IJkdijk analysis Sellmeijer determined a relation for the pipe volume and its length. This relation is based on the Sellmeijer rule and depends on the geometry shape term (F_G) and the normalized aquifer thickness. With neural network computations this relation has been for 1/8 and 1/10 of the seepage length. The relation is used in this study to validate the TPM on sand transport (rate). The relation reads:

$$V = \frac{d_{70}L V_1}{F_{scale}} \left(\frac{l}{0.1L} \right)^{\frac{\ln(V_2/V_1)}{\ln(0.125L/0.1L)}} \quad (\text{B.14})$$

In which is:

V	[m ³]	the volume of the pipe
l	[m]	the pipe length
V ₁	[-]	the volume term when pipe length is 1/10 of the seepage length. This value is related to the aquifer thickness – seepage length ratio. For the IJkdijk the volume term at this pipe length is 0.1036
V ₂	[-]	the volume term when pipe length is 1/8 of the seepage length. This value is related to the aquifer thickness – seepage length ratio. For the IJkdijk the volume term at this pipe length is 0.1398.

Appendix C - Sellmeijer (1988) versus Wang et al. (2014)

Below the differences and similarities between models of Sellmeijer (1988) and Wang et al. (2014) are elaborated based on a few characteristic points.

Model approach In the Sellmeijer model the piping mechanism consists of three processes. Two of these (laminar pipe flow based on Poiseuille, particle force balance based on White) determine the boundary condition for the third process (groundwater flow in the aquifer based on Darcy).

Wang et al. (2014) used the same approach with groundwater flow based on Darcy, particle force balance based on Howard and McLane (1988) and Lambe and Whitman (1979), and turbulent pipe flow based on Zhou et al. (2012).

Pipe flow Wang et al. consider turbulent pipe flow. A quasi-steady model was used, since the pipe flow in their model is unsteady. Quasi-steady is an unsteady process divided into a number of successive steady phases which enables the applicability of a steady model. This approximation holds for cases where the flow does not change quickly but facilitates the simplification of computation.

Sellmeijer (1988) assumes laminar flow because in the phase of limit equilibrium, the flow velocity remains low.

Pipe cross section Wang et al. (2014) assume a circular pipe with a constant pipe height in space and time. Erosion takes only place at the tip of the pipe.

Sellmeijer (1988) assumes a rectangular pipe of which the flow area increases in time due to erosion of the pipe wall. The pipe height increases from tip to exit point. The cross section of the pipe, or pipe height in case of Sellmeijer, determines the required pressure gradient to move a soil particle.

Model mesh In the Wang et al. (2014) model, the slope of the pipe is not necessarily constant. To account for a changing boundary, when the pipe develops, Wang et al. employed the element-free Galerkin (EFG) method. This is a mesh-free method that uses independent background meshes: the interpolating nodes are irrelevant to meshes and can therefore be added, removed or changed conveniently without modifying the integration meshes.

Sellmeijer used the finite-element method (FEM). In such a mesh, each point has a fixed number of predefined neighbors, and this connectivity between neighbors. The EFG method enables Wang et al. to simulate piping that develops with a variable angle (e.g. beneath a seepage screen), whereas the Sellmeijer model (FEM) only is able to simulate piping with a constant angle: the pipe trajectory is determined before piping starts.

Particles inception In both models piping depends on the forces acting on an individual particle. In the Wang et al. (2014) these include the seepage force, the gravity force and the drag force exerted by neighboring particles. This force balance was also used in the Sellmeijer 4-forces model. Recently, Sellmeijer changed this into a 2-forces balance. Consequently, the seepage forces were not included anymore (2-forces model). The

	2-forces model results in a smaller ΔH_{CRIT} (Deltares, 2012).
Pipe angle	<p>In both models the pipe may have an angle. In the Sellmeijer model this can only happen when the roof of the pipe (the impermeable clay dike) has also an angle: the angle is constant from exit to tip of the pipe.</p> <p>The model of Wang et al (2014) is able to simulate a pipe that for example follows the line of creep under vertical seepage screen (see Section 2.1.2). The pipe trajectory is determined by the least resistance the tip of the pipe encounters.</p> <p>In both models the single particle force balance is calculated to indicate the onset of piping. The angle of the pipe affects the particle weight force which determines together with the horizontal drag force the resistance to transport. A larger pipe angle (from entry to exit point) requires a larger pressure gradient to transport particles in the pipe. Hence, a larger pipe angle results in a larger ΔH_{CRIT}.</p>
Pipe flow	<p>Sellmeijer (1988) assumes a rectangular pipe (laminar flow) of which the flow area increases in time due to erosion of the pipe wall. The pipe height increases from tip to exit point, whereas Wang et al. (2014) assume a circular pipe (either laminar or turbulent pipe flow) with a constant pipe height in space and time. In the model of Wang et al. (2014) erosion takes only place at the tip of the pipe.</p>
Pipe exit	<p>In both models a preassigned pipe exists at the land side of the structure, so that groundwater flow streamlines at exit point converge already in the initial stage (Van der Zee, 2011). In the idealized geometry of Sellmeijer (1988) a preassigned crack channel connects the ditch landwards of the dike with the aquifer. Wang et al. (2014) use a predefined pipe with an initial pipe length of 3 centimeter.</p>
Erosion velocity	<p>The model of Sellmeijer (1988) does not determine the erosion velocity. According to Wang et al. (2014) the erosion velocity of piping is mainly determined by the local hydraulic gradient at the tip of the pipe.</p>
Geometry	<p>In the idealized dike geometry of Sellmeijer (1988) a clay dike is situated on top of a sand layer (multiple sub layers are optional). In this case no uplift of an overlying stratum has to take place. The model of Wang et al. (2014) consists of a nearly impervious surface layer and the underlying pervious layer.</p>
Aquifer soil	<p>The model of Sellmeijer (1988) is only valid for homogeneous sands, so that permeability and d_{70} are correlated (Van der Zee, 2011). Wang et al. (2014) do not specify this. Sellmeijer's design rule is derived from the idealized geometry with an (homogeneous) isotropic aquifer. Isotropic implies equal horizontally and vertically conductivity. However, in Mseep it is possible to define different horizontal and vertical conductivity (anisotropic). The model of Wang et al. (2014) assumes anisotropic aquifer conductivity.</p>
Dike failure	<p>The model of Wang et al. (2014) does not include dike failure. Both models relate pipe length to ΔH. The Sellmeijer model (1988) focusses on the critical situation. After this moment, progressive erosion occurs. Subsequent dike failure occurs when the pipe passes roughly thirty to fifty percent of the seepage length (Sellmeijer, 1988). The exact critical length is calculated with Mseep. Also Ojha et al. (2011) emphasized that the ΔH_{CRIT} is when pipe length has been developed about up to half</p>

of the base width. If a critical pipe length is reached in the model, the erosion does not stop anymore, but continues until the pipe has reached the upstream side (Ojha et al., 2011).

Appendix D - IJkdijk full-scale piping experiments

Table D-1 Details of all three IJkdijk full-scale experiments

		Test 1	Test 2	Test 3	Unit
Dike	Dike height	3.5	3.5	3.5	m
Geometry	Dike crest width	1	1	1	m
	Dike width (seepage length; parallel to seepage)	15	15	15	m
	Dike length (normal to seepage)	16.9	19	16.9	m
Aquifer geometry	Aquifer thickness	3	2.85	3	m
	Aquifer length (parallel to seepage)	33	33	33	m
	Aquifer width (normal to seepage)	9	11	9	m
Aquifer material	Aquifer sand material	125-200	250-350	150-250	μm
	Initial permeability	6.7	11.7	6.9	m/day
	Initial porosity	0.4	0.3	0.3	-
	Uniformity coefficient (d_{60}/d_{10})	1.6	1.8	1.6	-
	Particle diameter d_{70}	180	260	180	μm
	Particle diameter d_{10}	106	125	106	μm
IJkdijk test results	ΔH (at moment of first sand boil)	1.99	1.60	2.10	m
	Actual ΔH_{CRIT} (at moment of dike failure)	2.60	2.10	2.30	m
	Time sand boils (piping)	20.5-95	26.3-94.5	42.5-79.2	hour
	Time widening pipes	95-100	94.5-143	79.2-112	hour
	Time dike failure	100	143	112	hour
Sellmeijer	ΔH_{CRIT} predicted by Sellmeijer model	2.15	2.25	2.10	m
	Critical pipe length by Sellmeijer model	8	12.67	8	m
	Critical pressure head at tip by Sellmeijer model	0.450	0.870	0.437	m
	Submerged weight aquifer sand	22.5	24.7	21.2	kN/m^3
	Rolling resistance angle	33	33	33	deg.
	White's constant	0.25	0.25	0.25	-

Appendix E - Transient piping model neural networks

In this study the ΔH_{CRIT} , the critical pipe length, the ΔH at the first point of the equilibrium curve, the pipe length at the first point of the equilibrium curve, and the pressure at the tip of the pipe (when it has reached its critical length) is needed in the TPM. These five parameters can be retrieved from the Sellmeijer model (implemented in Mseep). Based on seepage length, aquifer permeability and aquifer thickness the five parameters will be predicted. As the relations are highly non-linear multiple regression was not successful. Five neural networks were trained to predict these five values so that the TPM is detached from Mseep. With use of batch file 312 different dikes (varying seepage length, aquifer permeability and aquifer thickness) were simulated in the Sellmeijer model and used to train the network. The prediction of the ΔH_{CRIT} by the neural network was validated with the current Sellmeijer rule and Sellmeijer model to check whether the network was over trained. As the Sellmeijer rule is not able to calculate the critical pipe length and pressure at the tip of the pipe, these predictions were only validated by the Sellmeijer model. In this Appendix the validation results are presented.

The lowest normalized absolute error (NAE) between the predicted data and test data (47 samples) has been determined by trial and error. The NAE of all five networks is 0.012 at most (1.2% difference on average between predicted data and test data). Therefore it is assumed that all networks sufficiently emulate the Sellmeijer model. For all five networks only one layer is used. This is kept as low as possible.

Table E-1 Neural network results

Neural network	Number of hidden neurons	Number of layers	Normalized abs. error (NAE) [-]	Mean absolute error (MAE) [m]
ΔH first point	6	1	0.0062	0.024
ΔH_{CRIT}	4	1	0.0059	0.019
Pipe length first point	9	1	0.0052	0.056
Critical pipe length	10	1	0.0083	0.061
Critical pressure at pipe tip	14	1	0.0118	0.0079

The top-left picture of the figures in this Appendix shows the ascended sorted Sellmeijer model outcome with blue dots. The red dots represent the prediction made by the neural network. The horizontal axis represents the number of simulation with the Sellmeijer model (each with a different dike parameter).

Critical head difference

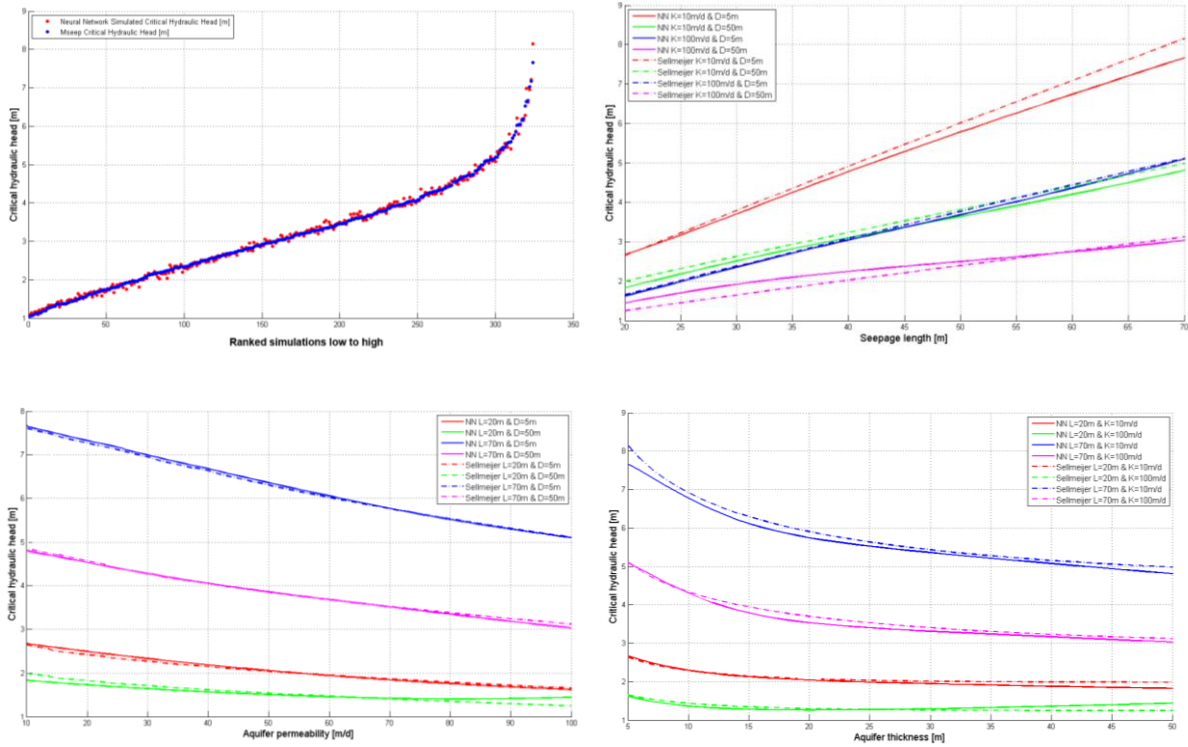


Figure E-1 Neural network predictions for ΔH_{CRIT}

Critical pipe length

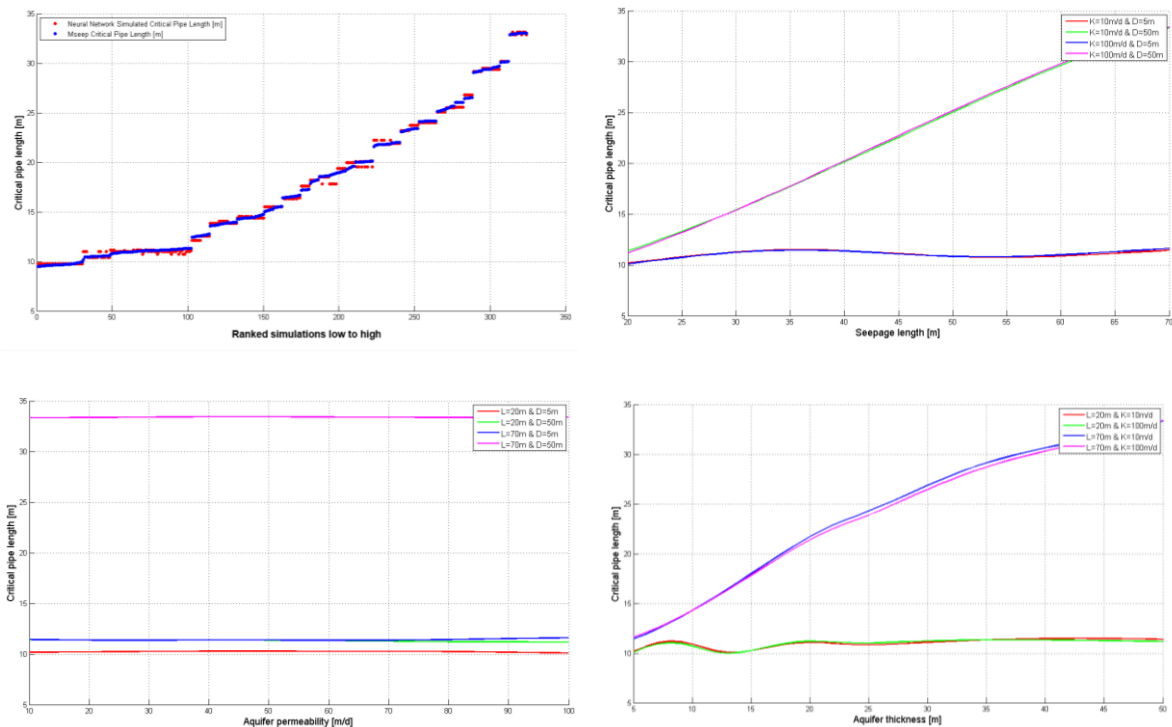


Figure E-2 Neural network predictions for critical pipe length

Critical pressure head at tip of the pipe

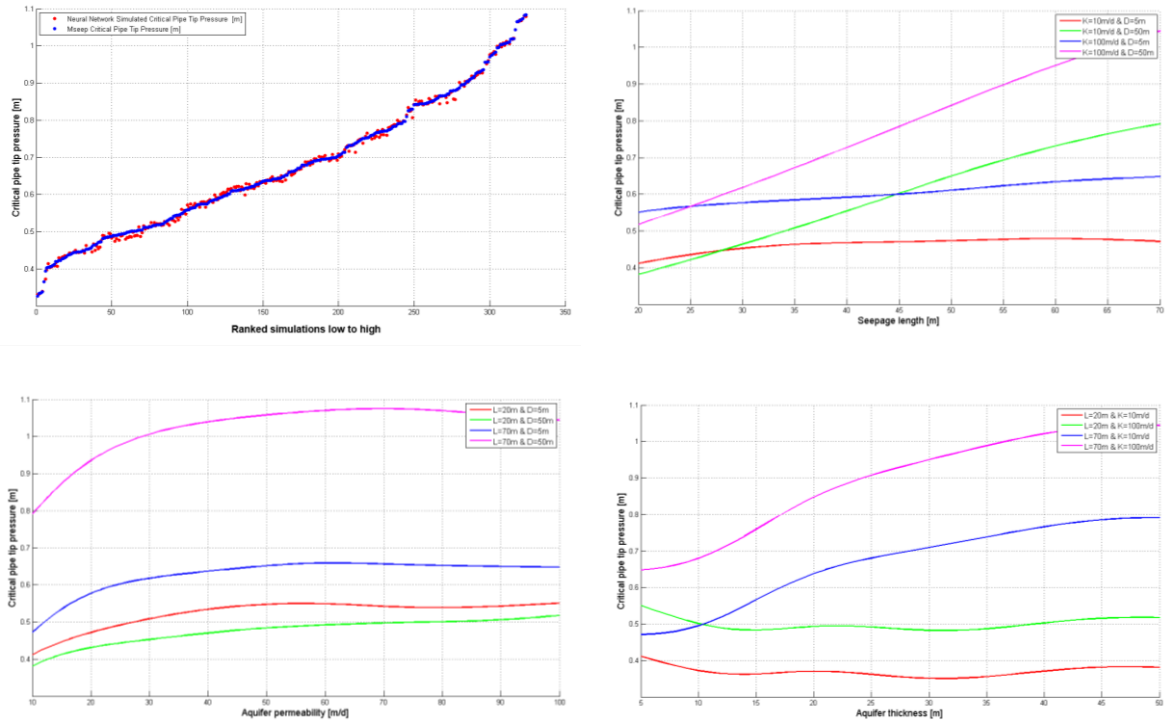


Figure E-3 Neural network predictions for critical pressure head at pipe tip

Head difference and pipe length of equilibrium curve's first point

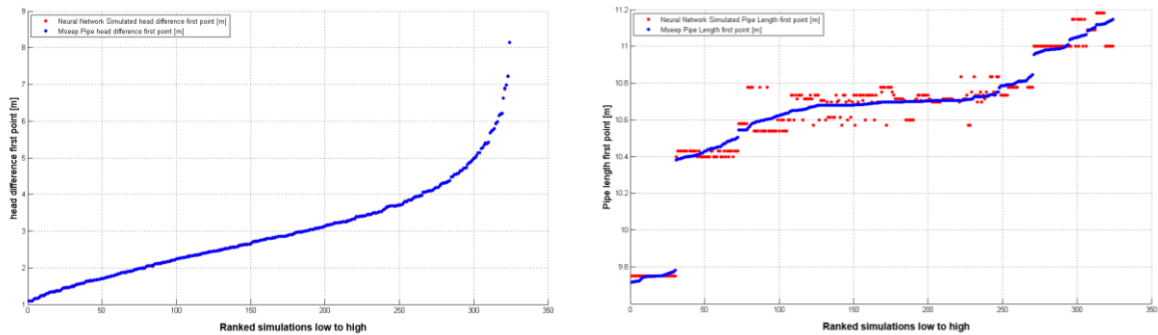


Figure E-4 Neural network predictions for critical pressure head at pipe tip

Appendix F - Transient piping model dike parameters

Performance of the TPM is investigated under constant and varying ΔH for dikes with varying seepage length, aquifer permeability, and aquifer thickness (figure F-1). In the analysis of the TPM the aquifer permeability is chosen as the reliability of Sellmeijer's rule is especially dominated by the uncertainty in permeability of the aquifer (Schweckendiek, 2010). The other two parameters, aquifer thickness and seepage length, have been selected in the result presentation as they are relatively easy to determine in reality and they represent dike geometry well. The height of a dike does not influence piping according to Sellmeijer (1988). The range of each parameter for primary dikes in the Netherlands is defined by a Grontmij expert judgment call.

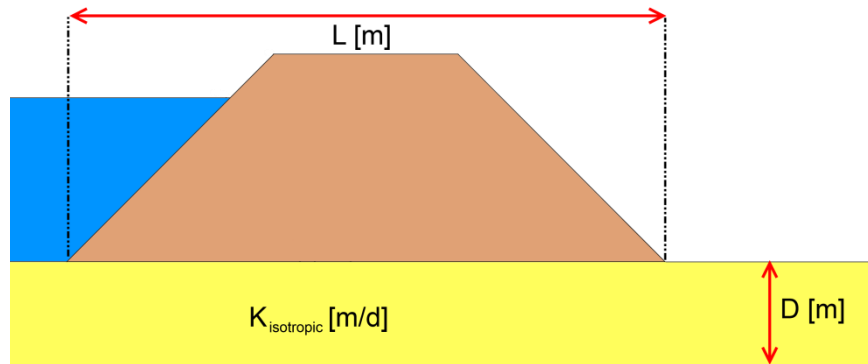


Figure F-1 Investigated dikes are varied with three dike parameters

Table F-1 Range of each investigated dike parameter

	Symbol	Low / small value	High / large value	Unit
Seepage length	L	20	70	m
Aquifer initial permeability	K	10	100	m/day
Aquifer thickness	D	5	50	m

Seepage length

In accordance with most common primary dikes the seepage length ranges from 20 to 70 meter. This is the distance between the inner and outer toe of the dike. A set dike slope of 1:2 is used as applied in the IJkdijk experiments. A minimal crest width (upper horizontal part of the dike) for primary dikes is about three meters so that traffic is possible on top of the dike (Grontmij, 2014).

Aquifer thickness

The Sellmeijer model assumes uniform aquifer thickness. In this study the aquifer thickness ranges from 5 to 50 meters. For primary dikes this is realistic range (Grontmij, 2014; DinoLoket, 2014). When the aquifer thickness is larger than the seepage length, the model of Sellmeijer is not valid anymore. It could be that Sellmeijer model then predicts a required seepage length longer than 18 times the ΔH . In the investigation this is the case with a seepage length of 20 and an aquifer thickness larger than 20 meters.

Aquifer permeability

The initial permeability of the aquifer ranges from 10 meters per day (upper limit fine sand) to 100 meters per day (very coarse sand) (TAW, 1994). In the IJkdijk test the initial permeability is about 10 m/d. In the investigation the permeability in horizontal and vertical direction is assumed to be equal. The neural networks, however, could have been trained with anisotropic aquifer permeability. Permeability is strongly dependent of the smaller grain fraction, the d_{10} (Sellmeijer, 1988; Van der Zee, 2011). D_{10} and d_{60} are correlated via the coefficient of uniformity C_u , (Hunt, 2005) where d_{60} and d_{10} are defined as the 60th and 10th mass percentile of a sand sample passing through a sieve with mesh size d [m].

The initial aquifer permeability and aquifer soil composition (e.g. grain sizes and porosity) are related. As the aquifer's grain sizes diameter and porosity increases, so does the permeability. Usually one calculates the permeability with a given porosity and grain size distribution. However, in this study the ΔH_{CRIT} (and critical piping time) is plotted as a function of aquifer permeability. The related initial porosity and grain sizes are calculated according Chapuis (2004). Wang et al. (2014) recommends this relation as the outcome is quite similar to the hydraulic conductivity of their experiment:

$$K = 1219.9 d_{10}^{1.565} \frac{n^{2.3475}}{(1 - n)^{1.565}} \quad (\text{F.1})$$

in which is:

K	[m]	the permeability of the aquifer
d_{10}	[m]	the tenth percentile of the particle size distribution
n	[m]	the (initial) porosity of the aquifer.

In this study the permeability ranges from 10 to 100 meters per day. The porosity is assumed to increase linear from 0.3 at low permeability and to realistic 0.4 at high permeability. This is done so that the particle size increase from low to high permeability is kept low (e.g. d_{70} of 675 μm instead of 1250 μm .) The porosity range of 0.3 to 0.4 is chosen because below the soil is packed tight and above the range the soil is packed loose regarding uniform sands (TAW, 1999). The tighter the soil is packed the more resistance to piping (van der Zee, 2011).

Now the tenth percentile of the particle size distribution is calculated according Chapuis (2004). However, in the Sellmeijer model the d_{70} must be defined. D_{60} and d_{10} are correlated through uniformity. The uniformity coefficient reads:

$$C = \frac{d_{60}}{d_{10}} \quad (\text{F.2})$$

In the IJkdijk experiments Baskarp sand was applied with a typical uniformity coefficient of 1.7 (Van Beek et al., 2012). A log-normal distribution between d_{60} and d_{10} is assumed to estimate d_{70} by interpolation.

$$d_{70} = 10 \text{ POWER} \left\langle \frac{70 - \left(10 - \frac{60 - 10}{\log d_{60} - \log d_{10}} * \log d_{10} \right)}{\frac{60 - 10}{\log d_{60} - \log d_{10}}} \right\rangle \quad (\text{F.3})$$

Conclusion

With a permeability increase from 10 to 100 meters per day and a porosity increase from 0.3 to 0.4 the 10 percentile of the grain diameter of the sand in the aquifer is calculated. Subsequently the 60 percentile of the grain diameter is calculated via the uniformity coefficient of 1.7. A log-normal distribution between d_{60} and d_{10} is assumed to estimate d_{70} by interpolation. The results are presented in figure F-2.

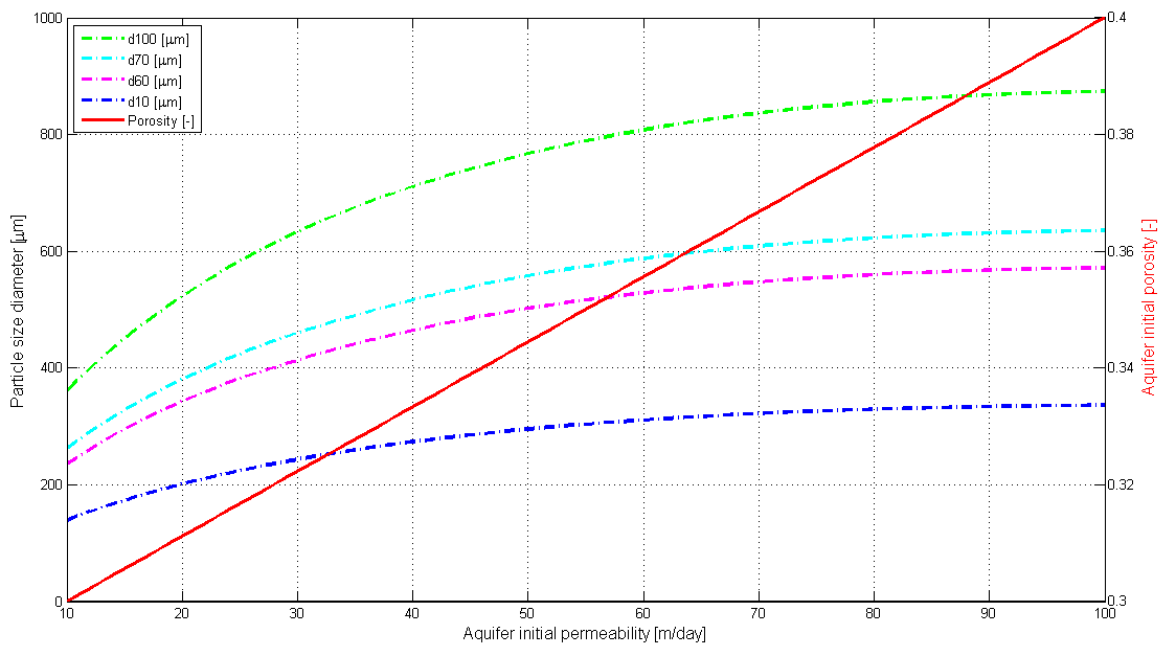


Figure F-2 The particle sizes of the aquifer sand and the aquifer initial porosity as a function of aquifer permeability